REFERENCE ONLY

UNIVERSITY OF LONDON THESIS

Degree PhD Year 2006 Name of Author WALLACE, A-S

COPYRIGHT
This is a thesis accepted for a Higher Degree of the University of London. It is an unpublished typescript and the copyright is held by the author. All persons consulting the thesis must read and abide by the Copyright Declaration below.

COPYRIGHT DECLARATION
I recognise that the copyright of the above-described thesis rests with the author and that no quotation from it or information derived from it may be published without the prior written consent of the author.

LOANS
Theses may not be lent to individuals, but the Senate House Library may lend a copy to approved libraries within the United Kingdom, for consultation solely on the premises of those libraries. Application should be made to: Inter-Library Loans, Senate House Library, Senate House, Malet Street, London WC1E 7HU.

REPRODUCTION
University of London theses may not be reproduced without explicit written permission from the Senate House Library. Enquiries should be addressed to the Theses Section of the Library. Regulations concerning reproduction vary according to the date of acceptance of the thesis and are listed below as guidelines.

A. Before 1962. Permission granted only upon the prior written consent of the author. (The Senate House Library will provide addresses where possible).

B. 1962 - 1974. In many cases the author has agreed to permit copying upon completion of a Copyright Declaration.

C. 1975 - 1988. Most theses may be copied upon completion of a Copyright Declaration.

D. 1989 onwards. Most theses may be copied.

This thesis comes within category D.

☑ This copy has been deposited in the Library of UCL

☐ This copy has been deposited in the Senate House Library, Senate House, Malet Street, London WC1E 7HU.

C:\Documents and Settings\lproctor\Local Settings\Temporary Internet Files\OLK8\Copyright - thesis (2).doc

The role of RET as a dependence receptor in enteric nervous system formation

Adam Spencer Wallace

Thesis submitted for the degree of PhD Developmental Biology

Neural Development Unit

Institute of Child Health

30 Guilford Street

London

WC1N 1EH

UMI Number: U592457

All rights reserved

INFORMATION TO ALL USERS
The quality of this reproduction is dependent upon the quality of the copy submitted.

In the unlikely event that the author did not send a complete manuscript
and there are missing pages, these will be noted. Also, if material had to be removed,
a note will indicate the deletion.

UMI U592457
Published by ProQuest LLC 2013. Copyright in the Dissertation held by the Author.
Microform Edition © ProQuest LLC.
All rights reserved. This work is protected against
unauthorized copying under Title 17, United States Code.

ProQuest LLC
789 East Eisenhower Parkway
P.O. Box 1346
Ann Arbor, MI 48106-1346

Abstract:

Enteric neurons are derived from vagal and sacral neural crest cell populations. Using human embryonic tissue aged 4-14 weeks of gestation the timing and pattern of gastrointestinal colonisation by vagal neural crest cells, and the development of interstitial cells of Cajal and the smooth musculature of the gut, were investigated using immunohistochemistry. Formation of both the enteric nervous system and smooth muscle involves rostrocaudal migration and maturation of these tissues. The gut is fully colonised by neural crest cells at week 7 and these cells first form the myenteric plexus external to the future circular muscle layer. Secondary centripetal migration to the submucosal plexus occurs at week 8 in the oesophagus and week 11 in the midgut. Smooth muscle appears at week 8, first as the circular muscle layer, with secondary formation of the longitudinal layer. ICCs are present from week 8 and develop in close association with the myenteric plexus in the midgut and hindgut. At week 14 all components required for a mature gut are present.

Rearranged during transfection (RET), a tyrosine kinase receptor and the most commonly linked gene to the enteric nervous system developmental disorder, Hirschsprung's disease, has been described *in vitro* as a dependence receptor, ie: expression of the receptor causes a cellular dependency on its ligand. In order to test whether RET functions as a dependence receptor *in vivo* constructs designed to perturb the caspase dependent cleavage of RET were introduced by electroporation of neural crest in E1.5 chicken embryos. Inhibition of Caspase-9 dependent apoptosis reveals a role for cell death in early control of neural crest cell numbers. No effect is observed when intracellular wildtype RET is introduced. However, introduction of a mutated form of RET induces a delay in the migration and differentiation of enteric precursors. These observations, combined with Tunel and *ret in situ* data, suggest a role for RET as a dependence receptor *in vivo* via a caspase-9 dependent mechanism.

Acknowledgements

I would like to thank all those who have assisted me during my PhD and in the production of this thesis.

Of the many people who have helped I must first thank my family for all their support and encouragment. I thank Alan Burns for his supervision, teaching and the opportunities he has provided me with these past three years. The Neural Development and Developmental Biology Units, Agnieszka Dziemba, Diane Austin, and Lucie Pompon for all their help, assistance and patience. I thank Piers Ruddle and Dianne Gerrelli for their help acquiring the human tissue and Andrew Stoker for his guidance as my secondary supervisor. Thanks also to Patrick Mehlen and Servanne Tauszig for all their help with the RET investigation. I would like to make special mention of Clare Faux and Dawn Savery for taking great care of me. Whether I needed help with protocols and techniques or just a friend they were there; they are my definitions of ace.

This work was kindly funded by a studentship from the Child Health Research Appeal Trust.

Table of Contents

Table of Figures:

Table of commonly used abbreviations:

CNS	Central nervous system
ECE-1	Endothelin converting enzyme 1
EDNRB	Endothelin receptor B
EGF	Epidermal growth factor
ENS	Enteric nervous system
ET-3	Endothelin 3
FGF	Fibroblast growth factor
GDNF	Glial cell-line derived growth factor
GFP	Green fluorescent protein
GFRα	GDNF family receptor alpha
GPI	Glycosyl phosphatidylinositol
HSCR	Hirschsprung's Disease
ICC	Interstitial cell of Cajal
Ig	Immunoglobulin
MEN	Multiple endocrine neoplasia
mRNA	messenger RNA
NCC	Neural crest cell
NTRN	Neurturin
PBS	Phosphate buffered saline
PDGF	Platlet derived growth factor
PNS	Parasympathetic nervous system
PSPN	Persephin
QCPN	Quail non-chick perinuclear antibody
RET	Rearranged during transfection
RTK	Receptor tyrosine kinase
SMA	Smooth muscle actin
SMADIP-1	SMAD interacting protein 1
WS	Waardenberg Shah syndrome

Chapter 1: Introduction

1.0 Introduction:

1.1 The Enteric Nervous System (ENS)

1.1.1 An overview of nervous systems:

The nervous system of an animal is responsible for the monitoring of internal and external stimuli, the processing of this input, the generation of original output in higher organisms, and the coordination of the activity of muscles and organs in response to these actions (Stein 1982). The central nervous system, which comprises the brain and spinal cord, is responsible for cognition and generates commands for the somatic portion of the peripheral nervous system. The somatic nervous system comprises afferent sensory neurons and efferent effector (motor) neurons and is responsible for voluntary skeletal muscle movement. The remaining portion of the peripheral nervous system is the autonomic nervous system which acts to maintain the homeostasis of the organism.

1.1.2 The autonomic nervous system

Homeostatic responses are separated from higher cognitive function and processed by reflex circuits for a rapid response. The autonomic nervous system deals with these involuntary responses to stimuli (Stein 1982). It can itself be further divided into the sympathetic, parasympathetic, and enteric nervous systems.

The sympathetic (SNS) and parasympathetic (PNS) nervous systems work synergistically or antagonistically in response to stimuli. As a generalisation the SNS can be thought of as responsible for initiating the "fight or flight" response, and the PNS it's opposite, exerting an energy saving influence over the muscles and organs it controls.

Independent of the SNS and PNS, the enteric nervous system (ENS) forms the third component of the ANS. Although capable of modulation by the SNS and PNS, it alone exhibits the ability to operate without extrinsic input. It is this ability that has earnt the ENS the nick-name "the second brain" (Gershon 1999).

1.1.3 The enteric nervous system, a component of the autonomic nervous system

The enteric nervous system consists of a twin coaxial network of neurons and glia that are located in the wall of the gastrointestinal tract. This arrangement of cells, extending from the oesophagus to the terminal portion of the gastrointestinal tract, rivals the spinal cord in terms of number of neurons (Furness and Costa 1987).

Enteric ganglia contain sensory and effector neurons like other components of the ANS. However, they also contain interneurons that form local circuits with sensory and motor neurons allowing the ENS to function independently of extrinsic input. Enteric neurons more closely resemble neurons

of the central nervous system than those of the ANS, using glia, cells analogous to astrocytes, instead of sheath cells to provide physical and nutritional support.

1.1.4 Structure of the ENS

Enteric neurons and their supporting glial cells are arranged into two plexi of ganglia at differing levels within the gut mesenchyme **(Fig 1.1)**. The outermost plexus is known as the myenteric (or Auerbach's) plexus and is located between the longitudinal muscle layer, towards the outside of the gut, and the circular muscle layer. Between the circular muscle layer and the mucosa is the submucosal or (Meissner's) plexus. Some model organisms, such as zebrafish, used to investigate the development of the ENS do not possess this second plexus and have only the myenteric plexus (Shepherd et al. 2004). Under high magnification these plexi appear as web-like structures of interconnected ganglia comprising tight groups of cells **(Fig 1.2)**.

The myenteric plexus, as indicated by its existence as the sole neuronal layer found in more primitive organisms, was probably the first to arise early in the evolution of chordates. It can be found along the full length of the gut in mammals and avians. The submucosal plexus by contrast, is not found in the stomach although it is present throughout the remainder of the gut. The myenteric plexus contains larger and more numerous ganglia than the submucosal plexus at any specific point of gut (Gabella and Trigg 1984; Burns, Pasricha, and Young 2004).

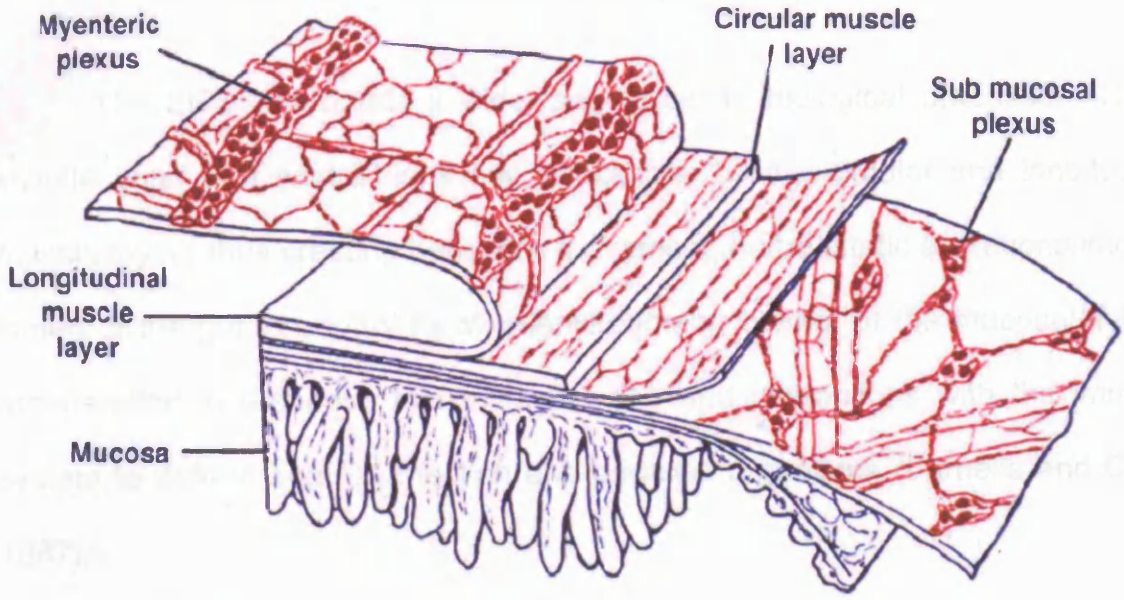

Figure 1.1: Organisation of the gut layers.

The myenteric plexus lies between the two main muscle layers of the gut, the outer longitudinal layer and the inner circular layer. The submucosal plexus lies between the circular muscle layer and the mucosa, which lines the gut lumen. (Modified from Furness and Costa, 1987)

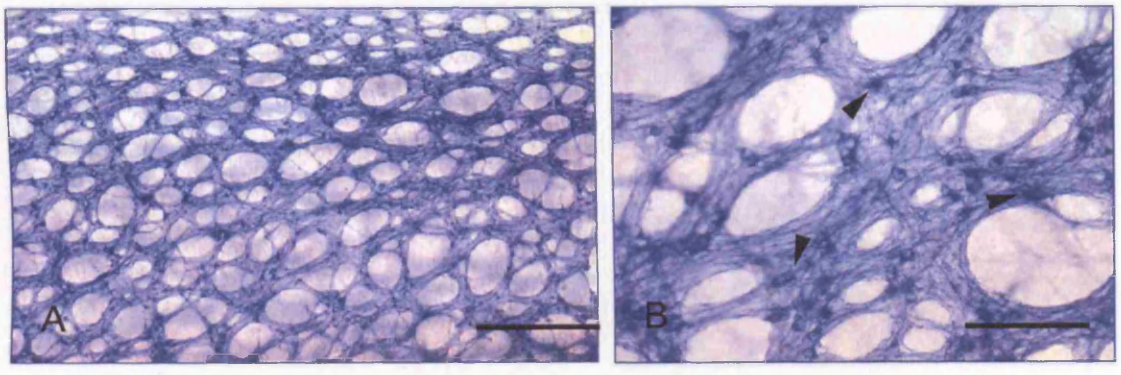

Figure 1.2: NADPH-diaphorase staining of chick hindgut at E14.5, myenteric plexus.

(A) Low magnification of NADPH-diaphorase staining of nitric oxide synthase containing neurons at E14.5 in the developing chick gut. (B) Same region of gut as in (A) shown at higher magnification. Individual NADPH stained neurons can be identified (arrowheads).
Scale Bars: (A) 50μm, (B) 10μm

1.1.5 Function of the ENS

The ENS commands a wide-ranging set of biological processes. These include control of contractions and relaxations by the circular and longitudinal muscle layers thus creating peristaltic movement, homeostatic secretions into the lumen of the gut to control its microenvironment; control of the mucosal lining's regeneration in response to continual wear; and interactions with the immune system to defend against infection and parasitic organisms (Furness and Costa 1987).

1.2 The Neural Crest

1.2.1 The neural crest

The neural crest is a transient population of cells unique to vertebrates. Arising from an epithelial to mesenchymal transition during neural tube closure the neural crest is located dorsal to the neural tube **(Fig 1.3)**. Cells migrate from this location early in development and give rise to various cell types throughout the body, including neurons of the PNS, the adrenal medulla, schwann cells of the ANS, neural crest-derived endocrine organs, melanocytes, craniofacial structures, cardiac outflow septum, and neurons and glia of the enteric nervous system (Le Douarin and Kalcheim 1999). Migration from the dorsal aspect of the neural tube by neural crest cells occurs along stereotypical pathways dependent upon the tissue target.

1.2.2 The neural crest gives rise to the ENS

The neural crest was identified as the origin of ENS precursors half a century ago. Using the chick embryo as a model, the effects of ablating various levels of neural tube, and associated neural crest were assessed. It was discovered that removing the post-otic hindbrain leads to aganglionic gut in the developing embryo (Yntema and Hammond 1954). This region, termed the vagal crest, was further specified following the development of a xenograft technique developed by Le Douarin in the 1960's which employed chicken embryos hosting quail tissue.

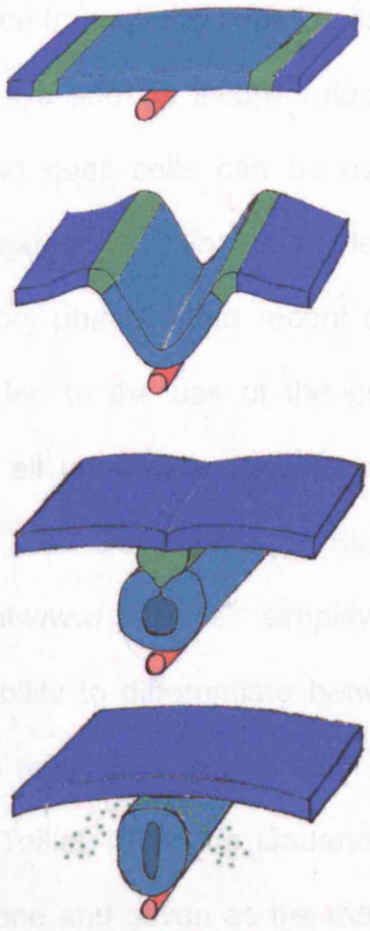

Figure 1.3: Formation of the neural tube and associated neural crest.

The neuroectoderm, which originally forms a sheet (light blue and green) above the notochord (red), elevates about the midline. The two opposing neural folds meet at the region joining the presumptive neural crest (green) and the future ectoderm (dark blue). At this point the neuroectoderm destined to become neural crest undergoes an epithelial-mesenchymal transition. Fusion of the ectoderm and neural tube (light blue) occur, resulting in the tube-like structure of the neural tube and the sheet of ectoderm above. Between these, the neural crest completes its transformation before migrating away from the dorsal aspect of the neural fold. Modified from UCLA - Crump Institute web notes. www.crump.ucla.edu

The success of this technique is due to the similar size and incubation period of the two species. Once transplanted quail cells can successfully migrate along their prescribed pathways and be incorporated into host tissue. At any stage after surgery chick and quail cells can be easily distinguished by the denser heterochromatin appearance within the nucleus of quail cells, before, during and after their migratory phase. More recent developments in antigenic markers of quail cells have led to the use of the quail non-chick perinuclear antibody (QCPN) to identify all quail cells (developed by Carlson & Carlson, University of Michigan, 1989; see Developmental Studies Hybridoma Bank for details, www.uiowa.edu/~dshbwww/), further simplifying and accelerating the investigative process. This ability to differentiate between the host and grafted tissue allowed Le Douarin to refine the precise axial level responsible for ENS precursors (Le Douarin and Teillet 1973). Le Douarin and colleagues identified the region between somites one and seven as the main source of vagal derived ENS precursors. They also identified a second source of crest cells that contributed to a lesser extent, and specifically to the hindgut, arising from the sacral region caudal to the 28th pair of somites **(Fig 1.4)**.

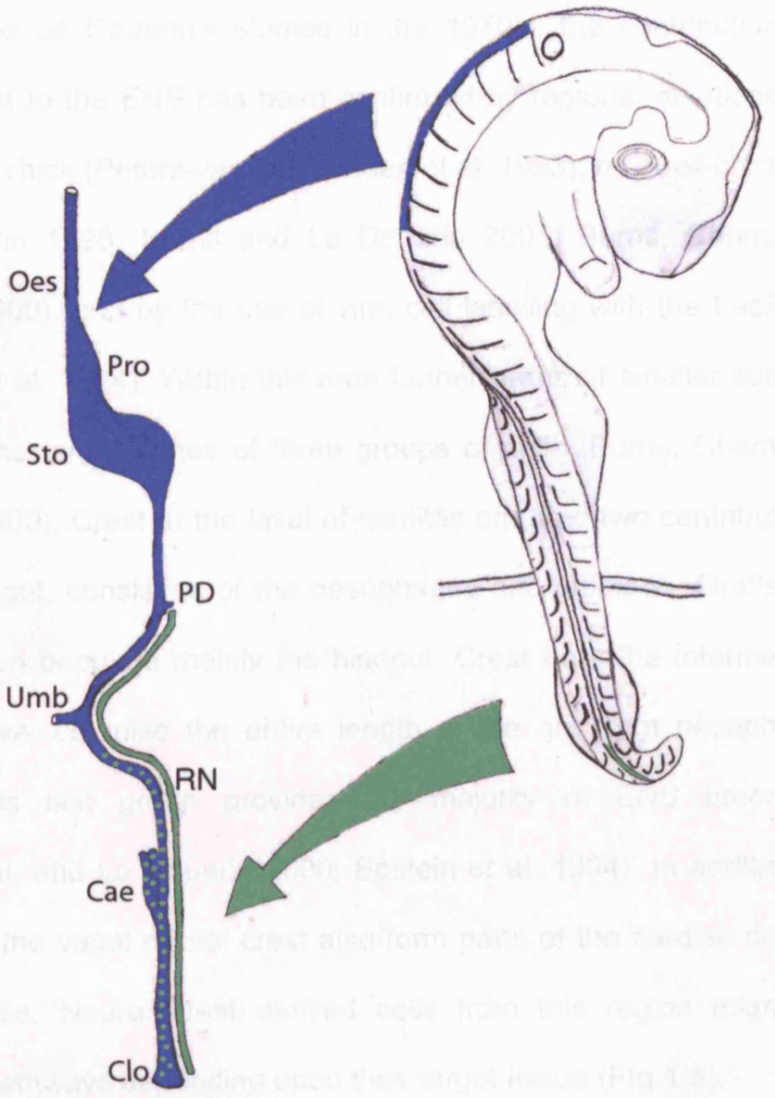

Figure 1.4: Vagal and sacral neural crest contribution to the enteric nervous system in the chick embryo.

Vagal neural crest cells from the level of somites 1-7 colonise the full length of the gastrointestinal tract (Blue arrow and shading). Sacral neural crest cells, originating from the region caudal to somite 28, form the nerve of Remak and then populate the colon and distal intestine (Green arrow, and dots).
Oes=Oesophagus, Pro=Proventriculus, Sto=Stomach, PD=Pancreatic Ducts, Umb=Umbilicus, Cae=Caecum, Clo=Cloaca, RN=Nerve of Remak

1.2.3 Vagal neural crest

Since Le Douarin's studies in the 1970's, the contribution of the vagal neural crest to the ENS has been confirmed by regional ablations of the neural tube in the chick (Peters-van der Sanden et al. 1993), by quail-chick grafts (Burns and Douarin 1998; Burns and Le Douarin 2001; Burns, Champeval, and Le Douarin 2000), and by the use of viral cell labelling with the LacZ marker gene (Epstein et al. 1994). Within this area further grafts of smaller sub-regions have revealed the target zones of three groups of cells (Burns, Champeval, and Le Douarin 2000). Crest at the level of somites one and two contributes exclusively to the foregut, consisting of the oesophagus and stomach. Grafts from somites six to seven populate mainly the hindgut. Crest from the intermediate somites, three to five, colonise the entire length of the gut from oesophagus to distal colon. This last group provides the majority of ENS precursors (Burns, Champeval, and Le Douarin 2000; Epstein et al. 1994). In addition to the ENS, cells from the vagal neural crest also form parts of the cardiac outflow tract and melanocytes. Neural crest derived cells from this region migrate along two different pathways depending upon their target tissue **(Fig 1.5)**.

Investigating the behaviour of mammalian vagal crest has involved cell-labelling techniques such as use of transgenic mice (Kapur, Yost, and Palmiter 1992), the lipophilic marker DiI (Pomeranz, Rothman, and Gershon 1991) or retrovirally delivered LacZ (Serbedzija and McMahon 1997) into the neural tube and neural crest cells. Mammalian systems are not well suited to ablative surgery as they develop *in utero*, and the extra-embryonic membranes must be kept

intact for effective embryo culture. However, vagal cells have been found to contribute to the ENS as they do in the chicken (Durbec et al. 1996b), but with some minor differences in the specificity of axial levels within this domain. Crest at the level of somites six and seven, which Durbec refers to as anterior trunk neural crest, gave rise to only foregut ganglia and dorsal root ganglia. The remaining vagal region, between somites one and five, gives rise to enteric ganglia along the full length of the gut.

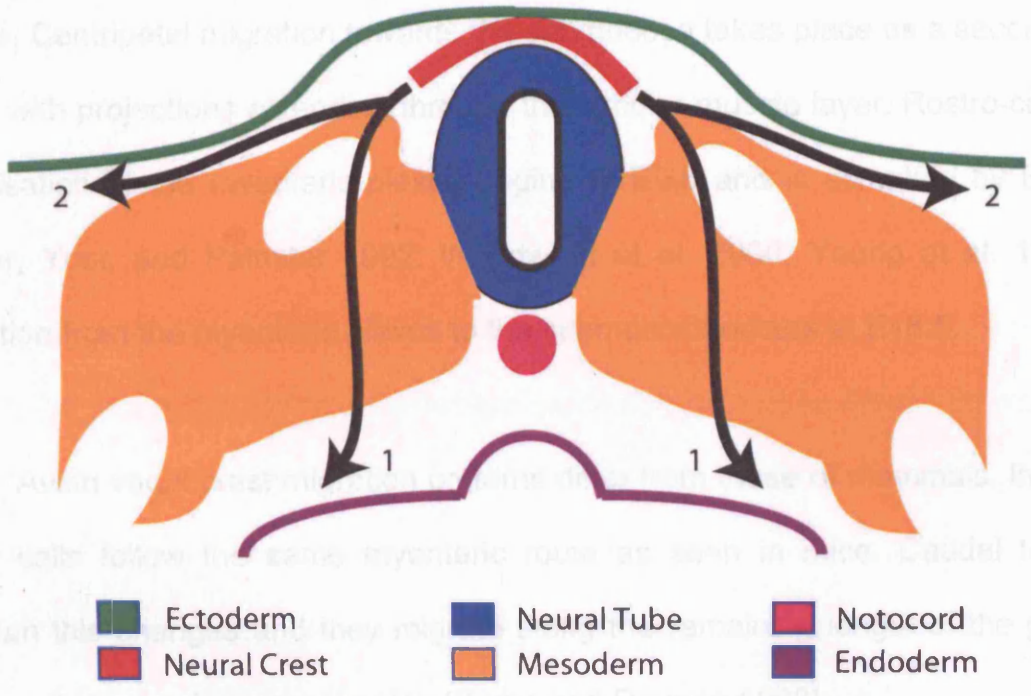

Figure 1.5: Migratory routes taken by early neural crest at rhombomere 7.

Early migratory crest cells from the region of rhombomere 7 migrate via one of the two routes shown above; 1) dorsoventral, 2) lateral. The lateral route is taken by neural crest cells destined to become melanocytes . The dorsoventral route is followed by those populations destined to form the ENS.

The pattern of migration by the vagal crest has been found to differ between the various animal models used to investigate ENS development. Zebrafish, the use of which has arisen more recently than that of mouse and chick, have a relatively simple ENS comprising a single plexus, the myenteric, which arises from vagal neural crest cells which migrate in a rostro-caudal direction, colonising the entire length of the gut (Shepherd et al. 2004).

The vagal NCC of mice migrate in a rostro-caudal wave through the gut mesenchyme in a region corresponding to the future position of the myenteric plexus. Centripetal migration towards the submucosa takes place as a secondary event with projections extending through the circular muscle layer. Rostro-caudal colonisation of the myenteric plexus begins at E9.5 and is complete by E14.5 (Kapur, Yost, and Palmiter 1992; Woodward et al. 2000; Young et al. 1998). Migration from the myenteric plexus to the submucosa occurs at E18.5.

Avian vagal crest migration patterns differ from those of mammals. Initially vagal cells follow the same myenteric route as seen in mice. Caudal to the caecum this changes and they migrate along the remaining length of the gut in the prospective submucosal region (Burns and Douarin 1998).

1.2.4 Sacral neural crest

The contribution of sacral crest to the ENS was initially overlooked but once reported sparked a quarter century's worth of research to clarify its role. Yntema and Hammond did not observe any enteric neurons in the chick gut when the vagal region was ablated, and so it was initially assumed that the ENS was derived from a single source (Yntema and Hammond 1954). However, use of the quail-chick grafting involving transplantation of the quail neural tube caudal to the 28th pair of somites into a chick host, allowed Le Douarin and Teillet to identify quail derived cells within enteric ganglia in the hindgut (Le Douarin and Teillet 1973). For twenty-five years conflicting findings concerning the precise contribution made by sacral crest to the ENS were reported.

Labelling sacral NCC with DiI and with retroviral introduced LacZ showed there to be sacral derived cells in the hindgut two days prior to the arrival of vagal derived cells in the chick (Pomeranz and Gershon 1990; Serbedzija et al. 1991). The contribution of sacral NCC to enteric ganglia appears greater in the chick than in the mouse but both have been found to contain labelled cells in the post-umbilical intestine (Serbedzija et al. 1991). Transplantation experiments in which hindgut was dissected and cultured prior to the arrival of vagal crest produced conflicting results. Some groups reported a complete absence of enteric neurons in the cultures (Nishijima et al. 1990; Kapur, Yost, and Palmiter 1992; Young et al. 1998; Young et al. 1996; Lecoin, Gabella, and Le Douarin 1996), while others reported the presence of neurons (Kapur 2000; Pomeranz and Gershon 1990; Pomeranz, Rothman, and Gershon 1991), but in reduced numbers. The lack of

neurons observed in these isolation and culture studies may have been due to the sacral population not having reached the gut at the time of dissection.

This issue was resolved, for avian species, by a comprehensive study utilising quail-chick grafting. Burns and Le Douarin utilised sacral grafts to address not only the presence of sacral derived enteric ganglia in the gut, but also the timing of their colonisation and their fate (Burns and Douarin 1998). These studies showed that enteric precursors originating from the sacral crest do not migrate directly into the gut. Instead they first migrate and form the nerve of Remak, then undergo a period of migratory senescence before undergoing a second period of migration resulting in colonisation of the gut several days later (Burns and Douarin 1998). The nerve of Remak, which is unique to avians, exists in close proximity to the mid and hindgut and plays a role in the regulation of gut motility through extrinsic projections (Smith and Lunam 1998; Lunam and Smith 1996). The formation of this nerve occurs as a distal-proximal migration between E4.5 and E6. Sacral derived NCCs appear in the myenteric plexus of the hindgut at E7.5, closely associated with fibres originating from the nerve of Remak. Between E7 and E10 sacral derived NCC are closely associated with these nerve fibres although they do not appear within enteric ganglia until E10. From E10 the number of sacral derived NCC in the gut begins to increase and contributes to enteric ganglia in larger numbers (Burns and Douarin 1998).

1.2.5 The relative invasive capacities of vagal and sacral crest

The contribution of sacral derived NCC to enteric ganglia of the hindgut is considerably less than that from the vagal population. At E16 the percentage of QCPN positive quail neurons, following a sacral graft, ranged from 17.4% in the distal-colorectum to 0.3% in the rostro-colorectum for the myenteric plexus, and 1.3% to 0.1% in the submucosal plexus (Burns and Douarin 1998). In embryos lacking the vagal contribution in the hindgut due to ablative surgery, sacral derived crest cells successfully migrated into the hindgut and differentiated (Burns, Champeval, and Le Douarin 2000). The number of sacral derived cells present in vagal-deficient hindgut exceeded the number in control gut, by a small but statistically significant degree. However, despite increased sacral derived NCC numbers, enteric ganglia in this region were infrequent and reduced in size indicating that sacral crest is incapable of adequately compensating for a lack of vagal cells.

To investigate the different behaviours and invasive capacities of the vagal and sacral derived crest, vagal-to-sacral and sacral-to-vagal grafts have been performed (Burns, Delalande, and Le Douarin 2002). When transplanted to the sacral region, vagal cells successfully colonised the hindgut but with significant differences to the patterns seen in controls. Migration of these transplanted cells appeared more rapid, colonising the mesenchyme of the gut at E4 having only formed a rudimentary nerve of Remak. Control embryos possessed no crest cells in the hindgut mesenchyme at this stage and the only quail cells present were adjacent to the gut wall as nerve of Remak precursors.

Vagal cells transplanted to the sacral region migrated in a caudal-rostral direction in opposition to the endogenous vagal cells migrating caudally. Transplanted cells colonised the hindgut, post-umbilical intestine and some reached the pre-umbilical intestine. These cells appeared to constitute the majority of neurons and glia in the myenteric and submucosal ganglia. Sacral cells transplanted to the vagal region failed to fully colonise the gut. These cells migrated to the level of the pre-umbilical intestine, with the majority of cells present in the myenteric plexus although a few cells were present in the submucosal plexus. This implies that both vagal and sacral derived crest are capable of responding to rostral and caudal migration signals. However, they differ in their ability to generate numbers of neurons and glia.

1.2.6 Developmental disorders affecting neural crest cells

Neurocristopathies are conditions resulting from defects in neural crest migration, survival or proliferation. Two main types of neurocristopathy exist; neural crest tumours and those conditions which result from a failure of NCC to migrate to their targets successfully. The affected structures in these disorders are commonly the adrenal medulla, Schwann cells of the ANS and neural crest-derived endocrine organs. Tumour type neurocristopathies may affect endocrine tissue or the nervous system, and include conditions such as pheochromocytoma, neuroblastoma, medullary carcinoma of the thyroid, carcinoid tumours, and neurofibromatosis. Defects in NCC migration along the gut result in Hirschsprung's disease, characterised by an absence of ENS cells in varying lengths of the hindgut. Conditions arising from migrational defects also

include Waardenburg syndrome, Aorticopulmonary septation of the heart, cleft lip/palate, frontonasal displasia, and Di George syndrome. Of these, Waardenburg syndrome (WS), which involves failures in migration of melanocytes and is characterised by a white forelock, is most commonly associated with HSCR (Pingault et al. 1998).

1.3 Hirschsprung's Disease – pathology and treatment

1.3.1 Hirschsprung's Disease

Hirschsprung's disease (HSCR) is the most common congenital defect affecting the gastrointestinal tract. First described by Harald Hirschsprung in 1886, HSCR affects 1 in 5,000 live births, although this frequency may range from 1-3 in 10,000, depending upon the ethnicity of the study population. Some exceptional, genetically isolated populations such as the Mennonites display rates ten times higher than this (Carrasquillo et al. 2002).

Most cases of HSCR are diagnosed soon after birth, but teenagers and adults may also be diagnosed if suffering milder forms. Generally an abdominal swelling **(Fig 1.6)** associated with failure to pass meconium within the first twenty-four to forty-eight hours of birth and vomiting of bile indicate HSCR in newborns. Young children and adults suffering mild HSCR may be diagnosed after suffering prolonged periods of diarrhoea and constipation, and they may also suffer anaemia.

Examination of the gut in HSCR cases reveals a grossly distended length of bowel proximal to a stretch of apparently normal gut, varying in length, which extends to the anus. Closer inspection of the distal gut reveals a lack of enteric innervation. With no control exerted over the musculature in this region a state of permanent contraction results, causing a blockage and proximal swelling. HSCR always affects the most distal gut although the aganglionic length varies affecting just the distal colon, known as short-segment HSCR, or the entire colon and

some of the distal intestine, termed long-segment HSCR. Eighty percent of HSCR patients suffer from the short-segment form (Passarge 1967; Garver, Law, and Garver 1985). Some cases of total intestinal aganglionosis have been reported (Seri et al. 1997) but such cases are extremely rare. Other conditions may be associated with HSCR, and are discussed below.

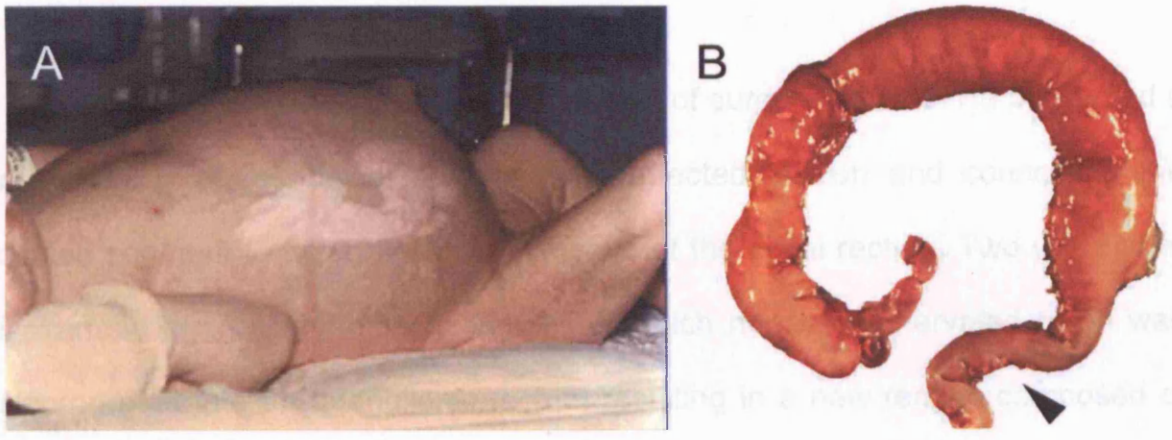

Fig 1.6: Hirschsprung's disease causes abdominal swelling.

(A) Neonate with swollen abdomen due to Hirschsprung's pseudo-obstruction (Photograph courtesy of Dr. P.Milla). (B) Region of contracted aganglionic bowel (arrowhead) and preceding distension of gut due to failure of faecal material to pass.

1.3.2 Treatment of HSCR

HSCR can be diagnosed using several techniques. Rectal biopsies may be carried out to assess the presence of ganglia although this is more often used to gauge the best point for resectioning the bowel. Barium enemas and abdominal x-rays allow for a relatively easy and low risk identification of HSCR cases. Once identified, surgery is performed to remove the aganglionic region and reconnect the functional bowel to the anus. Three forms of surgery (the definitive treatment for HSCR) can be used to restore gut function, each successful but differing in the potential complications that can result.

Orvar Swenson proposed the first form of surgery in 1948. He performed a resectioning of the bowel removing the affected portion and connecting the dilated segment to two or three centimetres of the distal rectum. Two years later Duhamel began performing operations in which normally innervated colon was incorporated into an aganglionic rectum resulting in a new rectum composed of half aganglionic and half ganglionic musculature. Most recently Soave introduced the technique of the endorectal pull-through. This process involves stripping the mucosa from the distal aganglionic rectum and passing the normally innervated colon through the sleeve of dysfunctional rectum. The function of the normal portion is used to propel material through the abnormal cuff.

These surgical procedures are not without their faults. Five percent of recipients of Swenson's surgery experience anastomotic leaks. Duhamel's surgery is prone to incomplete emptying of the aganglionic pouch. Soave's

treatment, although avoiding anastomotic leaks, suffers cuff abscesses and patients may require continued dilatations.

Ideally a method for repopulating this most terminal region using recovered precursor cells from fully functional bowel, and its incorporation into the functional extant ENS could be used to support the surgical procedure. Subsequent to the standard surgery the most terminal region would be subject to either a stem cell or gene therapy approach that could, perhaps with additional courses of therapy, restore functionality and result in a more satisfactory standard of life. To this end, an investigation of the signalling pathways controlling the formation of the enteric nervous system is desirable in order that we might better understand the conditions required for such a therapy to succeed.

1.3.3 Genetics of HSCR

HSCR arises from mutations in several known genes and does not display simple Mendelian inheritance. Whilst originally believed to be a multifactoral autosomal recessive disease, increases in patient survival to child-bearing age changed this idea as reports began to appear of familial cases consistent with autosomal dominant inheritance of HSCR (Lipson and Harvey 1987; Lipson, Harvey, and Oley 1990; Carter, Evans, and Hickman 1981). Variable penetrance and severity of HSCR cases indicates a complex and multifactoral origin of this condition. Overall males display higher levels of penetrance than females, 4:1

(Badner et al. 1990), although within families affected by HSCR this sex bias decreases as the severity of cases increases (Holschneider and Puri 2000).

HSCR occurs as an isolated trait in 70% of cases, while 18% are linked to other congenital defects. A higher proportion of familial cases appears to be associated with secondary congenital defects than for spontaneous HSCR. Several defects, including cleft palate, polydactyly, cardiac septum defects and craniofacial abnormalities, display higher than expected incidence within the 18% of cases associated with other defects (Spouge and Baird 1985). The remaining 12% of HSCR cases are linked to chromosomal abnormalities of which the vast majority are trisomy 21 (90%).

Several genes have been associated with HSCR cases in humans and others have been observed to create HSCR-like hypoganglionosis or aganglionosis in mutant mice. The key genes associated with HSCR are RET, GDNF, GFRα1, ET-3, EDNRB, ECE-1, SMADIP-1, Phox2B and Sox10. RET is implicated in the majority of identified HSCR cases, with around a half of familial and a third of spontaneous cases having mutations in this gene (Seri et al. 1997) **(Table 1.1)**.

Table 1.1:

Gene	Product	Species with known mutants	Frequency in HSCR
RET	Co-receptor for GDNF	Mouse, Human	20-25%
GDNF	Primary ligand for RET/GFRα1	Mouse, Human	Unknown (rare)
GFRα1	Co-receptor for GDNF	Mouse	Not Significant
NTN	Ligand for RET	Human	Single family
EDNRB	Receptor for ET-3	Mouse, Rat, Human	5-10%
ET-3	Ligand for EDNRB	Mouse, Human	5-10%
ECE-1	ET-3 converting enzyme	Mouse, Human	Rare
Sox10	Transcription factor	Mouse, Human	<5% (limited data)
SMADIP-1	Transcription factor	Mouse, Human	Rare*
Phox2B	Transcription factor	Mouse, Human	Rare

* Higher incidence rate in cases displaying HSCR and mental retardation.

Modified from Kapur RP, Gut 2000 December; 47 Suppl 4:iv 81-83.

1.4 Genetic pathways associated with HSCR and gut aganglionosis

1.4.1 The RET Pathway

1.4.1.1 Receptor Tyrosine Kinases

Receptor tyrosine kinases (RTKs) are transmembrane glycoproteins responsible for the transduction of signals for cell differentiation and growth (Schlessinger and Ullrich 1992). All multicellular organisms examined thus far have been shown to possess RTKs, with fifty having been described in vertebrates alone. RTKs are organised into groups according to their structural properties rather than by their function. However, structurally related RTKs appear to have similar roles. Amongst the ligands identified for RTKS are ephrins, epidermal growth factor (EGF), fibroblast growth factor (FGF), glial cell line-derived growth factor (GDNF), insulin, nerve growth factor (NGF), platelet derived growth factor (PDGF) and vascular endothelial growth factor (VEGF) (Hubbard and Till 2000).

RTKs usually consist of an extracellular ligand binding domain, which may be glycosylated, linked to the cytoplasmic signalling domain by a single transmembrane alpha helix. The extracellular portion can contain a variety of discrete globular domains including immunoglubulin (Ig)-like domains, EGF–like domains, fibronectin type III-like domains and cysteine rich domains. The organisation of the intracellular domain is simpler comprising a juxtamembrane region, then the tyrosine kinase domain and finally the carboxy-terminal region.

Two processes are required for the activation of RTKs, namely the enhancement of intrinsic catalytic function and the creation of binding sites to recruit downstream signalling proteins. In order to be activated, a RTK undergoes essential autophosphorylation at the tyrosine residues in its cytoplasmic domain (Mohammadi et al. 1996; Ellis et al. 1986; Kendall et al. 1999; Fantl, Escobedo, and Williams 1989) as a consequence of oligomerisation of the protein, an event mediated by ligand binding. Autophosphorylation of the activation loop in the kinase domain, which contains between one and three tyrosine residues, stimulates the kinase activity of the protein. This in turn acts by catalysing the γ phosphate of adenosine tri-phosphate (ATP) to hydroxyl groups of tyrosine residues on target proteins (Hunter 1998). Autophosphorylation of the juxtamembrane region, kinase insert or carboxy-terminal domain results in the creation of docking sites for phosphotyrosine recognising molecules.

The mechanism used to trigger autophosphorylation of an RTK is oligomerisation of a given receptor (Ullrich and Schlessinger 1990). Ligand binding of the extracellular domain induces a structural rearrangement facilitating the autophosphorylation in the cytoplasmic domains. For receptors such as RET which bind dimeric ligands, the dimeric receptor is the competent signalling form (Durick et al 1995) and this degree of oligermisation is probably sufficient in most instances. Other RTKs may require further steps for signalling to occur. For example, a dimeric ephrin is insufficient to initiate the complete range of responses that arise from a tetrameric ephrin (Stein et al. 1998).

1.4.1.2 RET

The Rearranged during transfection (RET) proto-oncogene encodes one such receptor tyrosine kinase (Takahashi, Ritz, and Cooper 1985). The genomic sequence of RET in humans is approximately 55KB, containing 20 exons (Pasini et al. 1995) at position 10q11.2 (Ishizaka et al. 1989). Homologues of RET have been found in vertebrates and invertebrates including *Drosophila melanogaster* (Hahn and Bishop 2001). Alternative splicing of this sequence generates three isoforms of RET named for the number of residues at the C-terminal end of the protein; RET9, RET43 and RET51 (Tahira et al. 1990; Myers et al. 1995). All three isoforms undergo transcription, but mRNA expression of RET43 is sparse and its sequence is less well conserved between species than that of its' sibling isoforms (Myers et al. 1995). Furthermore, RET43 protein has not been shown to be transcribed in cells. The amino acids in these c-terminal tails differ not only in their number but also their sequence. The number of tyrosine residues within the isoforms also varies. RET9 contains the sixteen tyrosines positioned in the nonvariable domains and RET51 contains an additional two within its 51 amino-acid tail (Myers et al. 1995).

The extracellular structure of RET contains four serial cadherin-like motif repeats and a cysteine rich domain (Iwamoto et al. 1993). Cadherins are Ca^{2+} dependent cell-cell adhesion molecules utilising tandemly repeated extracellular domains to effect this adhesion. Calcium binding to these cadherin domains is believed to protect the molecule from degradation by inducing linearisation and increased rigidity of the extracellular domain (Nagar et al 1996). It is also thought

that this process aids in the dimerisation of cadherins. RET displays properties which conform with these hypotheses; in the absence of calcium RET fails to fold properly within the endoplasmic reticulum (van Weering et al. 1998), while in the presence of calcium it is resistant to trypsin activity (Takahashi et al. 1993) and its dimerisation upon ligand binding is dependent upon calcium (Nozaki et al. 1998).

RET can be activated by the binding of four known molecules structurally related to the TGF-β superfamily, namely glial cell line-derived neurotrophic factor (GDNF), neurturin (NTRN), artemin (ARTN) and persephin.(PSPN). These secreted molecules possess activity in a variety of tissues (Ibanez 1998; Kotzbauer et al. 1996; Milbrandt et al. 1998; Baloh et al. 2000; Baloh et al. 1997; Creedon et al. 1997). Binding of these ligands is mediated by co-receptors collectively known as GDNF family receptor α (GFRα). GFRαs are glycosyl phosphatidylinositol-linked (GPI-linked) membrane receptors. Each member of the family specifically binds to one GDNF family ligand; GFRα1 – GDNF, GFRα2 – NRTN, GFRα3 – ARTN and GFRα4 – PSPN. This specificity can break down *in vitro* with GDNF able to bind GFRα2/3 and ARTN or NRTN able to bind GFRα1 (Baloh et al. 1997; Creedon et al. 1997; Jing et al. 1997; Sanicola et al. 1997). RET cannot bind any ligand independently and must bind a complex of GFRα and GDNF family ligands (Airaksinen and Saarma 2002). The localisation of RET at the cell membrane may be dependent upon whether it binds the membrane-bound or soluble form of GFRα1 **(Fig 1.7)**.

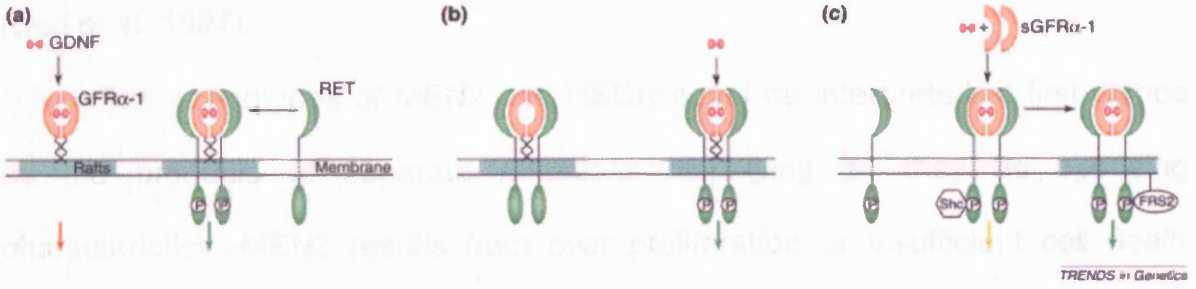

Figure 1.7: Possible mechanisms of RET activation.

(A) GPI-linked, lipid raft bound, GFRα1 dimers assemble with GDNF. RET is then recruited inducing dimerisation and autophosphorylation. (B) In an alternative view, RET and GFRα1 assemble as a pair of dimers at lipid rafts and bind GDNF secondarily which stabilises the complex. (C) The binding of soluble GFRα1 by GDNF which then binds and allows transactivation of RET outside of the lipid raft. Localisation of RET to the lipid raft is then induced by binding FRS2 (Fibroblast growth factor receptor substrate 2).
Taken from (Manie et al. 2001).

1.4.1.3 Conditions associated with defects in the RET pathway

RET has been linked to both the congenital defect Hirschsprung's disease (HSCR) and multiple endocrine neoplasia type 2 (MEN2). MEN2, is characterised by medullary thyroid carcinoma and is caused by activation of the RET receptor (Borrello et al. 1995).

RET linked HSCR accounts for over 50% of observed familial cases (Attie et al. 1995). RET mutations display incomplete penetrance, the figures for which are significantly higher for males (72%) than females (51%). RET mutations also contribute to greater than 33% of sporadic cases. RET mutations have also been

associated with the most severe forms of HSCR, total intestinal aganglionosis (Seri et al. 1997).

The phenotypes of MEN2 and HSCR could be interpreted at first glance as the products of separate mutations displaying as they do opposing characteristics. MEN2 results from over proliferation or insufficient cell death whereas HSCR is due to inadequate proliferation/survival or inappropriate cell death. However, cases of MEN2 have been reported to co-segregate with HSCR (Decker and Peacock 1998; Decker, Peacock, and Watson 1998).

1.4.1.4 RET pathway mutants

Mouse mutants of RET, GDNF and GFRα1 have been generated to further investigate the RET signalling pathway. Non-isoform specific RET knockouts display aganglionosis of the entire intestine accompanied by renal dysplasia (Schuchardt et al. 1994). The ENS of the oesophagus and stomach are only partially affected (Durbec et al. 1996b; Yan et al. 2004). It should be noted that only homozygous knockout mice develop this phenotype, unlike humans in which a single null mutation can be sufficient to result in HSCR. Also renal dysplasia is extremely rare in HSCR cases. More detailed investigation of RET signalling has involved the targeted knockout of the RET9 and RET51 isoforms thus generating mono-isoformic (mi) RET9 and RET51 mice (de Graaff et al. 2001). In these isoforms miRET9 has only RET9, whereas miRET51 has only RET51. RET43 was not included in this work due to its lower sequence conservation between species and the lack of proven protein expression. miRET9 mice display no obvious change from their wild-type counterparts'

enteric phenotype, suggesting no role for the RET51 isoform in ENS cell guidance or survival. The miRET51 mice display aganglionosis of the colon, a phenotype more HSCR-like than that observed in non-isoform specific knockouts of RET in mice, indicating that the RET9 isoform is required for normal ENS development (de Graaff et al. 2001). The miRET51 mouse model provides the most accurate model of HSCR available in mice.

GDNF deficient mice display intestinal aganglionosis and kidney agenesis (Moore et al. 1996; Pichel et al. 1996; Sanchez et al. 1996) similar to RET deficient mice, whereas mice lacking GFRα1 have aganglionosis of the small and large intestines (Enomoto et al. 1998; Cacalano et al. 1998). Both RET and GDNF null mice have defects in their dorsal root and sympathetic ganglia. GFRα1 null mice do not exhibit this phenotype (Tomac et al. 2000).

Gene knockdown studies in zebrafish have also contributed substantially to our understanding of the effects of absence of GFRα1 in the developing ENS (Shepherd et al. 2004). Zebrafish, unlike birds and mammals, possess two orthologs for GFRα1; GFRα1a and GFRα1b (Shepherd, Beattie, and Raible 2001). The expression of both these forms, and GFRα2, have been inhibited in zebrafish using morpholinos, (short sequences of RNA designed to bind to and inhibit specific mRNAs). Treatment with GFRα1a morpholinos resulted in a reduced number of enteric neurons particularly in the distal gut. Co-injection with the GFRα1b morpholino led to a total lack of enteric neurons. Embryos treated with GFRα1b or GFRα2 morpholinos alone displayed no enteric phenotype;

GFRα2 did not modify the affects of GFRα1a/b when co-injected, and is therefore not directly involved in this pathway. These studies highlight the essential requirement of GFRα1 for normal development of the enteric nervous system, with some degree of redundancy present between the GFRα1a and GFRα1b forms in zebrafish.

1.4.1.5 Downstream targets of RET

RET-ligand binding is likely to result in the two halves of the RET homodimer coming close enough to each other for trans-autophosphorylation to occur. Four of the eighteen tyrosine residues in RET51 become docking sites for proteins with specific interaction molecules (Liu et al. 1996). GDNF-dependent signalling induces activation of the phosphatidylinositol 3-kinase (PI3K) and the mitogen-activated protein kinase (MAPK) pathways. The MAPK pathway requires the activation of the extracellular-regulated kinases (ERKs), c-Jun amino-terminal protein kinases (JNKs), p38 MAPK and the big MAP Kinase (BMK1) ERK5 (Encinas et al. 2001; Hayashi et al. 2001; van Weering and Bos 1998; Jhiang 2000; Hansford and Mulligan 2000). RET can also activate Rho family GTPases including Rho, Rac and Cdc42 which alter the actin cytoskeleton involved in cell motility and neurite outgrowth (Murakami et al. 1999; Fukuda, Kiuchi, and Takahashi 2002). **(Fig 1.8)**

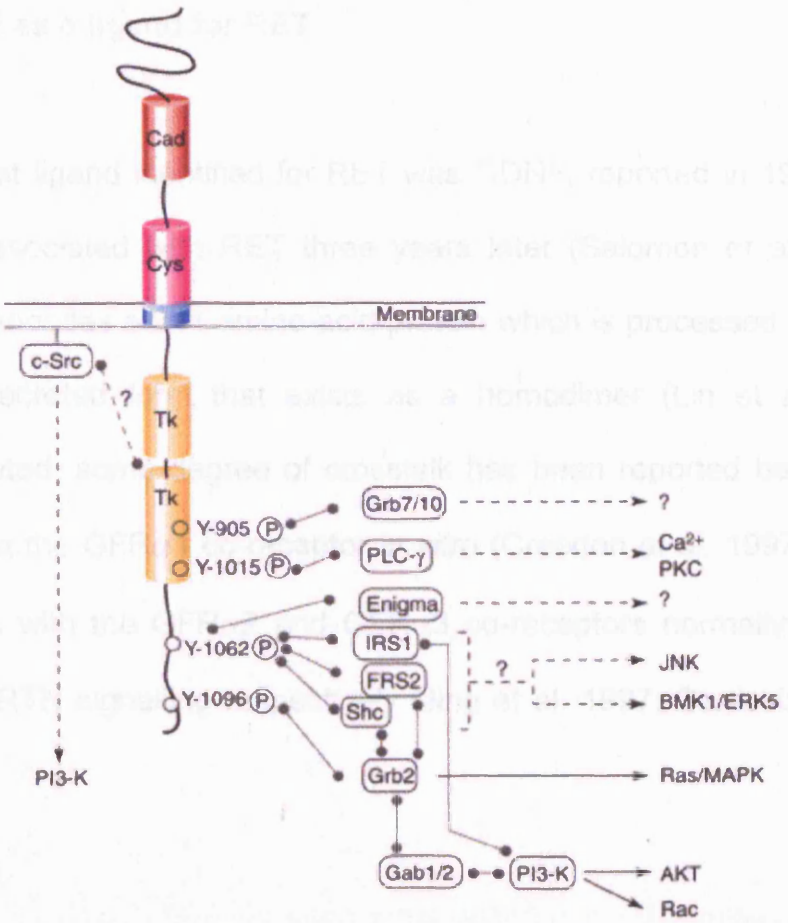

Figure 1.8: Downstream targets of RET.

Activation of RET results in autophosphorylation (P) of tyrosine residues in the cytoplasmic domain. This provides docking sites for signalling partners as shown by solid linkers. In addition to these c-Src is thought to interact directly through an unknown site.
Cad - cadherin domain, Cys – cystine rich domain, Tk – tyrosine kinase domain.
Y-(number indicating residue position) Y-1096 is only present in the RET51 isoform.

Taken from Manie et al (2001).

1.4.1.6 GDNF as a ligand for RET

The first ligand identified for RET was GDNF, reported in 1993 (Lin et al. 1993) and associated with RET three years later (Salomon et al. 1996). The GDNF gene encodes a 211 amino-acid protein which is processed to form a 134 amino-acid secreted form that exists as a homodimer (Lin et al. 1993). As previously stated, some degree of crosstalk has been reported between GDNF and NTRN via the GFRα1 co-receptor *in vitro* (Creedon et al. 1997), and can in turn crosstalk with the GFRα2 and GFRα3 co-receptors normally dedicated to NTRN and ARTN signalling respectively (Jing et al. 1997; Sanicola et al. 1997) **(Fig 1.9)**.

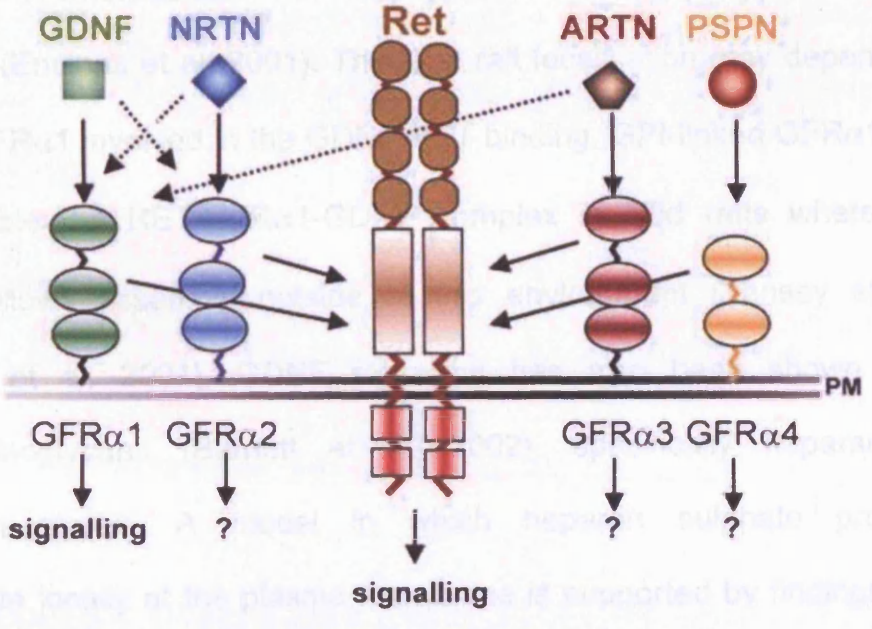

Figure 1.9: Interactions between RET/GDNF family ligands/GFRα co-receptors: Modified from Sariola and Saarma (2003).

GDNF was initially identified as a neurotrophic factor (Lin et al. 1993) but has since been linked to processes including cell proliferation, migration, survival and differentiation (Chalazonitis et al. 1998a; Hearn, Murphy, and Newgreen 1998; Heuckeroth et al. 1998; Taraviras et al. 1999; Worley et al. 2000; Young et al. 2001). Activation of PI3K appears to be essential for many responses to GDNF-mediated RET signalling. Both PI3K and MAPK are involved in migration and neurite outgrowth but the function of PI3K cannot be compensated for by MAPK (Natarajan et al. 2002). Cell proliferation depends upon PI3K activity as shown by the reduction in cell proliferation observed in cells cultured with PI3K inhibitor (Focke et al. 2001). Differentiation also seems dependent upon PI3K activity (Pong et al. 1998). The manner in which the PI3K or MAPK pathway is selected is unclear but it has been suggested that RET found in lipid rafts may favour MAPK whereas RET not associated with these rafts would activate other pathways (Encinas et al. 2001). This lipid raft localisation may depend upon the form of GFRα1 involved in the GDNF-RET binding. GPI-linked GFRα1 is thought to assemble the RET-GFRα1-GDNF complex in lipid rafts whereas soluble GFRα1 allows assembly outside of this environment (Tansey et al. 2000; Paratcha et al. 2001). GDNF signalling has also been shown to require glycosaminoglycans (Barnett et al. 2002), specifically heparan sulphate glycosaminoglycan. A model in which heparan sulphate proteoglycans concentrate locally at the plasma membrane is supported by findings that show GDNF activates RET even in cells depleted of surface heparin sulphates, if GDNF is found in high enough concentrations (Barnett et al. 2002).

1.4.1.7 GFRα1 is a co-receptor for GDNF

The GFRα1 gene is located at position 10q26 (Eng et al. 1998; Gorodinsky et al. 1997) in humans and a region of chromosome19 in mouse with high homology to human 10q24-26 (Puliti et al. 1997). The human gene contains 9 exons (Eng et al. 1998) which undergo alternative splicing (Shefelbine et al. 1998) to form both the GPI-linked and soluble forms. GPI-linked GFRα1 is recruited to the plasma membrane by TGF-β. In the absence of TGF-β, GDNF signalling is only viable if soluble GFRα1 is available (Peterziel, Unsicker, and Krieglstein 2002). As mentioned above, GFRα1 is a high affinity co-receptor for GDNF although it may also bind other GDNF family ligands (Sanicola et al. 1997). In addition to acting as the high affinity co-receptor for GDNF in RET dependent signalling (Airaksinen and Saarma 2002), GFRα1 binds GDNF in signalling which is independent of RET (Popsueva et al. 2003; Pezeshki, Franke, and Engele 2001).

1.4.1.8 RET expression in the ENS

RET expression is first detected in the mouse at E8.5 in the undifferentiated neuroepithelium of the neural tube (Pachnis, Mankoo, and Costantini 1993). The cells positive for RET at this time appear to be neural crest cells emigrating from rhombomere four. No other emerging neural crest cell populations express RET at this stage. The first RET expression observed in

enteric precursors appears at E9.0-9.5 in the mesenchyme of the third and fourth branchial arches through which the neural crest are known to migrate. Twelve hours later, RET-positive streams of cells migrate from these areas towards the foregut. At subsequent time points the RET-positive cells are migrating further down the gut until at E14.5 the entire myenteric plexus has been colonised (Kapur, Yost, and Palmiter 1992; Young et al. 1998). Although no secondary marker was used in these experiments, results would appear to be consistent with RET marking the majority of migrating and postmigratory cells of the ENS in the mouse.

The earliest reports of positive RET expression in the chick were at HH5 in the primitive streak and Henson's node (Robertson and Mason 1995). At HH10 the region of the neural tube from the level of somite seven up to the boundary of rhombomeres five and six was positive for RET expression (Robertson and Mason 1995). This presented as a gradient strongest at the rostral end. Stage 18 embryos were reported to express RET in pharyngeal arches one to four, the region surrounding the otic vesicle and in the region of the developing sacral crest. E3.5 embryos retained expression in the structures seen at stage 18 and RET positive cells were also found in the developing foregut (Homma et al. 2000; Schiltz, Benjamin, and Epstein 1999).

At E4.5 RET-positive cells had migrated down the gut to the level of the yolk stalk and RET-positive cells were present in the caudal nerve of Remak (Schiltz, Benjamin, and Epstein 1999). RET-positive cells had colonised the gut to the level of the caecum at E5.5 in which high levels of RET were observed.

Between E6 and E7 vagal-derived NCC migrated into the colon, as did projections from the nerve of Remak which was well formed at E8. At this time, clusters of RET positive cells were present along the entire length of the gut connected by faintly stained protrusions.

In the experiments of Shiltz et al, a secondary marker, HNK-1, was employed to assess RET expression through immunohistochemistry with respect to the entire migrating neural crest population (Schiltz, Benjamin, and Epstein 1999). This approach revealed that not all neural crest cells were RET positive. Initially a low percentage of HNK-1 positive cells were also positive for RET but this number increased with the age of the embryo. In order to confirm this low level of RET protein, in situ hybridisation was used to assess mRNA levels. This revealed that some HNK-1 positive cells express neither the RET protein or mRNA. Most significantly of all, the cells at the wavefront of colonisation did not appear to express RET, in contrast to the expected result in which RET would be present at the wavefront to respond to the chemo-attractive effect of GDNF, which is expressed in the gut mesenchyme (Natarajan et al. 2002). Data from our laboratory relating to both the vagal and sacral populations of migrating crest has also revealed an absence of RET from the wavefront cells (Delalande, Cooper, and Burns 2003).

1.4.2 Endothelin-3 Pathway

1.4.2.1 Endothelin-3

Endothelin-3 (ET-3) is a member of the endothelin group of vasoactive peptides that consists of three members; Endothelin 1, 2 and 3. Endothelin 1 was cloned by Inoue et al in 1989 and the sequences for two related peptides, ET-2 and ET-3, were isolated from genomic fragments (Inoue et al. 1989). ET-3 expression was later documented in the hypothalamus (Bloch et al. 1989). ET-3 encodes a 230 amino-acid peptide precursor that includes ET-3 and a 15 amino-acid precursor called the ET-3-like sequence. The ET-3 sequence is located at position 20q13.2-q13.3 and a homologue maps to chromosome 2 in mouse (Bloch et al. 1989; Malas, Peters, and Abbott 1994; Arinami et al. 1991; Malas, Peters, and Abbott 1994; Arinami et al. 1991) Once cleaved to the functional form by Endothelin converting enzyme 1 (ECE-1) (see below), ET-3 acts as a soluble ligand for Endothelin Receptor B (EDNRB).

1.4.2.2 ECE-1

ECE-1 is responsible for the proteolytic cleavage of endothelins from their big endothelin form to the biologically active peptide (Schmidt et al. 1994). Located at position 1p36.1 (Matsuoka et al. 1996; Albertin et al. 1996) the ECE-1 gene encodes a predicted 770 base open reading frame which undergoes alternative splicing to form two variants (Shimada et al. 1995; Yorimitsu et al. 1995). ECE-linked HSCR cases have been reported (Hofstra et al. 1999) but are extremely rare.

1.4.2.3 Endothelin receptor B

There are two forms of endothelin receptors, selective (EDNRA – specific to ET1) and non-selective (EDNRB) (Takayanagi et al. 1991). EDNRB encodes a 442 amino-acid transmembrane receptor peptide which exhibits strong homology to rat sequences (Nakamuta et al. 1991). In addition to these two forms, a splice variant of EDNRB named ETB-SVR, identical to EDNRB except at the C-terminal domain, has been shown to be expressed as mRNA in the lungs, kidney and skeletal tissue (Elshourbagy et al. 1996).

1.4.2.4 Endothelin pathway diseases and Mutants

ET-3 homozygous null mouse mutants display Waardenburg-Hirschsprung like symptoms, with enteric and pigmental defects (Baynash et al. 1994; Kunieda et al. 1996; Gariepy, Cass, and Yanagisawa 1996). ET-$3^{-/-}$ animals die within a few weeks of birth. These observations in mice were supported by demonstrating a homozygous substitution/deletion of ET-3 in one Waardenburg-Shah patient (Edery et al. 1996) and a mis-sense mutation observed in a second patient around the same time (Hofstra et al. 1996). The affected region of gut in ET-3 knockout mice lies between the terminal hindgut and the caecum. It has been shown that ET-3 inhibits the differentiation of NCCs into neurons through interactions with its receptor EDNRB *in vitro* (Wu et al. 1999). This process may act to balance the effects of GDNF-induced differentiation and proliferation.

Additionally, in lethal spotted mice (*ls/ls*), a spontaneously occurring null mutation in ET-3, an abnormal arrangement of the extracellular matrix is seen in the caecal region, the caudal limit to successful vagal neural crest cell colonisation in these animals. In addition the enteric smooth muscle of *ls/ls* mice displays a developmental delay (Rothman, Goldowitz, and Gershon 1993). One effect of this delay is an accumulation of laminin-1 by the cells destined to become smooth muscle (Rothman et al. 1996). Vagal neural crest cells express a laminin-1 receptor upon entering the foregut. Laminin-1 promotes the differentiation of neural crest cells into a neuronal phenotype, thus in combination with the increased differentiation already occurring due to the lack of ET-3, the pool of neural crest cells is insufficient to allow complete gut colonisation. Neural crest cells competent for ET-3 are incapable of migrating through explants of *ls/ls* terminal gut grown in culture, and *ls/ls* neural crest cells successfully pass through corresponding wildtype hindgut, indicating that the mesenchyme environment is the cause of the failure in colonisation (Rothman, Goldowitz, and Gershon 1993). Additionally ectopic pelvic ganglia are present in *ls/ls* mice suggesting that the sacral crest fails to reach the hindgut due to premature differentiation during migration.

EDNRB mouse mutants exist in the form of the spontaneously occurring piebald lethal mutant ($Ednrb^{sl}$) and the engineered knockout $Ednrb^{tm1Ywa}$ (Hosoda et al. 1994). The $Ednrb^{sl}$ mouse results from a 1cM deletion about the EDNRB locus (Roix et al. 2001) whereas the $Ednrb^{tm1Ywa}$ strain was specifically engineered via replacement of a 4.2kb exon 3 containing fragment with a neomycin selective cassette. Both these strains have aganglionosis; however the

phenotype exhibited by the generated knockout when crossed with the $Sox10^{Dom}$ is more severe than that of the naturally occurring mutation under the same conditions (Cantrell et al. 2004). This may indicate that the genetic background of the piebald lethal strain has undergone some selection for aganglionosis suppression.

EDNRB is normally expressed in enteric ganglia and the surrounding mesenchyme of the gut (Wu et al. 1999). This expression can be disrupted by failures in the Sox10/Pax3 transcription factors. For example, in *splotch* mice ($Pax3^{-/-}$) there is an absence of EDNRB expression in the enteric ganglia although it is retained by the mesenchyme (Lang et al. 2000a).

1.4.3 *Sox genes*

1.4.3.1 Sox genes

Sox genes were discovered in the early 1990s as a family of genes related to the testis determining factor gene Sry found in mammals (Gubbay et al. 1990). Since then homology based screening has added many more members to this group (Denny et al. 1992; Wright, Snopek, and Koopman 1993; Cremazy et al. 1998), with twenty Sox genes having been identified in mouse and human (Schepers, Teasdale, and Koopman 2002). From these twenty genes, eight groups can be discerned based upon intron-exon structure and sequence. Sox genes contain the HMG (high mobility group) domain, alongside the TCF, MATA and HMG/UBF families (Laudet, Stehelin, and Clevers 1993; Soullier et al. 1999), which comprises a 79 amino-acid DNA binding domain (Gubbay et al. 1990). All HMG domain sequences appear highly conserved and are capable of binding the sequence AACAA(A/T)G (Wegner 1999).

1.4.3.2 Sox10

Sox10 is a member of the Sox family of transcription factors (group E) that has been linked to the neurocristopathy Waardenburg syndrome (Bondurand et al. 1999) and Waardenburg-HSCR (Pingault et al. 1998). Its sequence is highly conserved between human and mouse (Pusch et al. 1998) and encodes a 466 amino-acid peptide. The human gene has been mapped to position 22q12-q13 (Pingault et al. 1997). Sequence analysis indicates a common evolutionary origin

between Sox10 and Sox9, another member of the Sox family also involved in regulation of neural crest development (Cheung and Briscoe 2003).

Sox10 is expressed in neural crest cells but is subsequently down-regulated in all non-glial progeny (Kim et al. 2003; Paratore et al. 2002; Paratore et al. 2001). Both the gliogenic and neurogenic potential of neural crest cells are maintained by Sox10. Furthermore, forced expression of Sox10 inhibits neuronal differentiation (McKeown et al. 2005). In the absence of functional Sox10 neural crest derived-structures are present and initial neural crest formation appears normal (Southard-Smith, Kos, and Pavan 1998; Herbarth et al. 1998; Britsch et al. 2001). It can thus be deduced that Sox10 is not required for the initial specification of a neural crest fate, nor in the initial migration of these cells. The cells which would normally express Sox10 undergo apoptosis prior to maturing in $Sox10^{-/-}$ embryos (Southard-Smith, Kos, and Pavan 1998; Paratore et al. 2002; Kapur 1999).

1.4.3.3 SOX10 mutant models

The dominant megacolon (Dom) mouse model of HSCR arose spontaneously at the Jackson Laboratory (Lane and Liu 1984). Heterozygotes exhibit white pigment spotting and deficiencies in the number of myenteric ganglia at the level of the colon; homozygous mice die within two weeks of gestation. Sox10 was identified as the gene underlying the Dom (HSCR) mutation by positional cloning (Southard-Smith, Kos, and Pavan 1998). It was demonstrated that in these mice there is disrupted expression of both Sox10 and

EDNRB and a loss of neural crest derivatives via apoptosis (Southard-Smith, Kos, and Pavan 1998). This body of work, and that of others (Herbarth et al. 1998), shows that Sox10 is essential for peripheral nervous system development.

More recently a LacZ knock-in of Sox10 was engineered into mice (Britsch et al. 2001). These animals show similar deficiencies to the Dom mice. However, the LacZ mice are null mutants, unlike the Dom mutation, which may possess dominant properties (Potterf et al. 2000).

1.4.3.4 SOX8 acts as a modifier of SOX10 induced enteric defects.

Sox8 is another member of the Sox family of transcription factors (group E) that is associated with HSCR. Located at position 16p13.3 it encodes a 446 amino acid sequence with 47% homology to Sox9 and Sox10.

$Sox8^{-/-}$ mice develop normally in utero, are viable and born at Mendelian ratios (Sock et al. 2001). These mice do, however, display a significant reduction in weight that may arise from metabolic deficiencies. The functional redundancies of group E Sox proteins (Sox9, Sox10) may explain the mild phenotype seen in these knockout mice. Despite the knockout of Sox8 having no effect on the enteric nervous system, Sox8 has been shown to act as a modifier of Sox10-induced HSCR. As described above, mice homozygous null for Sox10 die before or at birth but heterozygotes are born at Mendelian ratios with 20% displaying HSCR-like aganglionosis. Using LacZ knock-ins of both the Sox8 and Sox10 genes, it was shown that Sox8 increases the severity of the Sox10 phenotype

resulting in increased mortality of $Sox8^{lacZ/lacZ}Sox10^{+/LacZ}$ and $Sox8^{+/lacZ}Sox10^{+/LacZ}$ mice prior to birth (Maka, Stolt, and Wegner 2005). Additionally, the loss of even one copy of Sox8 dramatically increases the $Sox10^{+/LacZ}$ ENS phenotype. In these mice the aganglionic region extended rostral of the caecum for varying lengths into the small intestine.

1.4.3.5 SOX10 as a modulator of RET

Sox10 displays a weak, but reproducible, activity as a transcriptional activator in humans (Kuhlbrodt et al. 1998b; Kuhlbrodt et al. 1998a). The C-terminus contains a transactivation domain, and the N-terminus contains the synergistic enhancer of other transcription factors. Sox10 acts synergistically with Pax3 to modulate the expression of target genes (Lang et al. 2000b). Pax3 is a member of the paired-box-containing transcription factors (Goulding et al. 1991), and mutations in Pax3 may result in WS but without HSCR (Tassabehji et al. 1992). However, mice with mutant Pax3 (*Splotch*) (Epstein et al. 1993) possess defects in their enteric ganglia (Lang et al. 2000a). Pax3-WS patients are heterozygous for the mutations as homozygous loss is lethal (Ayme and Philip 1995).

Ret is one of the targets of the Sox10-Pax3 synergistic activation (Lang et al. 2000b). $Splotch^{-/-}$ embryos display reduced RET expression which would, as previously discussed, account for reduced enteric ganglia cell numbers. To test the ability of Pax3 and Sox10 to activate Ret, P19 cells were transfected with Pax3, Sox10 or both genes to assess the relative transcription of Ret in these

lines (Lang et al. 2000b). Sox10 alone does not result in a significant increase in RET levels. However, Pax3 or co-transfected Sox10 and Pax3 do result in significant increases. By using deletion constructs of the Ret enhancer region, a 45bp sequence required for the synergistic activation by Pax3-Sox10 was located which contains both transcription factor binding sequences. The interaction between these two transcription factors is a physical one. Immunoprecipitation using an antibody for Sox10 was also able to precipitate Pax3 but only if Sox10 was present in the reaction (Lang and Epstein 2003). Deletion mutants showed that the paired domain of Pax3 and the HMG domain of Sox10 are required for the physical interaction of these two proteins.

1.4.3.6 SOX10 regulates EDNRB expression

As previously mentioned, mice and humans with mutations of the EDNRB gene develop aganglionosis of the hindgut distal to the caecum (Hosoda et al. 1994; Puffenberger et al. 1994). Recent work extensively reviewed the effects of strain background on the $SOX10^{Dom}$ mutant mouse (Cantrell et al. 2004). The authors showed that the $SOX10^{Dom}$ mutant phenotype differs in penetrance and severity between the $B6.Sox10^{Dom}$ and $C3Fe.Sox10^{Dom}$ strains. Using polymorphic simple tandem repeats it was shown that B6 EDNRB haplotypes correlate with an increased severity and penetrance of aganglionosis though not of hypoganglionosis. Addressing the issue of gender, male heterozygotes were found to exhibit closer statistical means to the B6 homozgotes whilst female heterozygotes displayed statistical means closer to the C3Fe homozygotes, indicating a more severe phenotype in male heterozygotes compared to females.

In this work two strains of EDNRB deficient mice were used. The naturally occurring and established Ednrb^{sl} strain which results from a 1cM deletion about the EDNRB locus (Roix et al. 2001), and the generated knockout Ednrb^{tm1Ywa} (Hosoda et al. 1994). Interestingly it was found that the Ednrb^{tm1Ywa} strain resulted in a more severe phenotype than that seen in Ednrb^{sl}. This may be due to aganglionosis suppressing mutations having been bred into the Ednrb^{sl} strain.

Deletion studies of the region upstream of the EDNRB gene identified a 1kb enhancer region, between –1.2kb and –250bp of the start codon, specific to ENS phenotypes (Zhu et al. 2004). Binding sites for the transcription factor SOX10 were identified within this region and mutational studies of these sites indicate that SOX10 interacts directly with the EDNRB enhancer.

1.4.4 Mash-1

Mammalian acheate-scute homologue 1 (Mash-1) is a basic helix-loop-helix transcription factor, the human version of which (ASCL1) is located at position 12q22-q23 (Renault et al. 1995) and is predicted to encode a 238 amino acid protein (Ball et al. 1993). Mice homozygous for the null Mash-1 allele die at birth due to defects in respiration and feeding. Post-mortems revealed that the olfactory epithelium and sympathetic, parasympathetic and a portion of the enteric nervous systems were affected (Guillemot et al. 1993). The enteric nervous system of the oesophagus was most severely affected in Mash$^{-/-}$ mice (Sang et al. 1999). Inspection of the subclasses of enteric neurons revealed that

transiently catecholaminergic (TC) precursors, which give rise to the entire enteric population of serotonergic neurons, were absent.

1.4.5 Phox2B

Paired-like homeobox 2b (Phox2b), a protein of 314 amino acids (Yokoyama et al. 1996) located at position 4p12 (Amiel et al. 2003), is expressed in all ganglia of the autonomic nervous system including the ENS (Pattyn et al. 1997). Phox2B$^{-/-}$ mice generated by homologous recombination fail to correctly develop autonomic ganglia. Although Phox2B mutations are most commonly linked to congenital central hypoventilation syndrome (CCHS) it has also been associated with HSCR cases displaying a low level of penetrance (Benailly et al. 2003).

Phox2 genes are known to regulate the expression of Ret in the sympathetic and enteric nervous systems in mice, and are also necessary for the maintenance of Mash-1 expression. It is possible that Phox2B acts as a modifier determining the penetrance of other HSCR associated mutations in genes such as RET, either as a result of point mutations effecting protein function or through haplo-insufficiency. Haplo-insufficiency of Phox2B could result in reduced expression of RET predisposing towards HSCR.

1.4.6 SMADIP1

SMAD-interacting protein 1 (SMADIP1), also known as SIP1 or Zinc finger Homeobox 1B (ZFHX1B), is a member of the delta-EF1/Zfh1 family zinc finger homeodomain proteins found at position 2q22 (Wakamatsu et al. 2001). SMADIP1 interacts with activated full length receptor-mediated SMADs to co-repress expression of TGF-beta-controlled genes.

SMADIP1 has been linked to cases of HSCR (short segment) associated with microcephaly, mental retardation, hypertelorism, submucous cleft palate, and short stature. Amiel et al (Amiel et al. 2001) found that 8 out of 19 patients suffering HSCR and mental retardation possessed SMADIP1 deletions or truncations. These mutations, in addition to the frameshift, and nonsense mutations described (Wakamatsu et al. 2001; Yamada et al. 2001; Cacheux et al. 2001), suggest that the defects result from a haplo-insufficiency of the SMADIP1 gene. Mice generated with a Zfhx1b mutation comparable to that found in human patients revealed that SMADIP1 knockouts do not develop postotic vagal neural crest cells (Van de Putte et al. 2003). Thus SMADIP1 is essential for the formation of vagal neural crest cell populations.

1.4.7 BMP and Noggin

Bone morphogenetic proteins (BMPs) are a sub-group of secreted signalling molecules of the TGF-β family. Activation of BMP receptors results in SMAD phosphorylation and activation of the subsequent signalling cascade

(Zwijsen, Verschueren, and Huylebroeck 2003). They have already been shown to be involved in neural crest cell migration (Sela-Donenfeld and Kalcheim 2000; Sela-Donenfeld and Kalcheim 1999) and regulation of regionalisation of the gut (Faure et al. 2002; Smith et al. 2000). Their role in the control of development of enteric precursors is currently unclear.

BMP-2 and BMP-4 promote the differentiation of enteric precursors into TrkC-expressing Neurotrophin-3-dependent neurons (Chalazonitis et al. 2004). Overexpression of these signalling molecules effectively reduces proliferation within migrating precursor populations. When Noggin, a BMP antagonist, was expressed in the developing ENS using transgenic mice, the total number of neurons was increased but at the expense of the TrkC subset (Chalazonitis et al. 2004).

Conflicting data have arisen in another recent investigation into the expression of BMPs in the developing chick ENS (Goldstein et al. 2005). This study revealed that suppressing the phosphorylation of SMAD by BMPs, though expression of Noggin, resulted in a delay in the migration of enteric precursors. Furthermore enteric ganglia were reported as being reduced in size and the hindgut of experimental animals was hypoganglionic. The migration of these cells was delayed, but not subsequent events such as differentiation. This delay was not accompanied by apoptosis of the migrating precursors. To test the role of BMPs in ENS precursor migration collagen gel explants were performed. These revealed that BMP4 alone is insufficient to promote ENS migration, but can

modulate the effects of GDNF. Noggin significantly inhibited the distance migrated by neural crest cells in these experiments.

1.4.8 NT-3 and TrkC

Neurotrophin-3 (NT-3) was identified as an extension to the NGF, BDNF family of neurotrophins through low stringency PCR (Jones and Reichardt 1990) and is located at position 12p13 (Maisonpierre et al. 1991). It has been shown that NT-3 induces neural crest-derived cells to differentiate into neurons (Chalazonitis et al. 1994), specifically those expressing NADPH-diaphorase activity (Chalazonitis et al. 1998c) operating through the Trk-C receptor.

NT-3-deficient mice display severe defects in limb movement and die shortly after birth (Ernfors et al. 1994). These defects result from substantial loss of the sensory peripheral nervous system, although motor neurons were not affected. It has also been shown that disruption of the NT-3 gene results in cardiac defects consistent with failure of cardiac neural crest to migrate successfully (Donovan et al. 1996). Recent data reveals that $NT3^{-/-}$ mice exhibit a delay in the enteric innervation of the oesophagus by two days during development (Reddy and Kablar 2004).

1.5 Multiple pathways interact to successfully form a functional enteric nervous system

The above pathways and most likely a significant number not yet reported, interact and contribute to the formation of a functional enteric nervous system. Complex interactions balancing cellular migration, differentiation and proliferation result in neural crest cells migrating successfully from the vagal and sacral regions to the appropriate areas of gut mesenchyme. A general overview of the principal players in ENS formation is shown **(Fig 1.10)**.

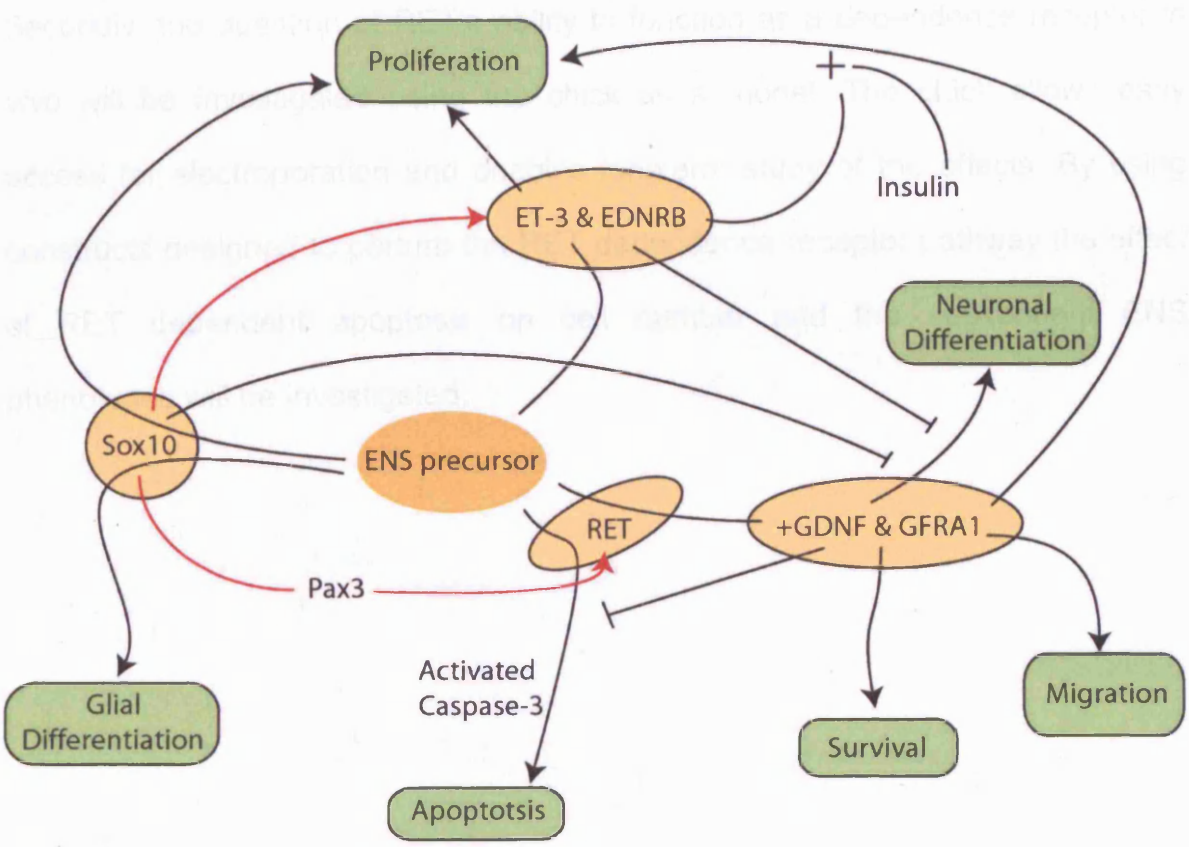

Figure 1.10:

Complex interactions between multiple pathways control enteric precursor fate. Black linkers indicate fates as dictated by expression and interaction of proteins. Red arrows indicate modification of gene expression by transcription factors.

1.6 Aims

The aims of this thesis are twofold and address distinct questions surrounding ENS formation. Whilst the spatiotemporal pattern of colonisation and migration of ENS precursors, enteric smooth muscle and intersticial cells of Cajal are well documented in model organisms there is a paucity of information concerning early development in Humans. Using immunohistochemistry to label these three cell types the aim is to fully describe the development of a normal functional bowel between weeks 4 and 14 of embryonic development.

Secondly, the question of RET's ability to function as a dependence receptor *in vivo* will be investigated using the chick as a model. The chick allows easy access for electroporation and enables longterm study of the effects. By using constructs designed to perturb the RET dependence receptor pathway the effect of RET dependent apoptosis on cell number and the subsequent ENS phenotypes will be investigated.

Chapter 2: Materials and Methods

Details of solutions may be found on page 78.

2.1 Human embryonic and foetal material

Tissue for this research was obtained from two sources, the Human Developmental Biology Resource (HDBR), located at the Institute of Child Health, University College London, and funded by the Medical Research Council (MRC) and Wellcome Trust, with additional material from the Human Tissue Bank at Hammersmith Hospital, London, funded by the MRC. The HDBR provided all samples from weeks 4-12, with older samples up to week 14 provided by the source at Hammersmith hospital. Embryos were collected via surgical or medical termination of pregnancy (STOP/MTOP) and immediately transferred to the lab in ice cold DMEM. Staging was carried out according to the Carnegie system. In embryos below seven weeks of gestational age, practical dissection of the gut was not possible, so these samples were processed as whole embryos. Embryos of week seven and older had their gastrointestinal tracts dissected free, and pinned out in a Sylgard-coated petri-dish prior to fixation. Embryos recovered during the time course of this investigation were fixed in 4% PFA in PBS; in those which had been retrieved from archives 4% PFA fixation had been followed by 70% ethanol storage. Post fixation, tissue was prepared for wax embedding or cryosectioning. For wax embedding samples were first dehydrated using an alcohol series of increasing concentration, 70%, 95%, 100%, 100% (1x5mins), then cleared in histoclear (2x10mins). Samples were left in wax at 56°C overnight then embedded. For cryosectioning tissue was cryoprotected in 15% sucrose in PBS overnight then transferred into gelatin 7.5%, sucrose 15% in PBS. Tissue

was orientated during gelatin cooling in blocks and snap-frozen in liquid nitrogen-cooled isopentane at –60°C. Samples were stored at –20°C.

2.2 Sectioning

Transverse sections were cut from whole embryos and dissected gut segments. Sections were obtained at a thickness of 6μm from wax blocks and 10-14μm from frozen blocks. All sections were placed on Superfrost Plus microscope slides. Adjacent sections were prepared for double label immunohistochemical staining protocols.

2.3 Immunohistochemistry

Slides were initially treated to remove supporting media. Wax sections were placed in Histoclear (3x5mins) then rehydrated through a descending series of alcohol (1x5min each) to PBS. Frozen sections were incubated for 30 minutes in PBS warmed to 37°C to remove the cryoprotectant. Primary antibodies (Table 2.1) were applied overnight at 4°C in a humid box. Slides were then washed in PBS (3x5mins) and treated with appropriate secondary antibodies (Table 2.2) for one hour at room temperature. Following further washing in PBS (3x5mins) labelled slides were visualized either with the fluorescent marker Alexa 488 (Molecular Probes Inc), or Cy3 (Amersham Pharmacia Biotech), or with the reaction product diaminobenzidine (DAB) (Sigma) as shown in Table 2.3.

Following DAB staining, sections were dehydrated through an ascending series of alcohols (1x5min each), cleared in Histoclear (2x5mins) and mounted in DPX (Fisher Scientific). Fluorescent-labelled sections were mounted in Fluoromount-G (Southern Biotech).

Table 2.1: Primary antibodies used, source, species and dilution.

Primary Antibody	Species	Dilution	Source
$P75^{NTR}$	Rabbit	1:250	Promega
c-kit	Rabbit	1:100	DAKO
α-Smooth muscle actin	Mouse	1:200	DAKO
PGP9.5	Mouse	1:100	Affiniti
QCPN Supernatant	Mouse	1:3	U' of Michigan

Table 2.2: Secondary antibodies used, source, species and dilution.

Secondary Antibody	Dilution	Source
Goat anti-rabbit IgG biotinylated	1:100	Southern Biotech
Rabbit anti-mouse IgG biotinylated	1:100	Southern Biotech

Table 2.3: Visualisation agents used, source, and dilution.

Visualisation	Dilution	Exposure Time	Source
DAB	1:50	10-15 minutes	Sigma
Streptavidin Cy3	1:400	30 minutes	Amersham
Streptavidin Alexa 488	1:200	30 minutes	Molecular Probes
Streptavidin-HRP	1:100	1hour	Southern Biotech

Images were captured on a Zeiss Axiophot microscope equipped with a Hamamatsu C4742-95, or Leica DC-500 digital camera, using openlab (v3.11) and Firecam (v1.20) software respectively. Figures were assembled and annotated in Adobe Photoshop.

Controls were performed for each experiment consisting of known positive control tissue and a negative control with no primary antibody applied.

2.4 Constructs

The constructs used in this work were produced and kindly provided by Servane Tauszig and Patrick Mehlen of the University of Lyon.

Table 2.4: Plasmids used in Chapter 4.

Construct	Plasmid	Promoter
PcDNA3	PcDNA3	None
RET9-ICD707N	pJ7Ω	CMV
RET9-ICwt	pJ7Ω	CMV
Caspase-9DN	PcDNA3	CMV

2.5 *DNA Preparation*

Bacterial Transformation:

Competent cells (50µl of DH5α) were thawed on ice for 10-15mins before adding 1µl of the desired plasmid and leaving on ice for a further 30 mins. Cells were subjected to a heatshock for 45 seconds in a water bath set to 42°C. Immediately after the heatshock 950µl of SOC media was added and the cells were placed in a shaker at 37°C for 1 hour. Ampicillin was added to pre-prepared bacterial plates (10cm diameter): 40µl Amp50 + 160µl water per plate. Transfected bacteria were added to plates using aseptic conditions and placed in an oven at 37°C overnight to grow.

Plasmid preparation: Using Qiagen Midiprep kit. (Details of solutions on page 77)

A single colony picked from a recently transformed plate, or scrape from glycerol stock solution, was placed in 200ml LB broth with 200µl Amp50 at 37°C overnight in a shaker/incubator. The resulting cells were cold centrifuged in 50ml falcon tubes for 15mins at 6000xg.The supernatant was removed and the pellet resuspended in 4ml of buffer P1 (to which RNase A has been added) by vortexing and/or pipetting up and down until no cell clumps remained. To this 4ml of buffer P2 was added and mixed thoroughly but not violently and incubated at room temperature for 5 mins maximum. 4ml of P3 buffer was then added and again mixed thoroughly but not violently and incubated on ice for 15 mins.

The mixture was centrifuged for 30mins at >20000 x g at 4°C, the supernatant was removed and respun for 15 mins under the same conditions. During this time a Qiagen-tip was equilibrated with 4ml of Buffer QBT. The supernatant was removed and added to the equilibrated Qiagen-tip, this passed into the resin by gravity flow. Washes of the tip with 2x10ml of Buffer QC followed, and then the DNA was eluted with 5ml of Buffer QF, collecting the elute in a 10ml tube.

DNA was precipitated by adding 3ml of isopropanol, mixing and centrifuging at 15000 x g for 30 mins at 4°C. The supernatant was removed and the DNA washed in 70% ethanol (200µl/tube), and spun for a further 15mins. After removing the ethanol the pellet was left to air-dry for 5 mins, the DNA was resuspended in 50µl H_2O and left on ice for 15 mins. Samples were then run through a spectrophotometer to determine concentration and purity.

2.6 Microsurgical Procedures

Neural Tube ablations:

Chick eggs were obtained from Henry Stewart & Co. Ltd and incubated in a humid forced-air incubator at 38°C. After positioning the egg on its side, 3ml of albumin was removed from the tapered end by syringe and discarded. A window was then cut into the top of the egg to allow access to the embryonic disc. A solution of equal parts Indian ink (Pelikan, Fount Indian No.17) and PBS was injected under the embryo by mouth pipette to aid in visualisation. A flame-drawn Pasteur pipette forming a slender tip was used to inject the ink/PBS.

Ablations of portions of the neural tube were performed on chick embryos at HH stage 10, prior to neural crest cell migration. All microsurgical procedures were performed with hand-crafted needles. A standard sewing needle was crudely ground down by bench grinder and then shaped on differing grain Arkansas stones until a very fine cutting tip was obtained.

To gain access to the embryo an initial cut of the vitreous membrane was made. A small drop of PBS was added to decrease interference by surface tension. The first cuts to the embryo were made laterally through the neural tube between the seventh and eighth somites and just rostral to somite one. Next the longitudinal cuts were made between these two points, cutting between the neural tube and the somites.

Once these four cuts had been made the neural tube from this area was removed. This requires further dissection to ensure the ventral midline has been properly separated from the remaining embryo. The neural tube was then removed by mouth pipette. The window of the egg was then sealed with clear adhesive tape and the egg was placed back in an incubator at 38°C.

2.7 Quail to chick neural tube grafts

The quail to chick interspecies graft is an extension of the ablation protocol. Essentially a chick host which has undergone neural tube ablation receives a corresponding region of neural tube from a quail donor (isotopic graft).

At HH stage 10 the chick and quail embryos are perfectly size matched for this procedure. The neural tube of the quail does not require trimming in width to fit the gap left in the chick host, and if the ablation is of a high enough quality will seat itself snugly in place.

To obtain donor quail neural tubes, quail eggs at stage HH10 were removed from their shell and placed into a dish containing PBS at a depth to cover the yolk. The embryonic disc was dissected from the yolk using fine dissecting scissors and placed in a Sylgard-coated shallow dish filled with PBS. The embryo was pinned out and the region of neural tube adjacent to somites 1-7 was crudely dissected free using fine scissors. The neural tube and attached somites was then transferred to another dish containing 2% pancreatin (Sigma) in PBS. After a period of approximately 10-15 mins the somites were dissected away from the neural tube. Fine mounted needles and a small gauge pipette were used to help gently remove the somites. Using a mouth pipette the neural tube was sucked up and down, the action of which removes the somites from the neural tube completely. The prepared neural tube was finally transferred to a third dish containing DMEM+10%FCS and placed on ice until ready for transplantation.

After transferring the quail neural tube to the area above the ablation by mouth pipette a dissecting scalpel was used to fine trim the length of the transplant tissue if required. The tissue was teased into place using any mark left to identify dorsal-ventral and anterior-posterior orientation. The egg was sealed with clear adhesive tape and returned gently to the incubator at 38°C.

2.8 Gene Electroporation

Electroporations were performed with a BTX ECM 830 square wave porator (Genetronics Inc), PM1000 cell micro-injector (Microdata Instruments Inc) and 5mm gold electrodes (Harvard apparatus Inc). Electrodes and injection needle were mounted in micromanipulators (Narishige) and embryos were visualized through a Zeiss Stemi SV11 stereomicroscope.

Electroporation settings for experiments involving one or both sides of the neural tube were; 20V, 5 pulses, 50ms pulse, and 950ms pulse interval with the electrodes approximately 5-7mm apart and injection pressure of 10psi. Injections were visualized using fast green at concentrations around 2.5%. Plasmids were mixed 50:50 (GFP: test construct). All DNA concentrations were at approximately 2µg/µl prior to mixing.

Electroporations were carried out on chick embryos between HH8-10. Solutions of desired constructs were injected into the neural tube at the level of approximately the 4^{th} somite with the needle pointing towards the anterior end of the embryo. Electrodes were placed at the level of the fourth somite with the anode electrode raised slightly with respect to the cathode. When both sides of an embryo's neural tube were electroporated, a second injection was made and the embryo rotated 180 degrees before the second pulse again located at the fourth somite.

Screening for successful electroporations was done on a LeicaMZ FLIII stereomicroscope using the Leica IM1000 software running a DC500 digital camera. E2.5 embryos that had been electroporated on one side of the neural tube were then dissected and placed in 4%PFA for 1.5 hours before being cryoprotected overnight at 4°C in sucrose solution (15%). Samples were then placed in gelatin for cryosection. Double sided electroporations were left until E14.5 when the gut was dissected along its full length and placed in 4%PFA overnight at 4°C for NADPH diaphorase staining.

2.9 3D reconstruction

Serial transverse sections were cut from whole embryos. Sections were obtained at a thickness of 15μm from frozen blocks, and were placed on Superfrost Plus microscope slides. Sections were immunohistologically stained and mounted (as described in section 4.3) prior to image acquisition (Leica DC500) in preparation for processing as a digital stack required for 3D reconstruction. 3D reconstruction was done using Improvision's Volocity Software Version 3.

2.10 Whole-mount NADPH-diaphorase staining

Dissected guts were stained with NADPH diaphorase after fixing with 4%PFA overnight at 4ºC. Guts were incubated in the dark at 37°C for 30 mins in a solution of 3ml PBS + 1.5mg NBT + 3mg βNADPH + 1.5μl Triton X-100. Samples were visualised under a Leica MZ FLIII stereoscope to assess crude relative cell number. Further images were taken of lengths of gut which had been placed under raised coverslips, slightly flattening the sample, using a 70% glycerol: 30% PBS mounting media and visualised under a Zeiss Axioplan 2 microscope. Images were taken using a Progres 3012 camera from Kontron Elektronik and compiled using Adobe Photoshop v.7.

2.11 Tunel staining (Terminal deoxynucleotidyl Transferase Biotin-dUTP Nick End Labelling)

Chick embryos were dissected at E1.5, E2, and E2.5 and fixed in 4%PFA for 1 hour at room temperature. They were then washed in PBS (2x5mins) before undergoing ascending serial dehydration in methanol, 25%, 50%, 75%, 100% (x2), for 15mins each on ice. If stored for later processing, embryos were kept in 100% methanol at –20°C.

Embryos were rehydrated in 10 minute washes of 75%, 50%, and 25% MeOH/PBT (PBT = PBS + 0.1% Tween 20) at room temperature. They were then washed in PBT (3x5mins) and incubated in 10μg/ml proteinase K/PBS at room temperature for: - E1.5 – 3.5mins, E2/2.5 - 4mins. Next embryos were washed in

2mg/ml glycine for 2mins to quench the PK activity and then further washed in PBT (2x2mins). Post fixation of tissue was carried out using 4%PFA for 20mins at room temperature. Embryos were washed again in PBT (5x5mins) and then fixed in pre-chilled ethanol : acetic acid (2:1) for 10 mins on ice. Further washing was carried out in PBT (3x5mins) before embryos were incubated for 1 hour at room temperature in equilibrium buffer (100-200μl). As much buffer as possible was removed from the tubes without risking damage to embryos before TdT enzyme was added to cover the embryos and left overnight at 37°C.

After washing with working strength stop buffer for 3 hours at 37°C, changing the solution every hour, embryos were then washed in PBT (3x5mins) before being subject to blocking with 2mg/ml BSA, 5% sheep serum in PBT for at least an hour at room temperature. Next embryos were incubated in antibody solution (1/2000 anti-dig Alkaline Phosphatase-conjugated Fab, 2mg/ml BSA, 1% sheep serum in PBT) for either 2 hours at room temperature, or overnight at 4°C.

If the antibody was left on for 2 hours, embryos were washed with 2mg/ml BSA/PBT (2x10mins) and then washed overnight at 4°C agitating in a large volume. If the antibody had been left on overnight embryos were washed with 2mg/ml BSA/PBT (4x1hour) and then left overnight at 4°C agitating in a large volume.

The next day embryos were washed in fresh NTMT at room temperature (3xmins), and transferred to glass pots. Placing 1ml of freshly made NTMT into

each pot and adding 17μl of NBT/BCIP mix, embryos were incubated in the dark for 10-15mins whilst agitating. They were then washed in PBT (3x5mins), and fixed in 4%PFA for 30mins at room temperature, before further washing in PBT (3x5mins). To store embryos for later photographing they were placed in PBT (1% Tween 20) with a drop of sodium azide at 4°C in the dark.

2.12 In situ Hybridisation

RNA probes were synthesised for RET and Sox10 (Table 2.4) using DIG labelling. 1μl of linearised probe was added to the synthesis solution and left at 37°C for two hours: DEPC-H_2O (23.5μl), 5x buffer (8μl), 100μm DTT with polymerase(4μl), DIG RNA labelling mix (2μl), 100u/μl RNAsin (0.5μl), 10u/μl RNA polymerase (1μl). Meanwhile a 2μl aliquot was removed and run on 1% agarose gel. 2μl of DNase-1 was added for fifteen minutes at 37°C. Afterwards 80μl of DEPC-H_2O was added and the RNA precipitated using 10μl 4M LiCl, 300μl ethanol for twenty minutes on ice. RNA was then spun for 15 mins at 15000rpm and washed in 70% ethanol and allowed to air-dry. After redissolving in 120μl DEPC-H_2O this precipitation step was repeated. Finally RNA was resuspended in DEPC-H_2O to 0.1μg/μl and stored at -20°C.

For wholemount *in situs* embryos were collected at daily intervals between E1.5 and E4.5. Embryos aged E4.5 underwent dissection to remove the gut, whereas earlier stages were processed intact. After dissection samples were

fixed in 4%PFA/PBS overnight at 4°C. If continuing at a later date fixed embryos could then be stored at 4°C in 1% PFA/PBS for several weeks.

Samples were washed in PBT twice for five minutes then dehydrated in a methanol/PBT series, 25, 50, 75, and 100% methanol for five minutes each. Embryos were washed in 6%H_2O_2/MeOH for one hour then methanol for five minutes. Samples were stored in methanol overnight at 20°C.

Table 2.5: *In situ* probe sources and detection methods.

Probe	Source	Detection	Source
RET	Vassilis Pachnis*	Anti-dig AP	Roche
Sox10	Paul Scotting**	Anti-dig AP	Roche

* National Institute of Medical Research ** University of Nottingham

Samples were rehydrated in a methanol/PBT series, 75, 50, and 25% Methanol, for five minutes each and then two five minute washes of PBT. Three twenty minute detergent wash steps followed this and then samples were left in 4%PFA/PBT for a further twenty minutes. They were then rinsed in PBT and washed a further two times for five minutes each. Further rinsing in an equal part solution of prehybridisation mix and PBT, at room temperature and at 70°C, preceded a wash of at least one hour in a 70°C waterbath with prewarmed prehybridisation mix. This was exchanged for prewarmed hybridisation mix (prehybridisation mix plus probe) and left overnight at 70°C in the water bath.

On the third day, four 30 min prewarmed solution X washes followed an initial rinse at 70°C. Samples were washed in equal parts Maelic acid buffer with tween (MABT)/Solution X for a maximum of ten minutes at room temperature then rinsed in MABT three times and washed in MABT for thirty minutes twice. An hour in 2% Boehringers blocking reagent (BBR)/MABT followed at room temperature, then between one and two hours in 20% Serum/ 2% BBR/ MABT. Finally embryos were left shaking overnight at 4°C in a solution of 20% sheep serum/ 2% BBR/ MABT plus anti-Dig antibody (1:2000).

The next day, after three MABT rinses, at least seven MABT washes of one hour were performed at room temperature. Samples underwent one last change of MABT and were left shaking overnight at room temperature.

The final step developed the staining. Four NTMT washes of ten minutes preceded the colour reaction step. This consisted of 12µl of NBT/BCIP stock solution being added to 2ml of NTMT and samples were left shaking on ice in the dark until the colour reaction developed. If the staining solution became purple it was replaced and the reaction continued. A ten minute NTMT wash cleaned the samples and then background was reduced through an initial ten minute PBT wash followed by an overnight wash when required. Samples were stored in PBT plus a drop of sodium azide at 4°C in the dark.

2.13 Solutions

Buffer P1: resuspension Buffer

50mM Tris-CL pH 8, 10mM EDTA, 100µg/ml Rnase A

Buffer P2: Lysis Buffer

200mM NaOH, 1% SDS (w/v)

Buffer P3: Neutralisation Buffer

3M potassium acetate pH 5

Buffer QBT: Equilibration Buffer

750mM NaCl, 50mM MOPS pH7, 15% isopropanol (v/v), 0.15% Triton x-100 (v/v)

Buffer QC: Wash Buffer

1M NaCl, 50mM MOPS pH 7, 15% Isopropanol (v/v)

Buffer QF: Elution Buffer

1.6M NaCl, 50mM Tris-Cl pH 8.5, 15% isopropanol (v/v)

Modified Carnoy's fixative:

Ethanol	60%
37% Formaldehyde	30%
Acetic acid	10%

PBT:

0.1% Tween-20 in PBS (1ml in 1l).

6% H_2O_2/MeOH:

30% H_2O_2	10ml
MeOH	50ml

Store at 4°C

Detergent Mix: (500ml)	Final Conc'	Volume
NP-40	1%	5ml
20% SDS	1%	25ml
Deoxycholate (Na^+salt)	0.5%	2.5g
1M Tris pH8	50mM	25ml
0.5M EDTA	1mM	1ml
5M NaCl	150mM	15ml
H_2O		429ml

Hybridisation mix:	Final Conc'	Volume
Formamide	50%	25ml
20x SSC	5x	12.5ml
20% SDS	2%	5ml
10% Boehringers blocking reagent	2%	10ml
tRNA	250µg/ml	1.25ml
Heparin	100µg/ml	100µl

Store at -20°C

Solution X: (50ml)	Final Conc'	Volume
Formamide	50%	25ml
20 x SSC	1%	2.5ml
H_2O		17.5ml

Store at 4°C

MAB: pH7.5

11.6g Maleic acid (100mM), 8.76g NaCl (150mM), 8g NaOH in 1l H_20. Autoclave.

MABT:

0.1% Tween-20 in MAB (1ml in 1l).

10% Boehringers Blocking Reagent:

100ml MAB, 10g BBR (powder at 4°C). Autoclave.

Store at -20°C

NTMT:	Final Conc'	Volume
5M NaCl	0.1M	2ml
1M Tris pH 9.5	0.1M	10ml
1M $MgCl_2$	5mM	5ml
Tween-20	0.1%	100µl
Water		to 100ml

Chapter 3: Spatiotemporal development of neural crest cells, smooth muscle and interstitial cells of Cajal within the human gastrointestinal tract.

3.1 Introduction

3.1.1 Overview

The developmental timings and patterns of migration of the vagal and sacral neural crest populations that colonise the ENS have been well documented in mouse and chick models (Burns 2005). However, there is a paucity of information concerning ENS development in human embryos. Ethical considerations and the difficulty of obtaining human embryonic and foetal material have been the main barriers to progressing in this area. Utilising tissue obtained from the Human Developmental Biology Resource (HDBR), jointly funded by the Medical Research Council and the Wellcome Trust, and from the MRC tissue bank at Hammersmith Hospital, London, we aimed to use immunohistochemistry to address basic questions relating to the formation of the functional innervation in the human gastrointestinal tract.

Functional gut requires the interaction of three components in order to generate successful motility; these are the ENS which comprises neurons and glia, the smooth muscle, and the interstitial cells of Cajal. The ENS generates signals, mediated by the ICCs, which control the activity of the gut smooth muscle. By using antibodies to $p75^{NTR}$ (the low-affinity neurotrophin receptor expressed by neural crest cells), α smooth muscle actin (SMA) (a structural protein expressed in the musculature of the gut), and c-kit (a receptor tyrosine kinase expressed by interstitial cells of Cajal) the appearance and development of these three cell types was documented.

3.1.2 The human enteric nervous system

As previously discussed in section 1.2, the ENS is derived from neural crest cells and their development is well understood in animal models. Prior to commencing this study the precise timings of ENS colonisation by neural crest cells was unknown in human embryonic development. Several ultrastructural and immunohistochemical studies of embryonic gut have previously been carried out, though these dealt with later stage embryos than available here from gestational week nine or ten (Fekete, Resch, and Benedeczky 1995; Fekete et al. 1996; Benedeczky, Fekete, and Resch 1993; Vaos 1989; Brandt, Tam, and Gould 1996). By this time neurons are present throughout the myenteric plexus along the entire length of the gastrointestinal tract.

To identify neural crest cells we chose to use the low-affinity neurotrophin receptor $p75^{NTR}$, a well recognised marker of neural crest (Baetge, Schneider, and Gershon 1990). In addition to labelling the neural crest derived ENS, some crest derived extrinsic nerve fibres associated with the gut, such as the vagus nerve, are also labelled.

3.1.3 Enteric musculature

The smooth musculature of the gastrointestinal tract, which is derived from lateral plate splanchnic mesoderm (Roberts 2000), consists of two components, the muscularis mucosae and the muscularis propria. The former structure sends projections into the mucosal layer and is thought to play a role in the lumenal mixing and absorbtion of gut contents. The latter comprises the longitudinal and circular muscle layers, and is involved in the motility of the gut.

The sequence in which these muscle layers form is well accepted. The circular muscle layer forms first, followed by longitudinal muscle and finally the muscularis mucosae. The precise developmental nature of the formation of these muscle layers is still unclear. Myoblasts can be induced by intestinal epithelium; however, studies have reported radial migrations by circular muscle into the presumptive longitudinal muscle layer region prior to the appearance of that layer (Masumoto et al. 2000). The role of these projections is unknown. It may be that they provide inductive factors to the mesenchymal cells in that region or they may simply incorporate themselves into that layer. Similar centripetal projections arise from the circular muscle layer towards the presumptive muscularis mucosae.

Adult gut smooth muscle is comprised mainly of α and γ isoforms of smooth muscle actin (Fatigati and Murphy 1984). α-smooth muscle actin (α-SMA) appears earliest within myoblasts and was chosen to act as the marker of smooth muscle in this investigation.

3.1.4 Interstitial cells of Cajal

Interstitial cells of Cajal (ICCs) were first described in 1895 by Cajal. These cells, which were first identified in the myenteric plexus of rabbits, were initially named interstitial neurons. Cajal suggested that due to their positioning between the muscle and ENS they may have been responsible for regulation of muscle activity. Since then ICCs have been found in several other locations of the gastrointestinal tract (Hirst and Edwards 2004). ICCs vary in their position relative to the two different plexuses and muscle layers depending upon the region of gut studied. The function of these cells is now known to alter with this positional change. Indeed six differing types of ICC have been identified using immunohistochemical staining (Burns et al. 1997).

ICCs can be identified by immunostaining for the transmembrane tyrosine kinase receptor c-kit (Wester et al. 1999; Ward et al. 1994; Huizinga et al. 1995), including within the human gut (Wester et al. 1999). The c-kit receptor is essential for the formation of a functional network of ICCs (Ward et al. 1995; Huizinga et al. 1995) although not all ICCs express c-kit (Torihashi, Horisawa, and Watanabe 1999). Three roles for ICCs have been suggested by morphological studies: 1) pacemaker cells of the musculature of the gastrointestinal tract; 2) facilitators of electrical activity within the gut; 3) mediators of neurotransmission between the ENS and musculature.

The precise germ layer origin of ICCs was unclear until comparatively recently. Staining shared between neurons and ICC, such as methylene blue and

silver chromate, convinced Cajal and others that they were of neural origin. Analysis of the cellular structure of ICC indicated a closer resemblance to fibroblasts and smooth muscle. This, combined with the close association of ICCs and enteric neurons, suggested a specialised support cell role (Thuneberg 1982; Thuneberg, Rumessen, and Mikkelsen 1982).

Work in both mammals (Young et al. 1996) and avians (Lecoin, Gabella, and Le Douarin 1996) revealed the non-neural crest origin of ICCs. Lecoin approached the problem with two sets of experiments. When vagal NC from quail embryos was grafted into chicks, ICCs in the gut did not contain the quail nucleus, and therefore were of chick origin. In the second experiment, organ culture using the chorioallantoic membrane of developing chick embryos was used to culture isolated E3.5 hindgut. At this stage NCC have not reached the hindgut (Burns and Le Douarin 1998) and so ICC development in the absence of crest cells could be assayed. In the cultured gut, c-kit expressing cells were found at the outer regions of the circular muscle layer. This would coincide with the correct location of ICC in association with myenteric ganglia in a normal hindgut. The work by Young et al in the same year (Young et al. 1996) used a similar approach to Lecoin by culturing E9.5-E14 mouse hindgut segments within the kidney capsule. Again gut explants of this age lack neural crest precursors and results from these experiments concur with Lecoin's findings that ICCs neither arise from the neural crest nor require its presence to differentiate. These studies have shown conclusively that ICCs are of mesenchymal origin

3.1.5 Aims

The purpose of this invesitgation is to describe the spatiotemporal development of functional human embryonic gut between weeks 4 and 14 of gestation. Using antibodies to previously described markers of neural crest cells, enteric smooth musculature and interstitial cells of Cajal the positions and origins of these three cell types will be catalogued and their relationship to each other compared.

Through the HDBR and MRC tissue bank multiple samples of each week were obtained if possible though in some instances only a single sample was availbale.

Table 3.1: Number of embryos collected for each gestational age.

Gestational age in weeks	4	5	6	7	8	9	11	12	14
N=	3	2	2	3	5	4	3	4	1

3.2 Results

3.2.1 Neural crest cells:

At week 4, the earliest stage examined, neural crest cells have already delaminated from the neural tube and begun to migrate ventrally along previously described pathways lateral to the dorsal aorta **(Fig 3.1 a)**. Crest cells migrate towards the midline ventral to the dorsal aorta and have reached the dorsal portion of the presumptive foregut **(Fig 3.1 b)**. The degree of gut colonisation by these NCC is sparse and at this stage of development they are distributed throughout the outer gut mesenchyme. More caudal in the presumptive midgut NCCs have colonised the ventral portion of the gut mesenchyme as well as more dorsally and are present within the outer regions of the mesenchyme in a diffuse and random pattern **(Fig 3.1 c)**. At week 5 there is no dramatic increase in the distance neural crest cells have migrated along the gut. In the foregut the dorsal half of the gut remains the only region colonised by NCC **(Fig 3.1 d)** and throughout the midgut NCC have colonised more ventral portions of the mesenchyme **(Fig 3.1 e,f)**. In the foregut, however, NCC have begun to coalesce into small interconnected groups thus beginning to form primitive ganglia **(Fig 3.1 d)**. The gut tube has increased in length by this time and the proximal and distal midgut regions do not differ significantly in their NCC colonisation patterns **(Fig 3.1 e,f)**. Like the NCC of the foregut, those in the midgut have begun to coalesce into tighter groups.

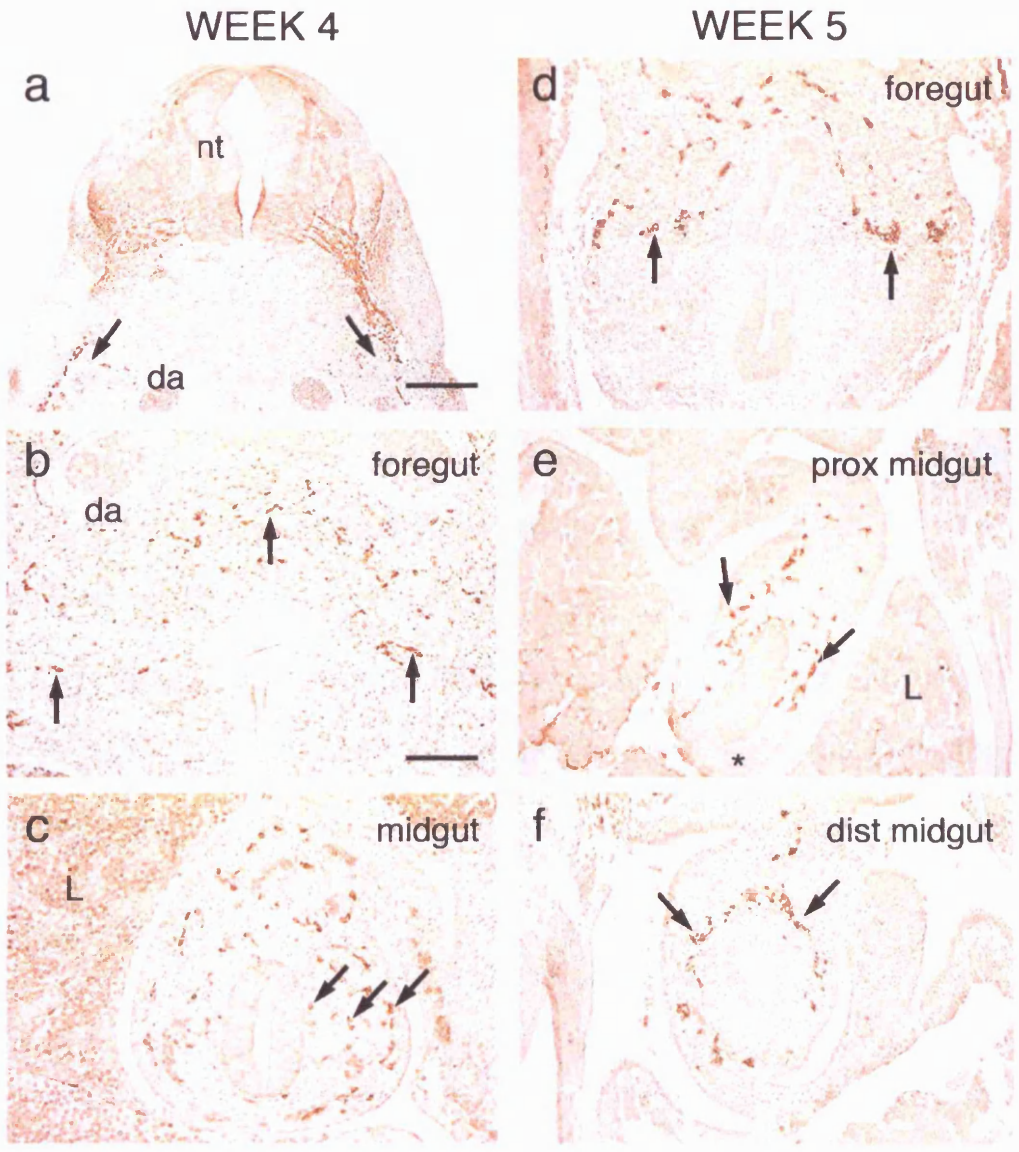

Figure 3.1. Development of p75NTR-immunopositive neural crest cells.

(a) At week 4, p75NTR-labelled cells (brown) migrated away from the neural tube (NT), as streams of cells (arrows) lateral to the dorsal aorta (DA). (b) NCC (arrows) were scattered in the dorsal aspect of the foregut mesenchyme. (c) In the proximal midgut, adjacent to the liver (L), NCC (arrows) were scattered across the width of the undifferentiated mesenchyme. (d) At week 5, NCC were present in the dorsal foregut, where they had accumulated into small groups of cells (arrows). (e) In the proximal midgut, adjacent to the liver (L), NCC (arrows) were present throughout the majority of the mesenchyme, although the ventral aspect of the developing gut was sparsely colonised (asterisk). (f) In the midgut, small groups of NCC encircled the gut, with the majority of cells distributed in the dorsal gut wall (arrows). Scale bar = 200μm (a); 100μm (b-f).

-Dr.Alan Burns assisted in the production and presentation of this figure.

At week 6 the gut can be divided into foregut, midgut and hindgut, with the stomach present as a discernable structure. Encircling the lumen of the stomach, small aggregates of NCC are present in the outer mesenchyme approximating to the position of the future myenteric plexus **(Fig 3.2 a)**. Also present are extrinsic fibres protruding into the outer mesenchyme. In the midgut NCC have coalesced into small clusters of cells joined by $p75^{NTR}$ positive projections **(Fig 3.2 b,c)**. In more caudal midgut NCC have also coalesced, but here the clusters are less well defined and lack the distinct fibres linking them **(Fig 3.2 d)**. At higher magnification these clusters can be clearly seen to contain upwards of 3-4 cells **(Fig 3.2 e)**. Neural crest cells located more caudal in the midgut have not yet begun to form clusters and are restricted to a tight band in the outer mesenchyme **(Fig 3.2 f)**. The hindgut is not yet colonised by NCC at this stage **(Fig 3.2 f)**.

Distinct ganglia of the forming myenteric plexus are present in the eosophagus and stomach of week 7 embryos **(Fig 3.3 a,b)**. In the duodenum these distinct ganglia are not yet present. Instead NCC are arrayed as a condensed web of small clusters of cells in the region of mesenchyme approximating to the future myenteric plexus **(Fig 3.3 c)**. The same is true of the proximal and distal intestine although progressively more caudal regions appear less well developed, exhibiting few instances of coalescence at this time **(Fig 3.3 d,e)**. At week 7 the hindgut is colonised by NCC **(Fig 3.3 f)**, and these cells are arranged as a loose web of cells dispersed widely throughout the mesenchyme.

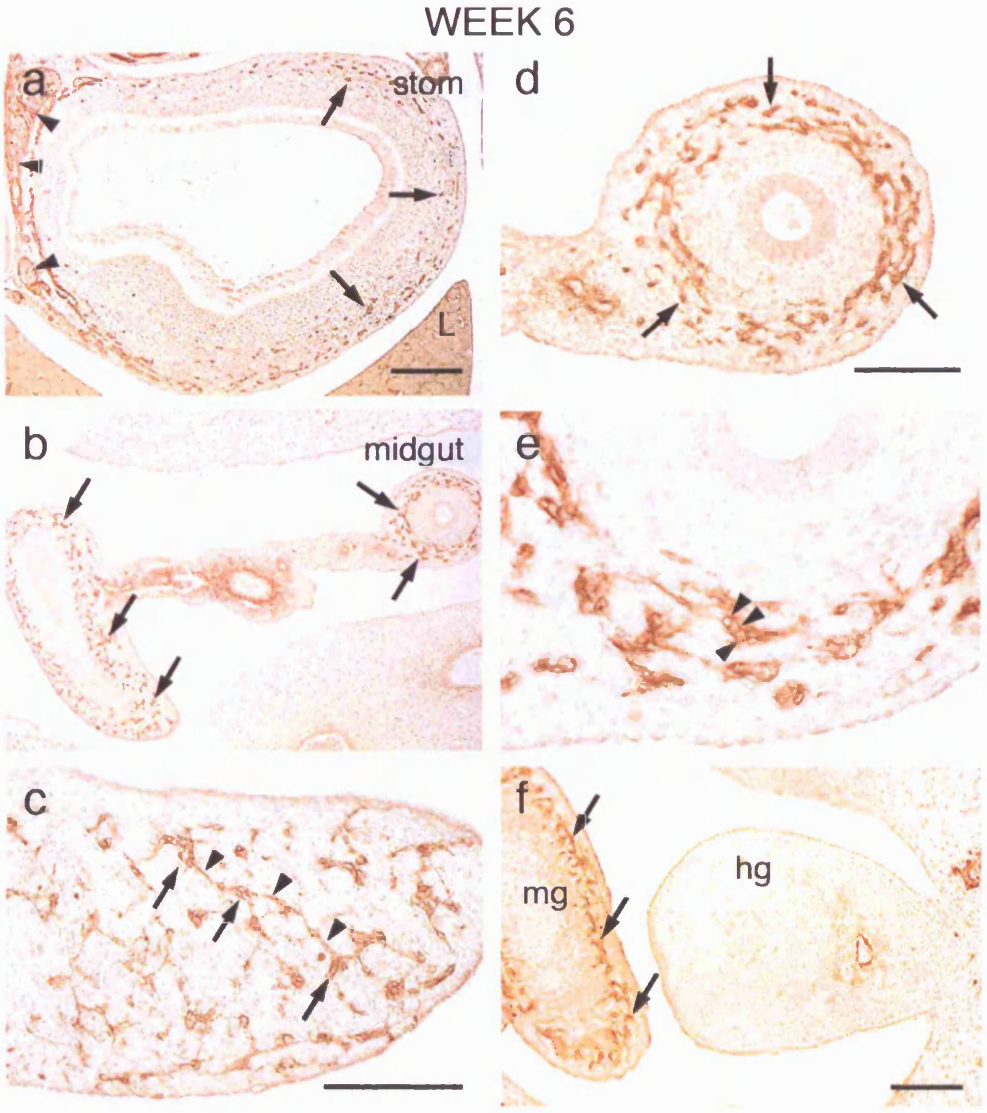

Figure 3.2. Development of p75NTR-immunopositive neural crest cells.

(a) At week 6, NCC (brown) were distributed within the wall of the stomach (arrows). p75NTR-immunostaining, corresponding to the vagal nerve and its branches, was also present adjacent to the stomach (arrowheads). (b-e) In the midgut, NCC (arrows) were present in the outer layers of the developing gut. Groups of cells (c, arrows), were interconnected by fine immunopositive fibres (c, arrowheads). Individual cell bodies could be identified within the small cell clusters (e, arrowheads). Although the midgut contained many NCC, the hindgut was free from crest cells (f). L, liver; mg, midgut; hg, hindgut.
Scale bar = 200μm (a, b); 100μm (c, d, f,).
-Dr.Alan Burns assisted in the production and presentation of this figure.

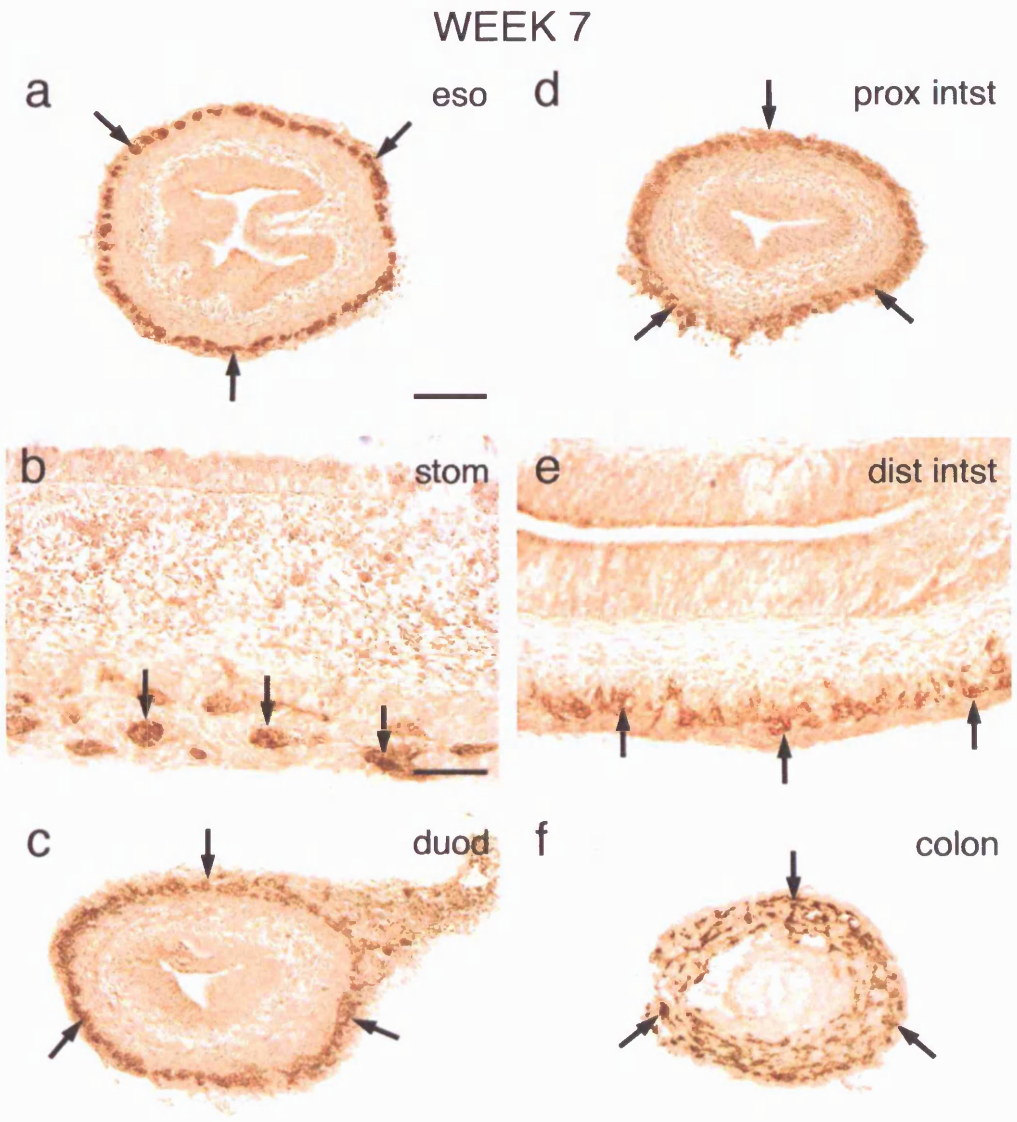

Figure 3.3. Development of p75NTR-immunopositive neural crest cells.

(a) At week 7, p75NTR-immunostaining (brown) was observed in the esophagus, in cells located external to the circular muscle layer (arrows). (b) In the stomach, labelling was apparent in groups of cells (arrows) within the muscle layers, corresponding to primitive ganglia. (c, d) In the duodenum and proximal intestine respectively, immunostaining (arrows) encircled the gut in a ring external to the circular muscle layers. (e) In the distal intestine, p75NTR-positive cells (arrows) were distributed within the developing muscle layers. (f) In the colon, immunopositive cells (arrows) were scattered throughout the undifferentiated gut mesenchyme. Scale bars = 100μm (a, c, d, f); 50μm (b, e).

In the eosophagus of week 8 embryos discrete groups of cells are present within the myenteric ganglia **(Fig 3.4 a)**. Also present at this stage are protrusions into the submucosal plexus from the myenteric plexus in the oesophagus. The myenteric plexus of the stomach contains distinct ganglia and possesses an organised appearance **(Fig 3.4 b)**. From the duodenum to the distal colon a clear gradient of development is apparent **(Fig 3.4 c-f)**. In the duodenum, ganglia are well defined and tightly restricted to the myenteric plexus region, although they do not appear organised as yet **(Fig 3.4 c)**. In the proximal intestine neural crest cells are restricted to the outer mesenchyme **(Fig 3.4 d)**. The ganglia appear less well formed than those in the duodenum, being more bulbous and rounded in appearance. In the distal intestine, NCCs are arranged as interlinked clusters of cells rather than ganglia, and these are present in a wide band encircling the gut (**Fig 3.4 e)**. The hindgut contains NCCs organised as small interlinked clusters, dispersed throughout much of the mesenchyme **(Fig 3.4 f)**.

By week 11 the first migrations from the myenteric plexus to the sub-mucosal plexus occur in the midgut **(Fig 3.5 b,c)**. In the most rostral regions of midgut primitive submucosal ganglia are present **(Fig 3.5 c)**. More caudally the colonising streams of cells migrate through the circular muscle layer **(Fig 3.5 b)**.

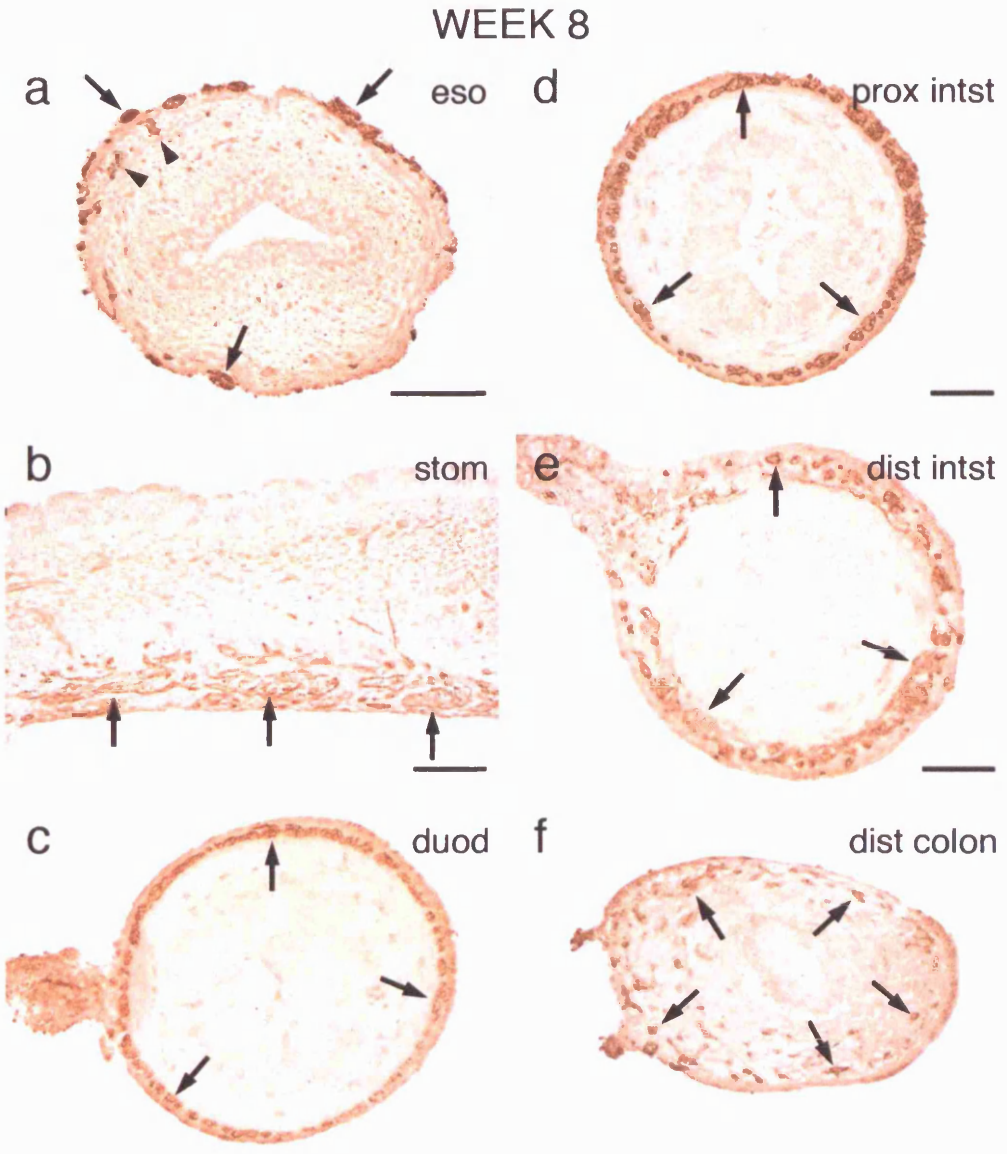

Figure 3.4. Development of p75NTR-immunopositive neural crest cells.

(a) At week 8, p75NTR-immunostaining (brown) was observed in the esophagus, in cells located external to the circular muscle layer (arrows) and as projections to the submucosa (arrowheads). (b) In the stomach, labelling was apparent in groups of cells (arrows) within the muscle layers, corresponding to primitive ganglia. (c, d) In the duodenum and proximal intestine respectively, immunostaining (arrows) encircled the gut in a ring external to the circular muscle layers. (e) In the distal intestine, p75NTR-positive cells (arrows) were distributed within the developing muscle layers. (f) In the colon, immunopositive cells (arrows) were scattered throughout the undifferentiated gut mesenchyme.
Scale bars = 100μm (a, c, d, f); 50μm (b, e).

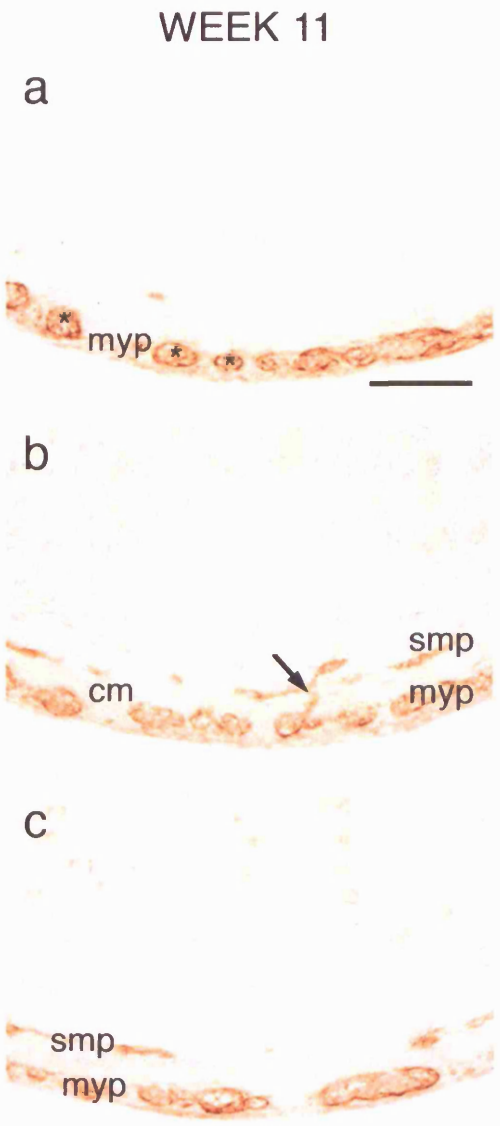

Figure 3.5. Development of p75NTR-immunopositive neural crest cells.

(a) At week 11, in the intestine, individual NCC-containing ganglia (asterisks) were apparent within the myenteric plexus region (myp) of the small intestine. (b, c) Projections (arrow) from the myenteric plexus cells, traversed the circular muscle layer (cm) and interconnected with areas of immunostaining in the presumptive submucosal plexus (smp) region. Scale bar = 50μm (a-c).

3.2.2 Smooth muscle development:

Weak αSMA staining is observed at week 7 in the foregut and midgut although this is barely observable (data not shown). A clear positive αSMA immunohistochemical signal appears along the length of the gut at week 8 of gestation **(Fig 3.6)**. The first muscle layer to appear positively stained is the circular muscle layer located internal to the forming myenteric plexus. This layer appears thickest in the eosophagus **(Fig 3.6 a)**, and is also the most well developed. In contrast to the developing circular muscle of the eosophagus the muscle in the colon appears as a thinner, more diffuse band of αSMA immunoreactivity, indicating a less well developed population of cells **(Fig 3.6 e)**.

By week 11 the full length of the gut possesses two distinct layers of strong SMA immunoreactivity corresponding to the circular and longitudinal layers, and also a weaker region which will develop into the muscularis mucosae **(Fig 3.7 a)**. Enteric ganglia, stained for $p75^{NTR}$, can be seen positioned between the circular and longitudinal muscle layers with occasional fibres protruding through the circular layer to the future submucosal plexus region. At week 12 the different layers appear more condensed and the difference in thickness can be seen, with the circular layer being noticeably thicker than the longitudinal layer **(Fig 3.7 b)**. At week 14 the musculature of the gut appears organised with the circular and longitudinal layers clearly defined by strong SMA immunostaining. These layers surround the $p75^{NTR}$-labelled enteric ganglia of the myenteric plexus, from which fibres protrude into the submucosal and muscularis mucosae. The muscularis mucosae is strongly stained for SMA immunoreactivity .

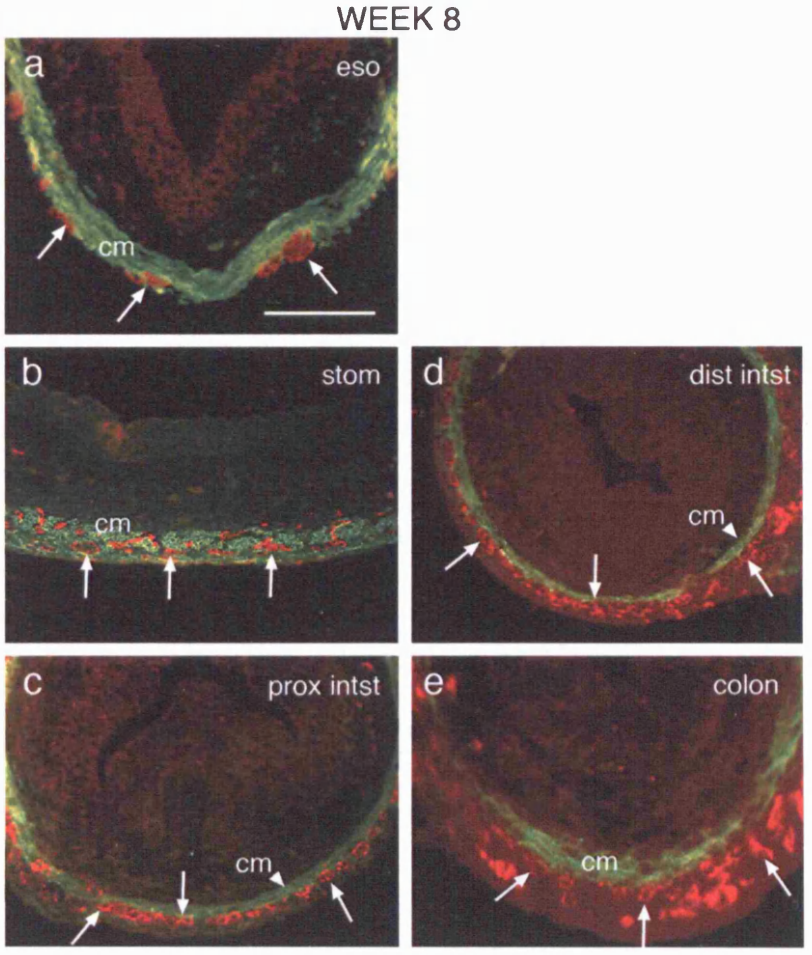

Figure 3.6. Development of SMA-immunopositive smooth muscle layers.

(a) At week 8, in the esophagus, the circular muscle layer (cm) was well developed and a dense band of cells was strongly immunopositive for SMA (green). p75NTR-positive cells (red) were grouped into presumptive ganglia (arrows), external to the circular muscle. (b) In the stomach, SMA labelling was apparent in the developing muscle layers (cm). p75NTR-labelled cells (arrows) were scattered throughout the smooth muscle. (c) In the proximal intestine, the circular muscle comprised a narrow band of SMA stained cells (cm, arrowhead). p75NTR-positive NCC were arranged external to the circular muscle, and had coalesced to form the presumptive myenteric plexus (arrows). (d) In the distal intestine, the circular muscle (cm, arrowhead) was less dense than in the proximal intestine. Some p75NTR-positive cells were grouped together as primitive ganglia (arrows), but the majority of labelled cells were scattered throughout the gut mesenchyme, external to the developing circular muscle layers. (e) In the colon, SMA-labelling was sparse and the circular muscle layer (cm) was at an early stage of development. p75NTR-positive cells (arrows) were scattered throughout the gut mesenchyme. Scale bars = 100μm (b, c, d); 50μm (a, e).

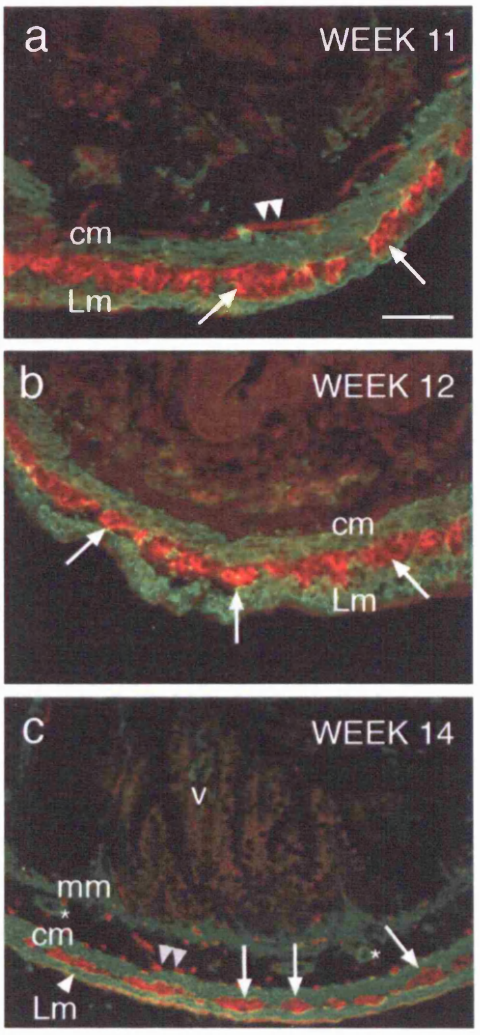

Figure 3.7. Development of SMA-immunopositive smooth muscle layers in hindgut.

(a) At week 11, SMA-staining (green) was apparent in the circular (cm) and longitudinal (Lm) muscle layers, located on either side of the p75NTR-positive (red) cells (arrows) of the presumptive myenteric plexus. Occasional areas of p75NTR immunoreactivity were also apparent in the region internal to the circular muscle layer, corresponding to the presumptive submucosal plexus (double arrowheads). (b) At week 12, the circular (cm) and longitudinal (Lm) muscle layers were strongly immunopositive for SMA. Between the muscle layers, p75NTR labelling was apparent in groups of cells comprising myenteric ganglia (arrows). (c) At week 14, SMA labelling was strong in the circular (cm) and longitudinal (arrowhead, Lm) muscle layers, and weak in the muscularis mucosae (mm), adjacent to the villi (v). The walls of blood vessel within the submucosa were also immunopositive for SMA (asterisks). p75NTR staining was present within ganglia of the myenteric plexus (arrows) and in nerve fibres within the submucosa (double arrowheads). Scale bars = 50μm (a, b); 100μm (c).

(Fig 3.7 c). Also stained are the walls of blood vessels running through the submucosa.

3.2.3 Development of the Interstitial cells of Cajal:

Immunoreactivity for c-kit, the marker for Interstitial cells of Cajal, begins to appear at week 9. Diffuse staining, in the future position of ICCs associated with the myenteric plexus, is present in the mid and hindgut **(Fig 3.8 A,B)**. Already these c-kit positive cells are found in close association with the developing enteric ganglia **(Fig 3.8 B)**. ICCs become organised the most rapidly of the three tissues investigated here, and as a result identifying any rostrocaudal wave of development is difficult with the samples available. At week 11 the positive immunostaining for c-kit has narrowed to only those regions in close association with the forming myenteric ganglia **(Fig 3.8 C,D)**. By week 12 ICCs appear well organised, being closely and exclusively associated with the myenteric ganglia and bipolar in appearance **(Fig 3.8 E,F)**. ICCs at week 14 **(Fig 3.8 G)** appear closely associated with enteric ganglia of the myenteric plexus.

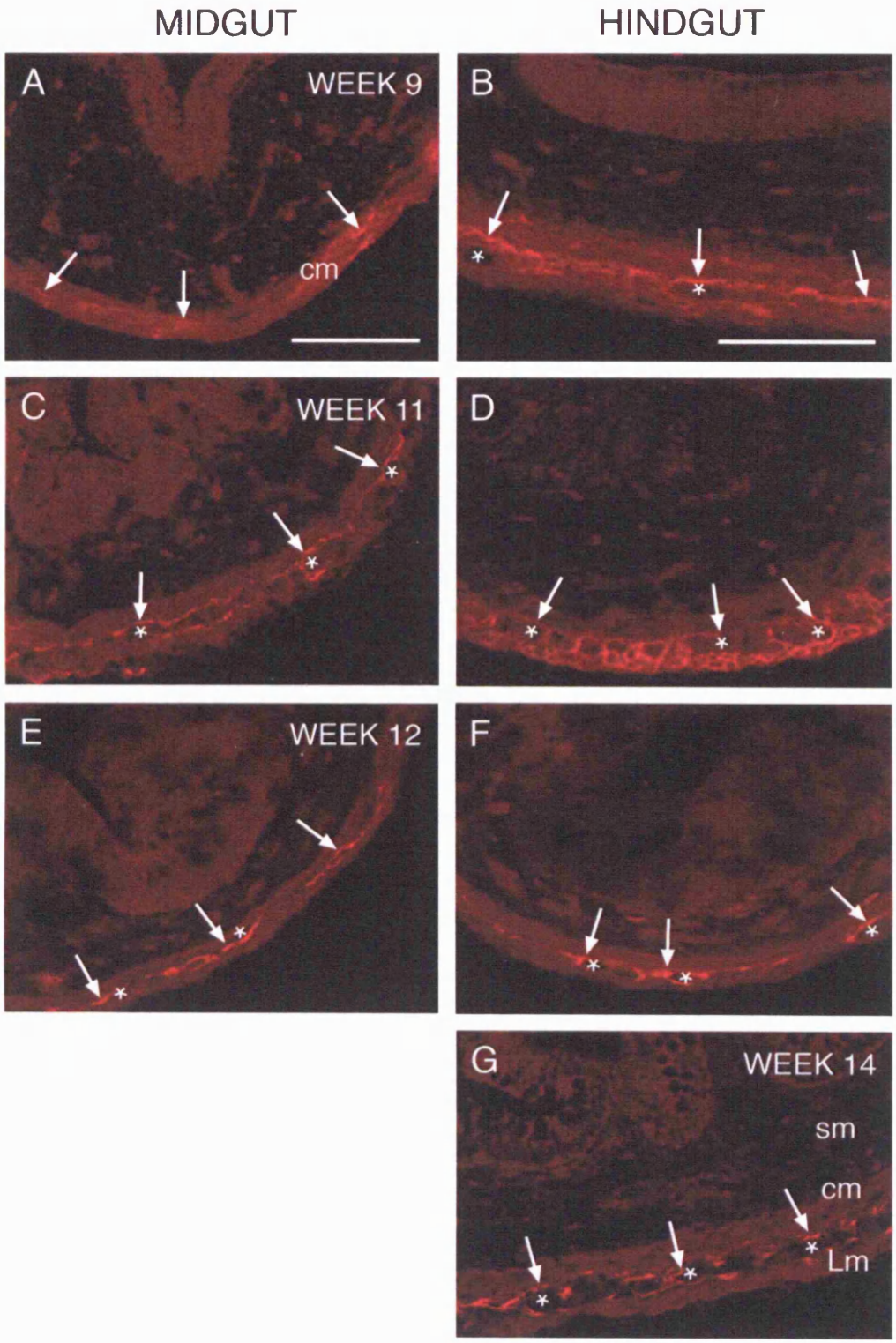
MIDGUT
HINDGUT
A
WEEK 9
cm
B
C
WEEK 11
D
E
WEEK 12
F
G
WEEK 14
sm
cm
Lm

Figure 3.8. Development of Kit-immunopositive interstitial cells of Cajal (ICC).

(A) At week 9, Kit immunostaining (red) was present at low levels (arrows) within the developing circular muscle (cm) of the midgut. (B) In the hindgut, immunolabelling (arrows) was apparent within the developing muscle. Unlabelled areas, corresponding to presumptive myenteric ganglia (asterisks) were apparent. (C) At week 11, in the midgut, Kit-positive ICC (arrows) were located on either side of the presumptive myenteric plexus cells (asterisks). (D) In the hindgut, Kit staining was widespread within the developing smooth muscle layers, particularly surrounding (arrows) the presumptive myenteric ganglia (asterisks). (E) In the midgut at week 12, Kit-positive cells (arrows) were restricted to the areas surrounding ganglia (asterisks), a pattern similar to that within the hindgut (F). (G) At week 14, in the hindgut, Kit-positive ICC (arrows) surrounded myenteric ganglia (asterisks). Kit staining was not observed within the submucosa (sm).
Scale bars = 100μm (A, C-F); (B, G).

3.3 Discussion

In this study the spatiotemporal colonisation of the human gastrointestinal tract by three cell types essential for the formation of a fully functional and co-ordinated neuromuscular apparatus in the gastrointestinal tract was documented: 1) The neural crest-derived enteric precursors, which contribute the neurons and glia of the ENS; 2) The enteric smooth muscle, which derives from splanchnic mesenchyme, and forms the contractile tissue of the longitudinal and circular muscle layers; 3) The interstitial cells of Cajal, also derived from mesenchyme, which mediate neuromuscular signalling and underlie the generation of the slow wave electrical activity of the smooth muscle. Immunohistochemistry using three well established markers for these cell types was employed to visualise their spatiotemporal development at known stages.

The low affinity neurotrophin receptor $p75^{NTR}$ has been extensively used to label NCC in species including *Xenopus laevis (Sundqvist and Holmgren 2004)*, mouse (Chalazonitis et al. 1998b; Young et al. 1998; Young et al. 1999; Young, Bergner, and Muller 2003), human (Fu et al. 2003), and other mammals including sheep, horse, cow, pig, rabbit and rat (Esteban et al. 1998). In agreement with the recent findings of Fu et al (Fu et al. 2003), $p75^{NTR}$-positive NCC were found to colonise the human gut in a rostro-caudal direction between weeks 4 and 7 of embryonic development (Wallace and Burns 2005). At week 4, $p75^{NTR}$-positive NCCs from the vagal region were found in the dorsal aspect of the foregut having migrated via a dorso-lateral route from the vagal region of the neural tube. As colonisation progresses these cells migrate in a rostrocaudal direction through

the gut mesenchyme, encircling the gut, proliferating and forming, first chains of cells and then primitive ganglia. This rostrocaudal pattern of migration is the same as that reported in other organisms such as fish (Shepherd et al. 2004), avians (Burns and Le Douarin 2001), mouse (Young et al. 1998), and most recently humans (Fu et al. 2003; Fu et al. 2004; Wallace and Burns 2003). Considering these comparable studies of NCC migration in conjunction with the rostrocaudal migration seen here, it can be surmised that vagal neural crest-derived enteric precursors colonise the entire length of the gut and contribute to at least the majority of neurons and glia along that length. This idea is further supported by work investigating the expression of RET in the developing human gastrointestinal tract, which showed that expression was confined to neural crest cell-derived populations (Attie-Bitach et al. 1998). At the time of this study no markers capable of segregating between vagal and sacral derived NCCs are available. Therefore it is impossible to state whether there is any sacral contribution to the ENS in humans, the timings thereof should this occur, or the extent to which they contribute. No $p75^{NTR}$ positive cells were observed in the hindguts of embryos prior to the arrival of the migration front of the vagal derived cells indicating that any sacral contribution arrives after the colonisation of the hindgut by the vagal derived NCCs, findings consistent with those in animal models (Burns and Douarin 1998).

In addition to the rostrocaudal migration of NCC along the gut between weeks 4 and 7, this study reveals a considerable amount of variation in the distribution of crest cells between differing gut regions at a single time point. For example, at week 7 although the entire length of the gut has been colonised by

NCC, their appearance differs greatly between the foregut, in which NCC have coalesced to form primitive ganglia, the midgut, in which NCC are loosely arranged in the outer mesenchyme, and the hindgut, in which NCC are scattered throughout the mesenchyme. Therefore the maturation of the ENS also occurs along a rostrocaudal gradient with the myenteric plexus forming in the oesophagus some three weeks prior to the hindgut.

After initially being scattered throughout the mesenchyme of the gut, the NCCs are restricted to the outer mesenchyme, thus forming a primitive myenteric plexus, consistent with the pattern seen in model organisms (Kapur, Yost, and Palmiter 1992; Gershon, Chalazonitis, and Rothman 1993; McKeown, Chow, and Young 2001; Burns and Douarin 1998). In these models the formation of the submucosal plexus occurs as a second centripetal colonisation event originating from the myenteric plexus with cells migrating through the circular muscle layer. Here centripetal migration by NCC from the myenteric to the submucosal plexus is observed in the oesophagus at week 8 and in the midgut at week 11.

The environmental cues which guide and trigger this secondary migration event remain to be fully determined. Ligands such as GDNF and ET-3, of the RET and EDNRB signalling pathways respectively, are expressed in the gut mesenchyme at these times (Suvanto et al. 1996; Natarajan et al. 2002; Leibl et al. 1999), although not in a pattern which coincides with the NCC migration through the circular muscle layer. Another prospective pathway determining this event is signalling through the receptor Deleted in Colorectal Cancer (DCC) and its ligand netrin1. DCC-expressing NCCs show an affinity for regions of high

netrin expression, which in the gut mesenchyme is the submucosal region (Jiang, Liu, and Gershon 2003). Therefore NCCs may possess the ability to enter the submucosal region from the very start of their migration, but as yet undetermined negative chemotactic signals restrict the initial domain available to that of the future myenteric plexus. Later this signal is removed and the chemoattractive properties of DCC and netrin1 act on a subset of ENS precursors to initiate centripetal migration and formation of the submucosal plexus. Such a system occurs in the chick where collapsin-1 initially inhibits neuronal projections from the nerve of Remak from penetrating the gut wall (Shepherd and Raper 1999).

Using antibodies against α smooth muscle actin (αSMA), a rostrocaudal maturation of enteric smooth muscle was observed beginning after NCC colonisation of the gut. A broad band of αSMA staining was evident at week 8 in the oesophagus, and week 11 in the hindgut, corresponding to the position of the future circular muscle layer. Other work has reported such gradients in smooth muscle maturation (Fu et al. 2004) but the link between immunohistochemical and structural development is poorly understood. Ultrastructural investigations of muscle development in the gut have not revealed such a gradient (Gabella 2002).

It was suggested recently by Fu et al (Fu et al. 2004), that the circular and longitudinal muscle layers appear at the same time during development of the gut in humans, and that they differentiate in a rostrocaudal manner between weeks 7 and 9. As stated above the accepted pattern of development in lab animals involves the formation of the circular muscle prior to the longitudinal

muscle. This investigation provides no evidence of any αSMA positive staining in the longitudinal muscle layer of the midgut and hindgut at week 8 whereas the circular muscle layer in these locations is αSMA positive at this stage. These findings suggest that the longitudinal muscle matures after the circular muscle. This is in agreement with reports of delayed longitudinal muscle maturation in the gut of the chick embryo using the smooth muscle marker 13F4 (Burns and Douarin 1998). The timings of muscularis mucosae formation observed here also co-incide with established patterns (Roberts 2000).

The transmembrane tyrosine kinase receptor c-kit and its ligand Stem Cell Factor (SCF) are essential for development of a normal ICC network (Ward et al. 1994; Ward et al. 1995), although a subpopulation of ICC do not express the c-kit receptor (Torihashi, Horisawa, and Watanabe 1999). Studies in avians show that during development the c-kit receptor is expressed at the outer boundary of the circular muscle and SCF is expressed within the circular muscle layer (Lecoin, Gabella, and Le Douarin 1996). A second source of SCF from enteric neurons has also been reported (Torihashi et al. 1996). This raises the issue of whether ICCs can form a complete and/or functional network in the absence of enteric neurons, as would be the case in HSCR. Evidence from aganglionic gut models in mice and chick suggest that the removal of enteric neuron sourced SCF does not inhibit the formation of functional networks of ICC (Wu, Rothman, and Gershon 2000); (Lecoin, Gabella, and Le Douarin 1996). However, the relationship between enteric neurons and ICCs in humans is still unclear with conflicting reports recently described (Huizinga et al. 2001; Rolle et al. 2002; Newman et al. 2003).

Using antibodies against c-kit ICCs were identified from week 9 in the intestine, after the colonisation by NCCs and differentiation of the smooth muscle. ICCs do not appear to mature in a rostrocaudal pattern like the other cell types reported here. ICC maturation is rapid; by week 11 they have become restricted to the area immediately adjacent to the developing myenteric ganglia. This pattern of association between the two cell types appears better defined in the midgut than hindgut at this time. Other reports of this association have been made recently from human foetal bowel (Kenny et al. 1999). This association suggests that in the absence of enteric neurons, such as in HSCR, the structure of any ICC network forming would be greatly disrupted, although not necessarily dysfunctional in all its activities. In contradiction to the timings observed in this study, Fu et al (Fu et al. 2004) describe the presence of c-kit positive cells within the myenteric plexus from week 12, with these cells migrating to the periphery of those ganglia at week 14. No c-kit positive cells were observed within the ganglia of the myenteric plexus in this study, although double labelling between c-kit and p75 was not carried out. The positioning of the staining found here indicates that the ICC are located at the periphery of the myenteric ganglia by as early as week 9 and certainly by week 11. The formation of the ICCs appears to occur some time after the formation of the ENS and smooth muscle, as has been reported in the mouse embryo (Wu, Rothman, and Gershon 2000).

Chapter 4: Investigating the role of RET in enteric nervous system development

4.1 Introduction

4.1.1 Ret, a dependence receptor candidate:

The role of the tyrosine kinase receptor RET has already been discussed in **section 1.4.1**, but this dealt with the classical neurotrophic properties of the RET protein. In addition to the established signalling roles there is mounting evidence to suggest that RET also functions as a dependence receptor (Bordeaux et al. 2000). The term dependence receptor describes a protein whose expression results in cellular dependency for its target ligand(s) (Bredesen, Mehlen, and Rabizadeh 2005). Thus in addition to any positive signalling roles which result in processes such as proliferation, survival , migration, or differentiation, so-called dependence receptors may tranduce negative signals inducing programmed cell death.

Candidate proteins displaying dependence receptor characteristics include those involved in nervous system development and tumour formation (Fang, Jass, and Wang 1998; Krygier and Djakiew 2001). Ret is no exception, playing a key role in ENS development and also being associated with the cancer, multiple endocrine neoplasia type 2 (Borrello et al. 1995).

To date, ten dependence receptors have been described: $p75^{NTR}$ (the low-affinity neurotrophin receptor), DCC (deleted in colon carcinomas), UNC5H1, UNC5H2, UNC5H3, AR (androgen receptor), RET, Integrin $\alpha_v\beta_3$, integrin $\alpha_5\beta_1$ and Ptc (patched – the sonic hedgehog receptor) (for review see (Bredesen,

Mehlen, and Rabizadeh 2005)). Of these, the majority are type 1 transmembrane receptors, whereas only Ptc and AR are not. RET is the only receptor tyrosine kinase identified as a dependence receptor thus far.

4.1.2 Cell death:

Cells inevitably die in multicellular organisms, although the manner in which they do so varies. Cell death can be a deliberate means to an end, a tool for sculpting developing tissues into their required shape. To simplify greatly, cell death can be thought of as organised or chaotic **(Fig 4.1)**. Chaotic cell death arises through necrosis, the lysing of a cell as a result of trauma, most commonly damage to the cell's plasma membrane. Organised, or physiological cell death takes the form of either autophagy or apoptosis, also known as programmed cell death (for review see Lockshin and Zakeri (2004)).

In necrosis, death can be caused through physical injury to the cell, by infection, infarcation, or inflammation. The uncontrolled manner of death may result in further injury or death to surrounding tissues as the cell lyses and its contents are released into the immediate area. In such cases toxins and infectious agents can then attack secondary targets.

Autophagic cell death is an extension of the day-to-day cellular process of autophagy, in which organelles are turned over as part of a normal metabolism and housekeeping process. Autophagic cell death is not apoptotic, but may take place as part of preparations for apoptosis in some cells.

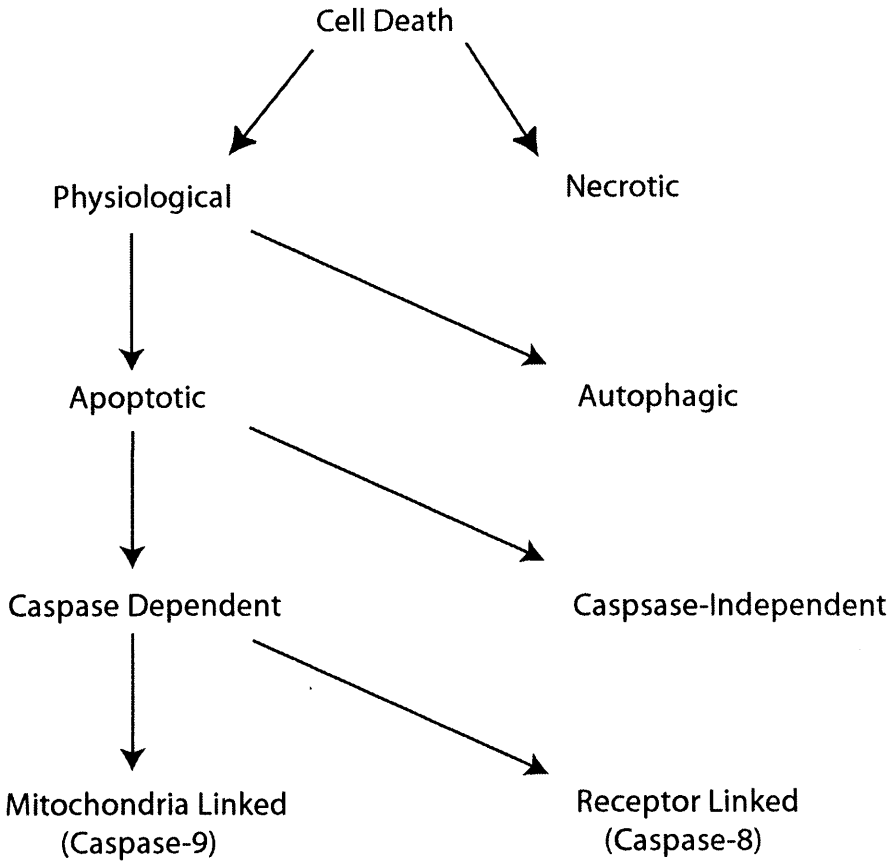

Figure 4.1:

Modified from Lockshin and Zakeri, 2004

4.1.3 Apoptosis:

Specific patterns of ultrastructural change are observed when a cell undergoes apoptosis. These events are part of the process which fragments the cell in such a way that the cell is destroyed without releasing its contents. Such apoptotic fragments are subsequently consumed by macrophages, limiting

damage to neighbouring cells. In addition to these ultraskeletal changes nuclear compaction is undergone and the cell's DNA is cleaved into small fragments.

Apoptosis can be either caspase dependent or caspase independent. Casapse dependent apoptosis can be due to endoplasmic reticulum stress, death receptor linked (via caspase-8) or mitochondria-metabolism linked (via caspase-9), also known as the intrinsic pathway. A Bcl-2 dependent non-mitochondrial/cytochrome-c linked system also presents a possible method of caspase activation (Marsden et al. 2002), although its precise pathway is unknown. It may not classify as a true third pathway but instead be a subset of caspase-8 related receptor linked apoptosis.

4.1.4 Caspases:

Caspases (cysteinyl aspartate-specific proteases) were first discovered in the nematode worm, *Caenorhabditis elegans*, and were recognised as being resposible for the programmed cell death essential for development of that organism (Ellis and Horvitz 1986). The *c.elegans* capase, CED-3, possessed close homology with the then human interlukin-1β-converting enzyme (ICE), now refered to as caspase-1 (Yuan et al. 1993). Caspase-1 has not been shown to regulate apoptosis itself but other members of the family do act as regulators of programmed cell death.

Caspases are produced as inactive zymogens which undergo internal cleavage to produce the final active state. Not all caspases are associated with apoptosis, but those that are can be divided into two groups based upon their actions, initiators and effectors (for review see Wang, Liu, and Cui (2005)). Initiatiors act to trigger effector capase activity by cleaving a procaspase zymogen into its active caspase form. These initiator caspases are not the exclusive machinery by which this can occur. Other non-caspase proteases can also induce effector caspase activity. Active effector caspases cleave target proteins releasing proapoptotic fragments. The functions of capases are 1) to arrest the cell cycle and inhibit DNA repair mechanisms; 2) inactivate the inihibitor of caspases machinery (XIAP); 3) dismantle the cellular cytoskeleton in an organised fashion for removal by phagocytes.

4.1.5 Caspase-9 and the Apaf-1 apoptosome:

Caspase-9 is amongst the most intensively studied caspases due to its essential role in the "intrinsic" pathway of apoptosis. It is encoded by a ~35Kb region and comprises 9 exons located at position 1p36.3-1p36.1 (Hadano et al. 1999). A wide variety of foetal and adult human tissues display caspase-9 expression. Expression is seen as early as E7 in the mouse embryo (Kuida et al. 1998) and is subsequently down-regulated at E15. Knockouts of caspase-9 result in apoptosis-deficient defects of the nervous system including enlarged and malformed cerebellum (Kuida et al. 1998). Analysis of caspase-3 expression in such mutants reveals caspase-9 to be a key regulator of the apoptotic cascade.

The intrinsic pathway refers to the activation pathway responsible for caspase-9 related apoptosis. Caspase-9 is activated primarily as a result of signals arising from mitochondrial damage, for example due to UV, toxins, Nitric Oxide, or in response to endoplasmic reticulum stress signals via caspase-12. Key to the mitochondrial activation of caspase-9 is Apaf-1.

Apaf-1 (apoptotic protease-activating factor-1) is activated through the release of cytochrome-c from mitochondria in response to apoptotic signals. It is the mammalian homologue of CED-4 found in *C.elegans* which has been shown to be an essential part of the highly organised apoptotic programming in that animal. Apaf-1 alone is a large protein of 130 kD which after activation by cytochrome-c oligomerises to form a 700-1400 kD caspase activating complex referred to as the Apaf-1 apoptosome. Multiple copies of caspase-9 are then recruited to the complex through caspase recruitment domain (CARD) binding, and this in turn recruits the procaspase-3 zymogen. The act of oligomerisation of caspase-9 when recruited to the Apaf-1 apoptosome likely induces self-activation of caspase-9, in turn leading to procaspase-3 activation.

The activation of initiator caspases is unusual in that like their effector relatives they undergo autocatalytic cleavage to acquire their active form. However, the activity of caspase-9 depends more on its incorporation to a larger complex than on its cleavage. Incorporation of cleaved caspase-9 into the Apaf-1 holoenzyme complex increases activity by 3 orders of magnitude compared to unbound procasapse-9 zymogen (Stennicke et al. 1999). Mutated caspase-9 with two mutations preventing cleavage of the zymogen to the recognised active form

is still incorporated and retains 40% of wildtype activity levels. It is unlikely that the marginal activity of caspase-9 when not part of the apoptosome is alone sufficient to activate caspase-3 and cleave downstream targets. Cellular apparatus exists to keep such low-level caspase activities in check.

Neurons are reported to use this intrinsic (mitochondrial) pathway of apoptosis, although there are notable exceptions which use receptor directed apoptosis (Raoul, Henderson, and Pettmann 1999; Schneider et al. 1999). Mice which are null for either Apaf-1 of caspase-9 exhibit gross encephalic malformations due to the lack of apoptosis in neuronal cell populations (Kuida et al. 1998; Cecconi et al. 1998). Deletion or impairment of Bax, another gene involved in the intrinsic pathway also results in reduced programmed neuronal cell death, and enables survival of nerve growth factor withdrawal (Deckwerth et al. 1996).

4.1.6 Evidence for RET as a dependence receptor:

As mentioned above RET possesses characteristics found in other known dependence receptors, namely involvement in nervous system development, and tumour susceptibility. It has been previously shown that RET behaves in the manner of a dependence receptor *in vitro* using 293T cells (Bordeaux et al. 2000). In these studies expression of RET in the absence of its ligand GDNF resulted in increased levels of cell death. Introducing GDNF to 293T cells expressing RET eliminated this effect and imposed a slight increase in survival compared to controls. These results are similar to those found for the relationship

between DCC and its ligand netrin-1. During investigations into DCC's role as a dependence receptor it was observed that it acts as a caspase substrate with cleavage occuring at Asp1290 (Mehlen et al. 1998). Mutating this site resulted in suppression of the proapoptotic effect of DCC expression in the absence of netrin-1. Investigating RET led to a similar mechanism being proposed for its function. RET also acts as a caspase substrate and is cleaved at two positions, Asp 708, and Asp 1017 by caspase-3 (Bordeaux et al. 2000). Mutation of either site resulted in suppression of the proapoptotic effect of RET in the absence of GDNF. The domain between Asp708 and Asp1017 does not share any similarity with the proapoptotic domain of DCC bordered by Asp1290, or indeed any other dependence receptor.

4.1.7 A mechanism for RET induced apoptosis:

As discussed in **section 4.1.3** effector Caspases are not produced in an active form but in the form of inactive pro-caspase zymogens. These zymogens do not possess sufficient activity to be responsible for cleaving either RET or DCC in the context described above. A novel mechanism for caspase activation is required for the apoptosis seen arising from the expression of either DCC or RET in the absence of their respective ligands.

The mechanism of DCC induced apoptosis has been studied and reveals a possible mechanism for novel caspase activation (Mehlen et al. 1998; Forcet et al. 2001). It was shown that caspase-3 activation in DCC dependent apoptosis was independent of caspase 8, Apaf-1 and cytochrome-c, yet dependent upon

caspase-9. This removes the possibility of an intrinsic pathway dependent system such as is detailed in **Fig 4.2**. Both caspase-3 and caspase-9 have been shown to interact with DCC in conjunction with DCC-interacting protein 13α (DIP13α). Whether this interaction is direct or indirect is unclear but the interactions were complementary: Caspase-9 interacted with DCC in conditions of ligand absence and caspase-3 interacted with DCC in the presence of ligand. Together these data suggest conformational change by DCC in response to ligand binding which acts to modulate a novel method of caspase activation and proteolytic cleavage.

RET may induce apoptosis by a similar method. It is known that RET dimerises when bound to its ligand GDNF and this may act to mask the caspase cleavage sites through a conformational change in the structure of the intracellular domain. Equally, though no evidence yet exists to directly support this, RET may interact either directly or indirectly with caspase-3 and/or caspase-9 to initiate its own proteolytic cleavage in the absence of GDNF.

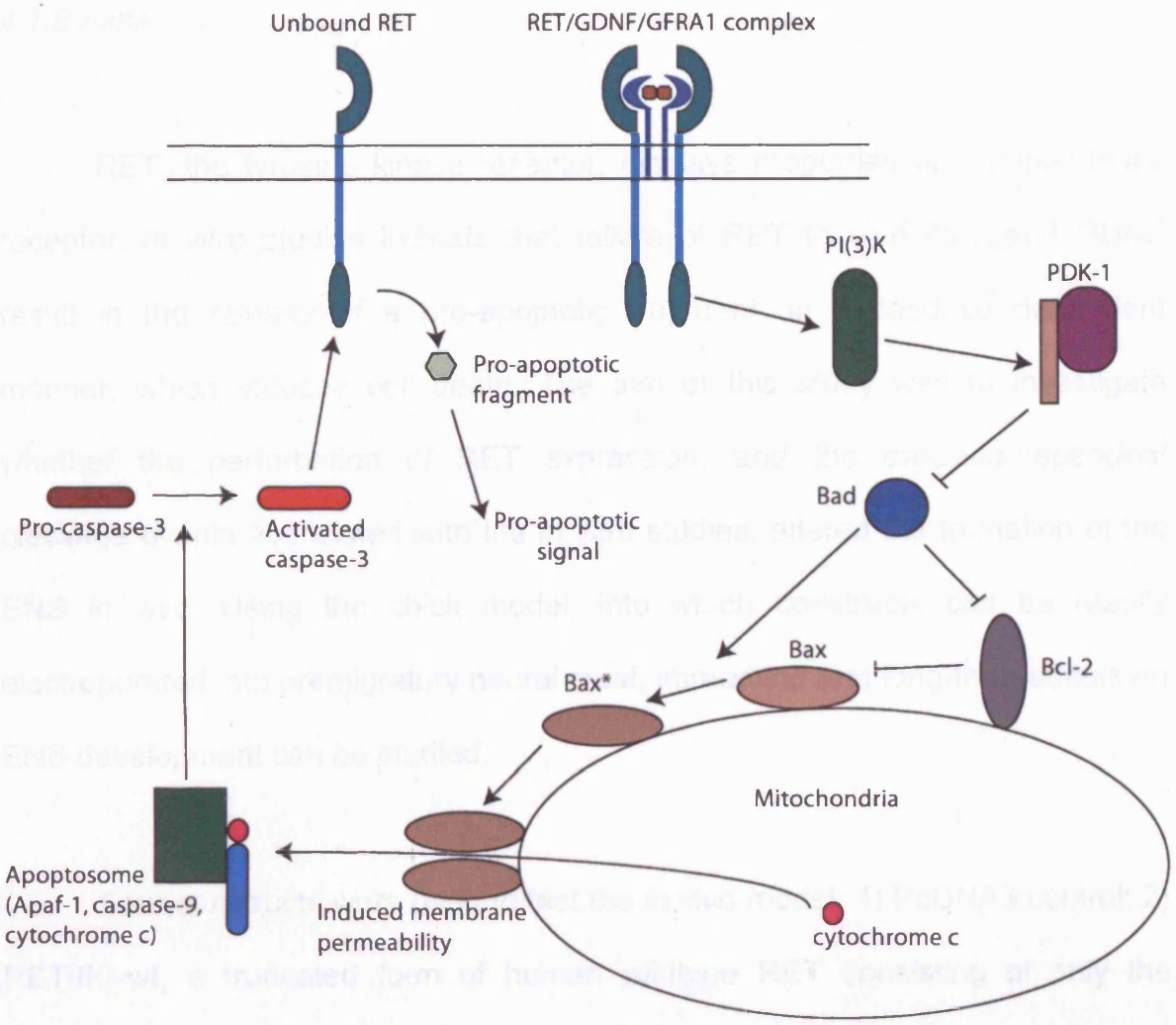

Figure 4.2: A possible system by which ligand withdrawal from RET may induce apoptosis:

One effect of RET-GDNF interaction is that the release of cytochrome c from mitochondria is inhibited by the PDK-1, Bad route shown. In the absence of RET signalling to PI(3)K this does not occur and leads to cytochrome c release and apoptosome assembly. In turn caspase-3 is activated and can cleave unbound RET releasing the apoptotic fragment. This leads to an amplification of the apoptotic response. Bax* indicates activated Bax.

4.1.8 Aims:

RET, the tyrosine kinase receptor, displays properties of a dependence receptor. *In vitro* studies indicate that failure of RET to bind its ligand GDNF result in the release of a pro-apoptotic fragment, in a caspase dependent manner, which induces cell death. The aim of this study was to investigate whether the perturbation of RET expression, and the caspase-dependent cleavage events associated with the *in vitro* studies, altered the formation of the ENS *in vivo*. Using the chick model, into which constructs can be readily electroporated into premigratory neural crest, immediate and long-term effects on ENS development can be studied.

Four constructs were used to test the *in vivo* model; 1) PcDNA3 control; 2) RET9IC-wt, a truncated form of human wildtype RET consisting of only the intracellular domain; 3) RET9IC-D707N, the same intracellular region as the wildtype RET but with a single point mutation at position 707; 4) Caspase-9DN, a dominant negative form of caspase-9. The purpose of the point mutation in the third construct was to prevent caspase cleavage at that site thus preventing release of a pro-apoptotic fragment **(Fig 4.3)**.

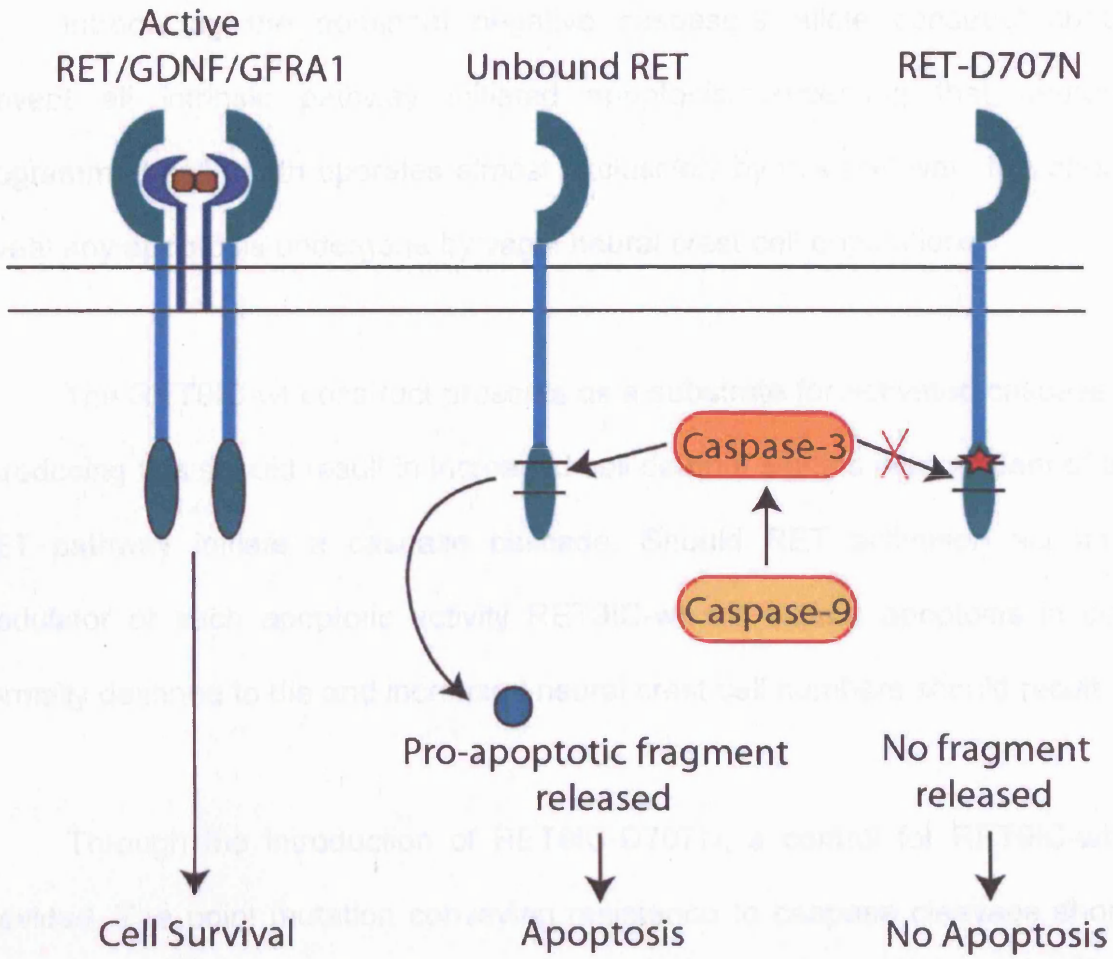

Figure 4.3: Caspase cleaves wildtype RET but not RET with mutation D707N.

When bound to its co-receptor and ligand, RET forms a dimer, autophosphorylates and adopts a conformation which masks the caspase cleavage sites at positions 708 and 1018. These caspase cleavage sites are available in unbound, monomeric, wildtype RET. Cleavage results in the release of a pro-apoptotic fragment. A single point mutation at position 707 removes the ability of caspase-3 to cleave at position 708 and prevents the release of the pro-apoptotic fragment.

Introducing the dominant negative caspase-9 allele construct should prevent all intrinsic pathway initiated apoptosis. Accepting that neuronal programmed cell death operates almost exclusively by this pathway, this should reveal any apoptosis undergone by vagal neural crest cell populations.

The RET9IC-wt construct presents as a substrate for activated caspase-3. Introducing this should result in increased cell death if signals independent of the RET pathway initiate a caspase cascade. Should RET activation act as a modulator of such apoptotic activity RET9IC-wt will initiate apoptosis in cells normally destined to die and increased neural crest cell numbers should result.

Through the introduction of RET9IC-D707N, a control for RET9IC-wt is provided. The point mutation conveying resistance to caspase cleavage should result in no increase in apoptosis within neural crest cells.

4.2 Results

4.2.1 In situ analysis of Sox10 expression within enteric precursors:

Sox10 was used as a marker of neural crest cells to establish a benchmark against which the expression of *ret* in NCC could be compared. At E2.5 *sox10* was expressed in vagal derived migratory neural crest cells within the region of the otic vesicle and pharyngeal arches **(Fig 4.4 A,B)**. Trunk neural crest in the early stages of migration also expressed s*ox10* and appeared as two lines running parallel to the midline **(Fig 4.4 C)**. Neural crest cells were seen migrating as streams between somites from this region of the neural tube. At E3.5 *sox10* expression was present in the area around the otic vesicle and within the developing dorsal root ganglia **(Fig 4.4 D,E)**.

At E4.5 *sox10* expression was present within vagal derived enteric precursors and was not detected in sacral derived neural crest **(Fig 4.4 F)**. The extrinsic, neural crest derived, vagus nerves also expressed *sox10* **(Fig 4.4 F,G)**. *sox10* expression was seen throughout the length of the gut, including oesophagus, proventriculus and stomach **(Fig 4.4 F-H)**.

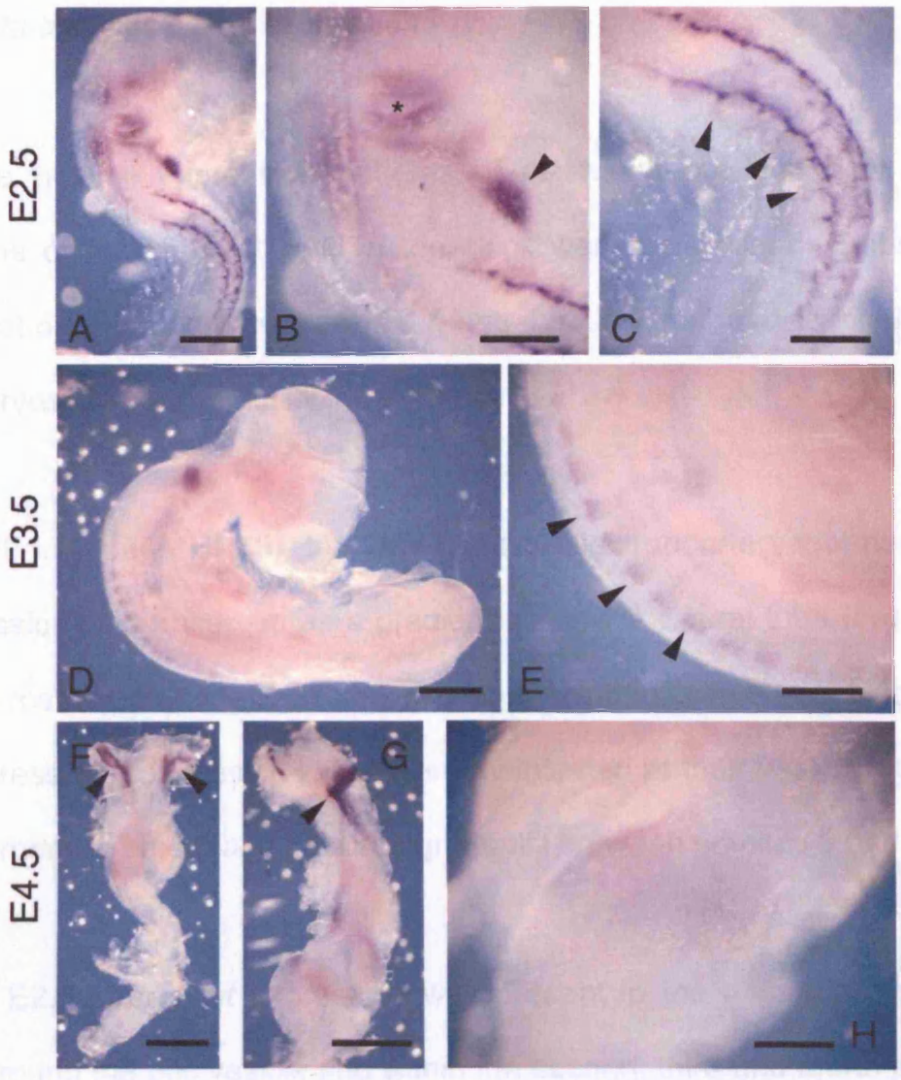

Figure 4.4: In Situ hybridisation with *sox10* probe.

(A) At E2.5 *sox10* expression was present in the region of the otic vesicle, 3rd pharyngeal arch, pharynx and in two lines parallel to the midline through the level of the truck. (B) High power image of the vagal region showing crest cells around the otic vesicle (asterisk) and pharynx (arrowhead). (C) *sox10* expression in early migratory neural crest of the truck level. Crest cells were seen migrating through the anterior part of somites (arrowheads). (D) *sox10* expression at E3.5 was difficult to assess in the region of the pharyngeal arches, some staining was visible around the otic vesicle. (E) High power showing *sox10* expressing cells in forming DRGs at E3.5 (arrowheads). (F) At E4.5 *sox10* expressing cells were present within the foregut and vagus nerves (arrowheads). (G) Higher power image showing expression in oesophagus, proventriculus and stomach. Also expressing *sox10* were the neural crest derived vagus nerves (arrowhead). (H) *sox10* expressing cells within the stomach.
Scale bars: 0.25mm C,H; 0.5mm A,B,E; 1mm D,F,G.

4.2.2 In situ analysis of Ret expression within ENS precursors:

The precise expression patterns of *ret* within pre and post migratory populations of neural crest cells in the chick were determined. Embryos were collected at daily intervals between E1.5 and 4.5, and the gut dissected free from E4.5 embryos.

At E1.5 (stage HH10), the time used to electroporate vagal neural crest, *ret* expression was observed as a gradient within the neural tube **(Fig 4.5 A,B)**. The most rostral point of expression, rhombomere 6, displayed the highest levels of *ret* expression. Expression levels were maintained at their peak throughout the length of rhombomere 6 and declined gradually between somites 1 and 5.

At E2.5 strong *ret* expression was present in the migratory neural crest located around the otic vesicle and within the second, third and fourth pharyngeal (branchial) arches **(Fig 4.5 C,D)**. A small number of *ret* expressing cells was present caudal to these regions in the location of the developing foregut **(Fig 4.5 C')**. No *ret* expression was seen within the neural tube at the level of sacral neural crest at this stage.

Wholemount *in situ* hybridisation for *ret*

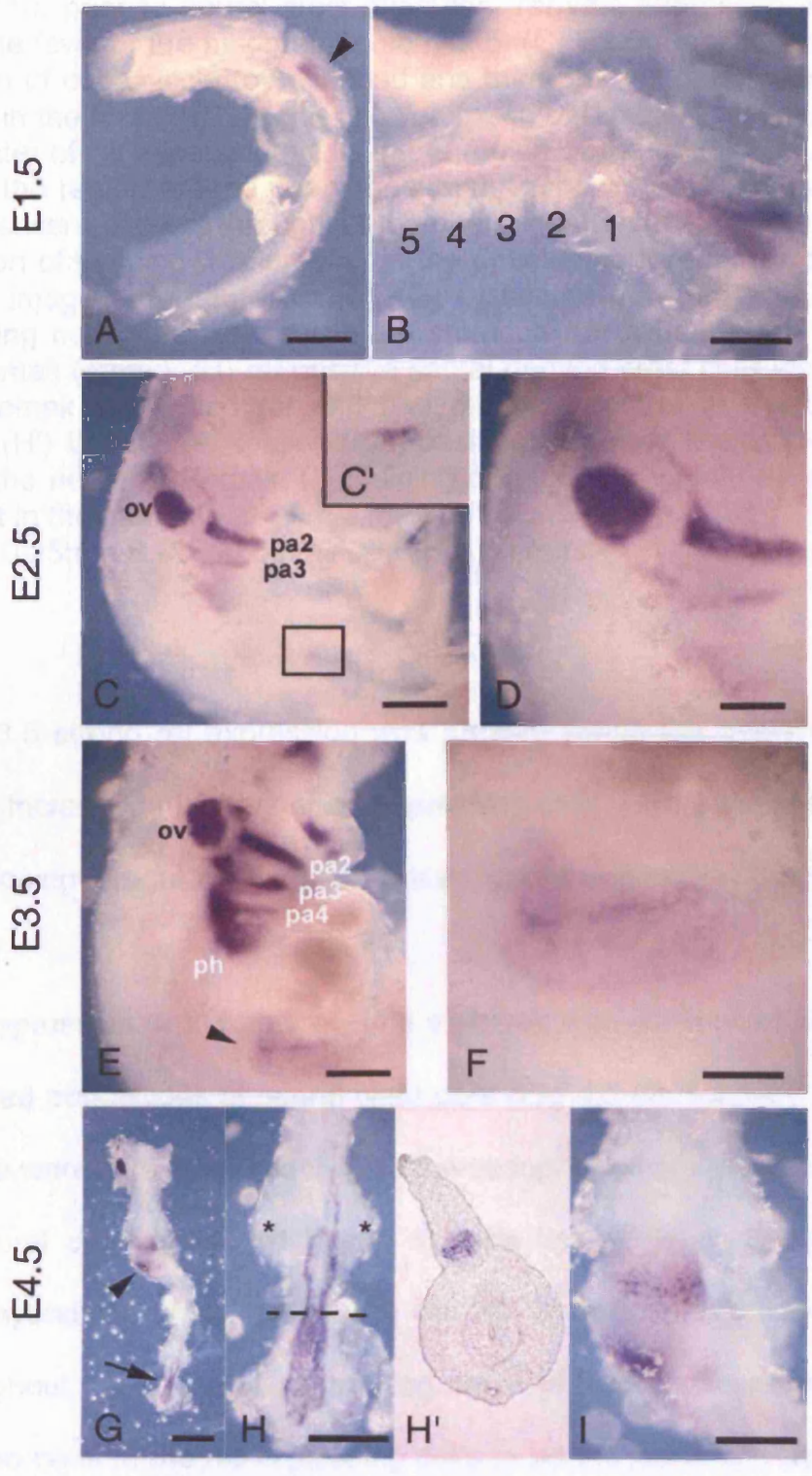

Figure 4.5: In Situ hybridisation with *ret* probe.

(A,B) at HH10, prior to neural crest migration, *ret* was expressed in the neural tube from the level of the hindbrain to somite 5. (C) E2.5 embryo, *ret* expression in the region of otic vesicle (ov), second and third pharyngeal arches (pa2, pa3) and weakly in the fourth. (C') Higher power image of boxed region in (C) showing a small cluster of *ret* expressing cells in the region of the developing foregut. (D) close up of the region around pharyngeal arch 2 showing *ret* expression. (E) *ret* positive cells were present throughout the pharyngeal arches, pharynx (ph) and a diffuse region of staining was present in the developing foregut (arrowhead). (F) High power image of foregut from (E). (G) Dissected gut from an E4.5 embryo, *ret* expressing cells were present in the stomach (arrowhead) and forming the nerve of Remak (arrow). (H) *ret* positive sacral derived crest cells which form the nerve of Remak expressed *ret* and had migrated rostral to the caecal buds (asterisks). (H') transverse section from position of dotted line in (H) confirmed staining of the nerve of Remak. (I) Staining of migrating vagal neural crest cells was present in the stomach.
Scale bars: 0.25mm B,D,F; 0.5mm A,C,E,H,I; 1mm G.

At E3.5 strong *ret* expression was present within the pharyngeal arches **(Fig 4.5 E)**. Increased numbers of *ret*-expressing cells were present in the region of the developing foregut but their location appeared unchanged **(Fig 4.5 F)**.

ret expression in the guts of E4.5 embryos was present within vagal and sacral derived populations of neural crest cells **(Fig 4.5 G)**. Extrinsic fibres of the vagus nerve were also seen attached to the oesophagus of dissected gut. Sacral derived neural crest cells had begun to form the nerve of Remak and had migrated beyond the caecal buds **(Fig 4.5 H)**. Strong *ret* expression could be seen throughout the length of the forming nerve of Remak. Transverse sections of this region confirm the *ret*-expressing cells to be the nerve of Remak **(Fig 4.5 H')**. Expression of *ret* within vagal derived neural crest cell populations was restricted to the stomach **(Fig 4.5 I)**. No *ret* expression was observed in the

oesophagus or lungbuds, structures which should already have been colonised by neural crest cells.

4.2.3 Tunel analysis:

In order to identify apoptotic cells within neural crest cell populations destined to form the ENS, Tunel staining was employed. Early stage E1.5 and E2.5 embryos were investigated as there is currently a paucity of information regarding apoptosis in ENS precursor populations during migration in the gut.

At stage HH10 apoptotic cells were observed along a significant portion of the neural tube **(Fig 4.6 A)**. The "salt and pepper" appearance of Tunel positive cells was limited almost exclusively to the dorsal aspect of the neural tube. At E2.5 Tunel positive cells could be seen in the regions surrounding the otic vesicle through which vagal neural crest cells migrate **(Fig 4.6 B,C)**.

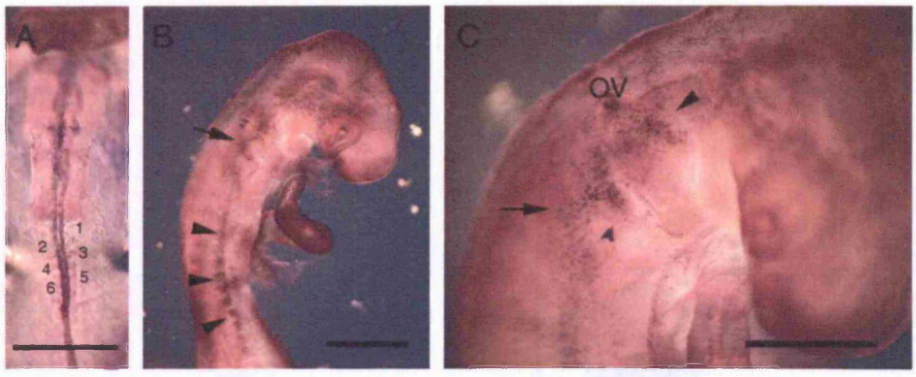

Figure 4.6: Tunel staining of E1.5 and E2.5 chick embryos.

(A) Tunel positive cells were located along the midline of the embryo in a pattern consistent with neural crest formation. An area of highest positive cell density was located between somites 2 and 7, the region corresponding to vagal neural crest. (B) Tunel positive cells were located in the region of migrating neural crest cells around the otic vesicle (arrow). Tunel cells were also seen in the dorsal tips of somites in the trunk region (arrowheads). (C) Tunel positive cells in the region of neural crest cells migrating towards branchial arch 3 (arrowhead), and ventro-posteriorly towards the 3rd pharyngeal pouch (arrow).
(Scale bars: 1mm.)

4.2.4 Electroporation of vagal neural crest does cells:

Electroporation is an invasive procedure for early stage embryos. Thus it was first checked that electroporated neural crest cells were viable, migrated successfully along established pathways and survived to form the ENS. To do this a GFP reporter was electroporated into HH10 embryos in the region of the vagal neural crest **(Fig 4.7)** and embryos were screened at E2.5 when NCC were migrating towards the gut and at E6 when NCC were forming the ENS within the gut. Wholemount fluorescence and cryosections revealed neural crest cells migrating successfully from the neural tube at E2.5 along the recognised dorsoventral pathway used by enteric precursors **(Fig 4.8 A,B)**. At E6 GFP positive cells were present in the stomachs of electroporated animals **(Fig 4.8 C)** implying that survival of this population is not affected.

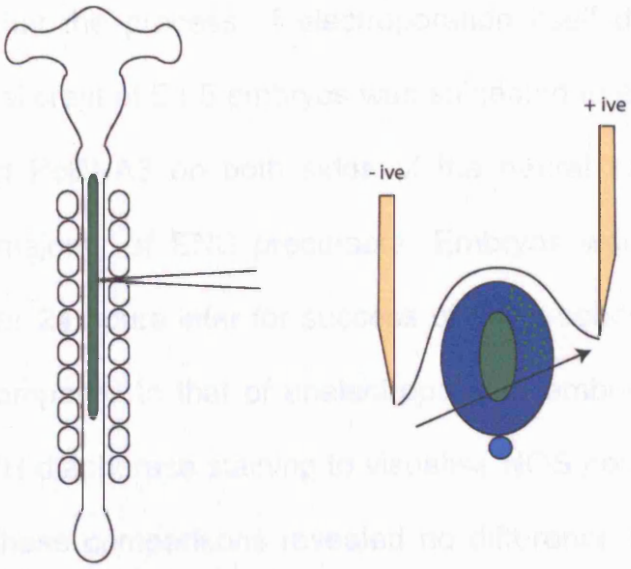

Figure 4.7: Electroporation of HH10 chick embryos.

Reporter and experimental plasmids were injected into the neural tube at the level of the third-fourth somites. Fast green was used to visualise the progress of the injected solution which is allowed to fill the region between somites 1 and 7. When placing the electrodes the anode was positioned above the level of the cathode. This results in a flow of current, and hence DNA, into the more dorsal aspect of the neural tube.

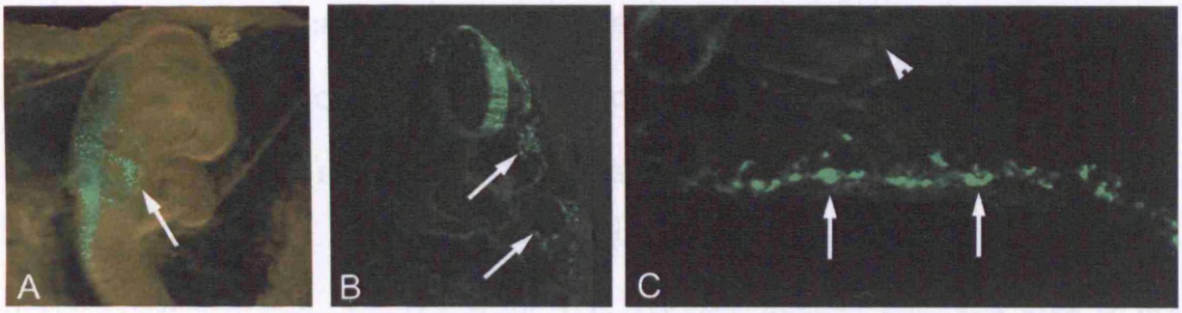

Figure 4.8: GFP labelled neural crest-derived cells migrate and survive in chick embryos.

GFP-labelled cells migrate and colonise the gut in chick embryos after electroporation. (A) E2.5 chick embryo 24 hours post electroporation, crest cells are migrating past the visceral pouch (Arrow). (B) 12um cryosection reveals the ventral path taken by GFP-labelled crest cells. (C) GFP-labelled cells form primitive ganglia (Arrows) in the stomach of E8 chicks (Arrowhead-mucosa).

To ensure that the process of electroporation itself did not affect ENS formation, the neural crest of E1.5 embryos was subjected to electroporation with the control plasmid PcDNA3 on both sides of the neural tube in an effort to electroporate the majority of ENS precursors. Embryos were again screened using a GFP marker 24 hours later for success of the procedure. The formation of the ENS was compared to that of unelectroporated embryos at E14.5 using wholemount NADPH diaphorase staining to visualise NOS neurons along the gut length **(Fig 4.9)**. These comparisons revealed no difference in the formation of the NOS-neuron networks between these animals.

4.2.5 Electroporation with Caspase-9DN results in an abnormal neural tube and increased numbers of neural crest cells: (The number of embryos studied was 12)

In contrast to a normal neural tube, which possesses a rounded dorsal midline, the majority of caspase-9DN electroporated embryos (7/9) displayed a slender protrusion or ridge **(Fig 4.10)**. This ridge appeared to co-incide with only the region subject to electroporation, with the remaining neural tube demonstrating a normal morphology. Interestingly, despite only one side of the neural tube having been electroporated this ridge contained tissue from the control side in addition to GFP positive tissue.

Sections immunofluorescently stained for the neural crest marker HNK-1 revealed that the numbers of neural crest cells migrating on the electroporated side of the embryo were increased. To visualise this further 3D reconstruction of

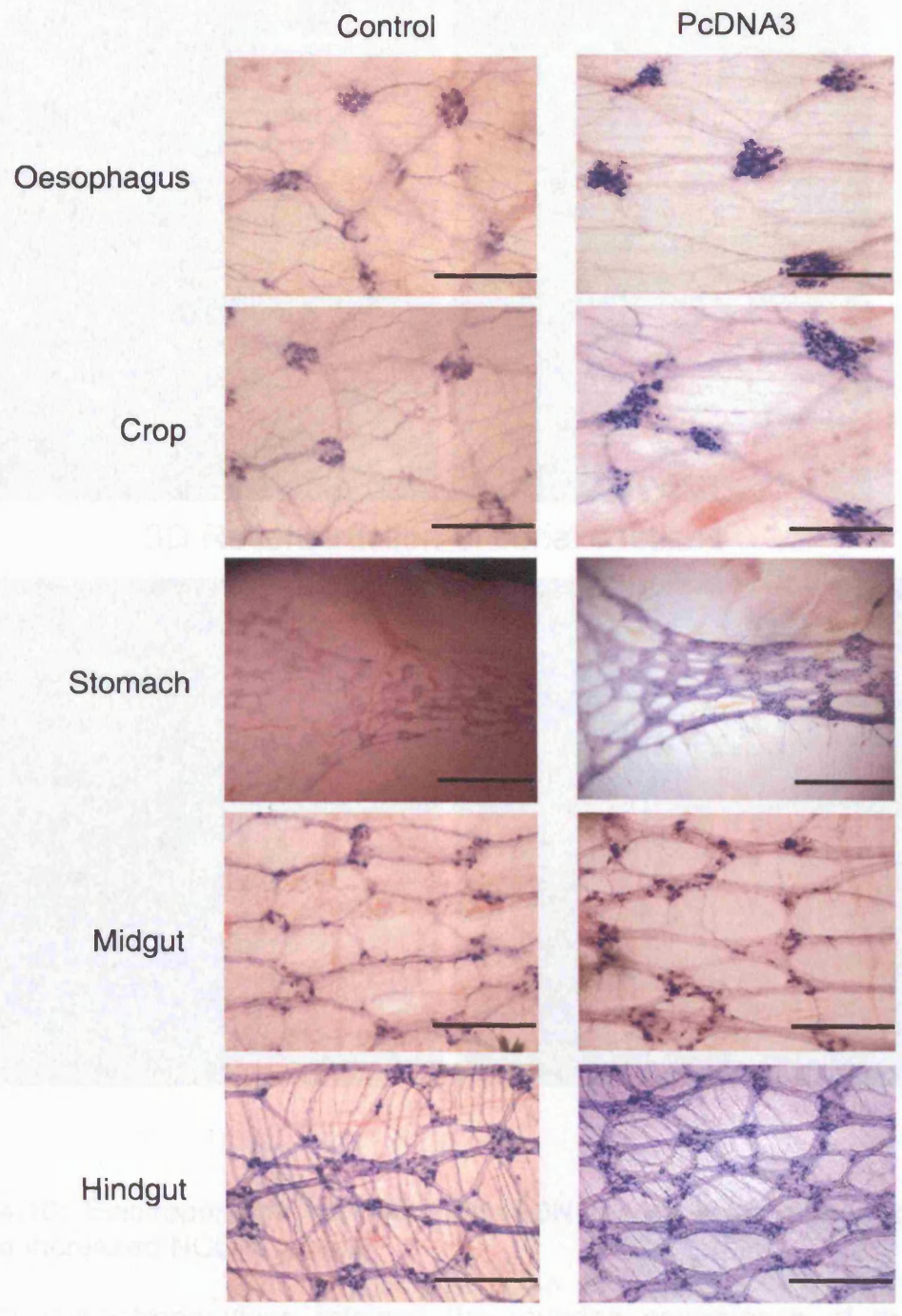

Figure 4.9: Electroporation does not affect ENS formation.

Electroporation with the control vector PcDNA3 results in a normal enteric phenotype at E14.5 as shown by NADPH-diaphorase staining for NOS neurons. Scale Bars: 20μm excluding stomach 1mm

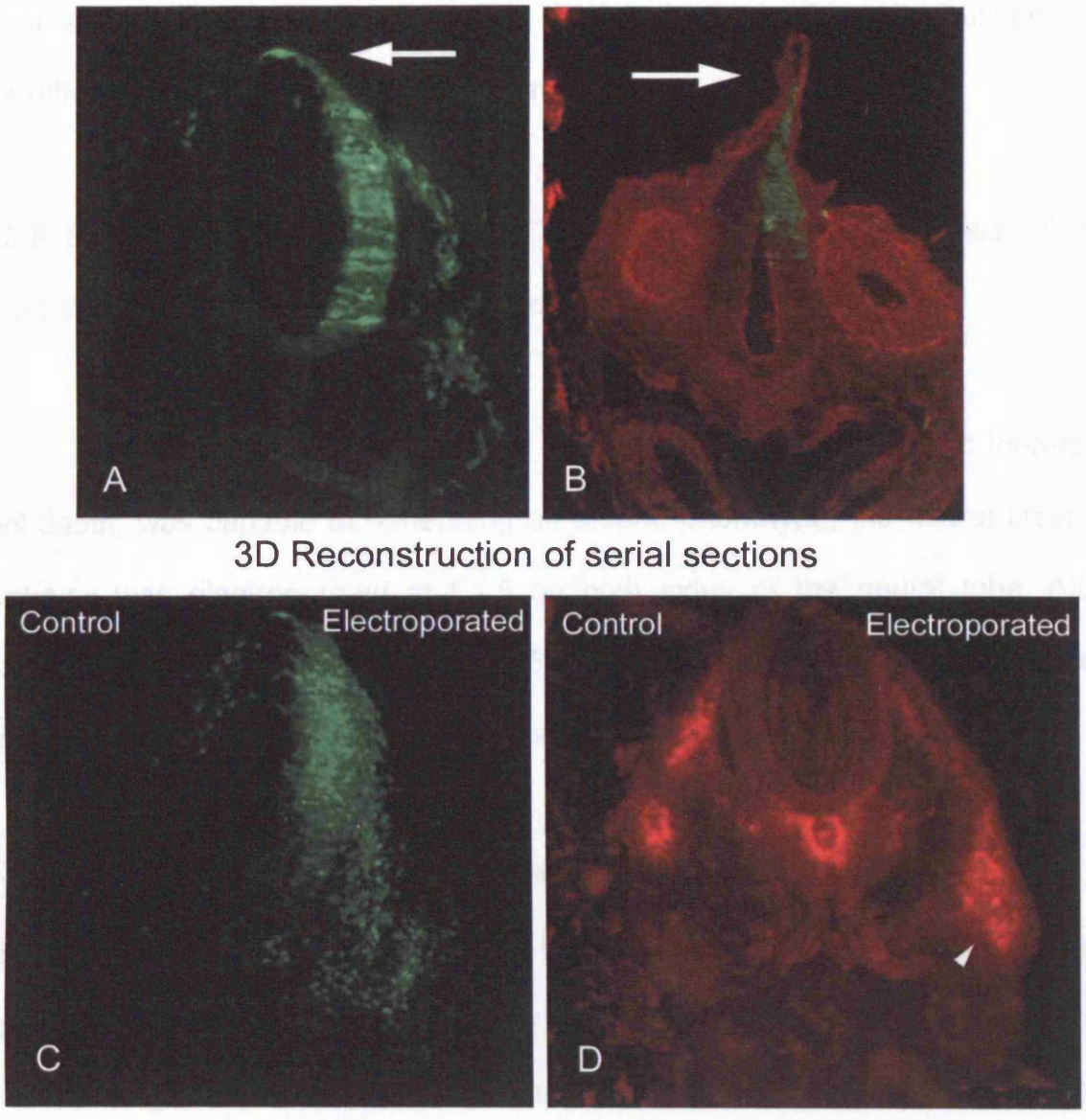

Figure 4.10: Electroporation with Caspase-9DN results in an abnormal neural tube and increased NCC numbers.

(A) Control electroporations retained the rounded appearance of the dorsal aspect of the neural tube (arrow) at E2.5. (B) However, Caspase-9DN electroporated embryos exhibited a pronounced protrusion from the dorsal midline in the region of electroporation (arrow). (C,D) 3D reconstruction of serial cryostat sections from a Caspase-9DN electroporated embryo. (C) GFP was expressed on the right-hand side indicating successful electroporation, the left-hand side serves as a control. (D) HNK-1 staining for migratory neural crest cells revealed more neural crest cells on the electroporated side (arrowhead) in comparison to the control side.

serial sections was used to generate a model which could be manipulated and the differences between populations compared.

4.2.6 Electroporation with Caspase-9DN results in hyperganglionosis of the foregut: (The number of embryos studied was 4)

To investigate whether inhibiting the activity of caspase-9, and therefore cell death, was capable of generating an enteric phenotype, the neural crest of embryos was electroporated at E1.5 on both sides of the neural tube. After screening, embryos were left until E14.5, at which time their guts were dissected and prepared for NADPH staining as described in methods **section 2.10**.

50% (2 of 4) of the animals which survived to this late stage (E14.5) displayed an enteric phenotype. Whilst the hindgut and midgut of these animals appeared normal when compared to controls their foreguts were distinctly different **(Fig 4.11)**. The oesophagus and crop of Caspase-9DN electroporated animals displayed hyperganglionosis. This hyperganglionosis appears as a network of ganglia of greater size and number than that present in controls. Despite these changes in number and size the overall pattern of ganglia appeared relatively normal possessing a honeycomb like structure.

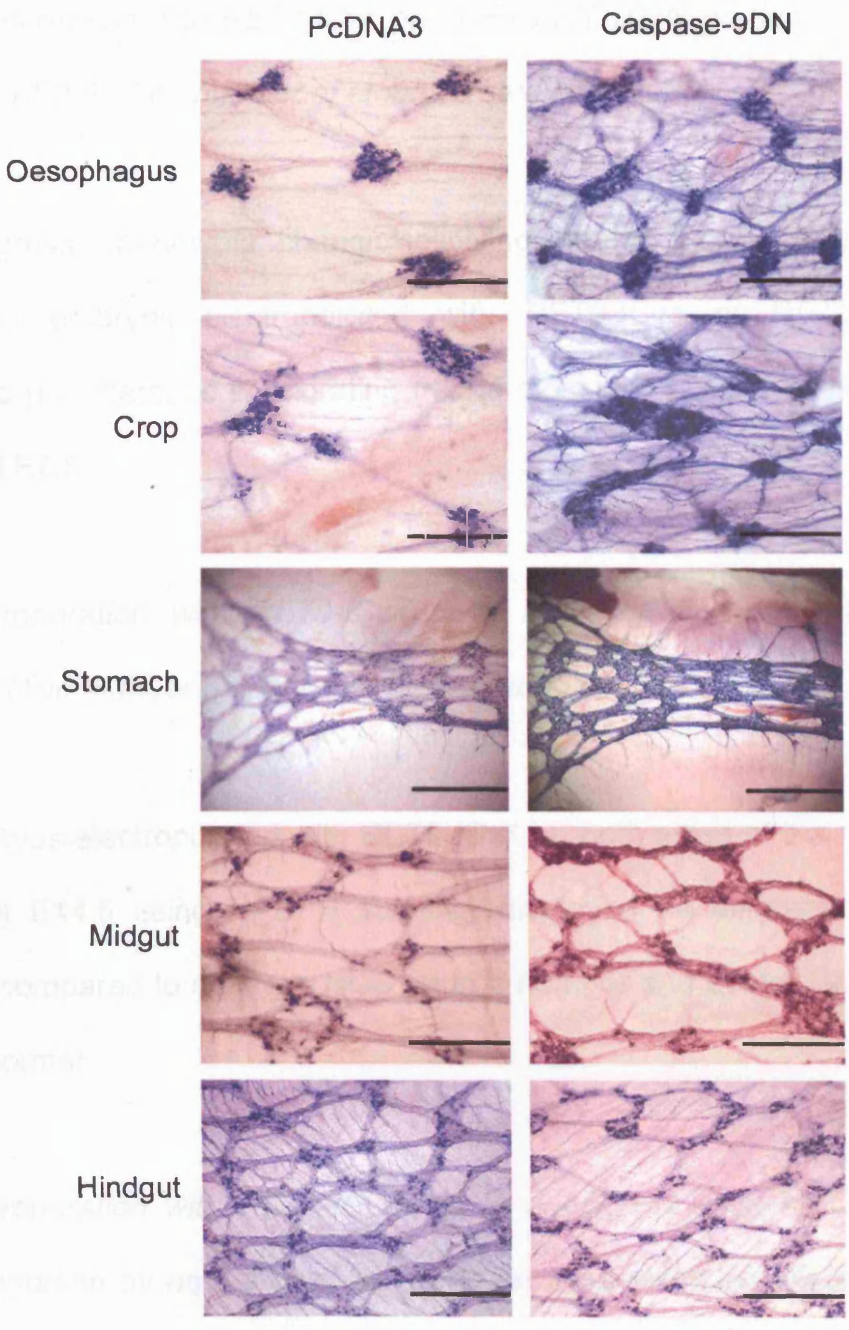

Figure 4.11: Caspase-9DN treated embryos display hyperganglionosis of the foregut.

Caspase-9DN electroporated embryos shown in the right-hand column display hyperganglionosis of the oesophagus when compared to controls (left column). This hyperganglionosis does not continue along the full length of the gut; cell numbers appear normal in the midgut and hindgut.
Scale Bars: 20µm excluding stomach 1mm

4.2.7 Electroporation with RET9-ICwt and RET9-ICD707N produce no apparent phenotype at E2.5: (The number of embryos studied was 20)

No gross phenotypic change involving neural tube morphology was observed in embryos electroporated with RET9-ICwt or RET9-ICD707N. Furthermore no difference in migrating neural crest cell number or position was observed at E2.5.

4.2.8 Electroporation with RET9-ICwt does not produce a different enteric phenotype: (The number of embryos studied was 5)

Embryos electroporated with RET9-ICwt on both sides of the neural tube, analysed at E14.5 using NADPH staining, displayed no difference in enteric phenotype compared to controls. NOS neuron number and overall ENS structure appeared normal.

4.2.9 Electroporation with RET9-ICD707N in quail/chick chimeras results in a delay of migration by neural crest cells and an associated ectopic plexus: (The number of embryos studied was 3)

As the GFP marker had been demonstrated to be diluted out of the NCC by E8 due to their highly proliferative nature, attempts were made to combine the electroporation procedure with a quail/chick interspecies graft. This was done to enable both highly specific targeting of the vagal crest, and the subsequent tracing of these cells using the anti-quail cell antibody QCPN.

Electroporated / grafted embryos were assessed by immunohistochiemical staining using the QCPN marker on cryosections.

Data were acquired for PcDNA3 and RET9-ICD707N graft/electroporation combinations. PcDNA3 electroporated embryos appeared normal with no change in neural crest number or in their spatiotemporal colonisation of the gut. Embryos electroporated with RET9-ICD707N displayed a delay in colonisation of the gut **(Fig 4.12 A-H)**. In addition to this delay ectopic cells were observed in E9.5 and E12.5 embryos **(Fig 4.12 I,J)**. These ectopic cells were located in the mucosal layer below the submucosal plexus and appeared to be forming an additional ectopic plexus.

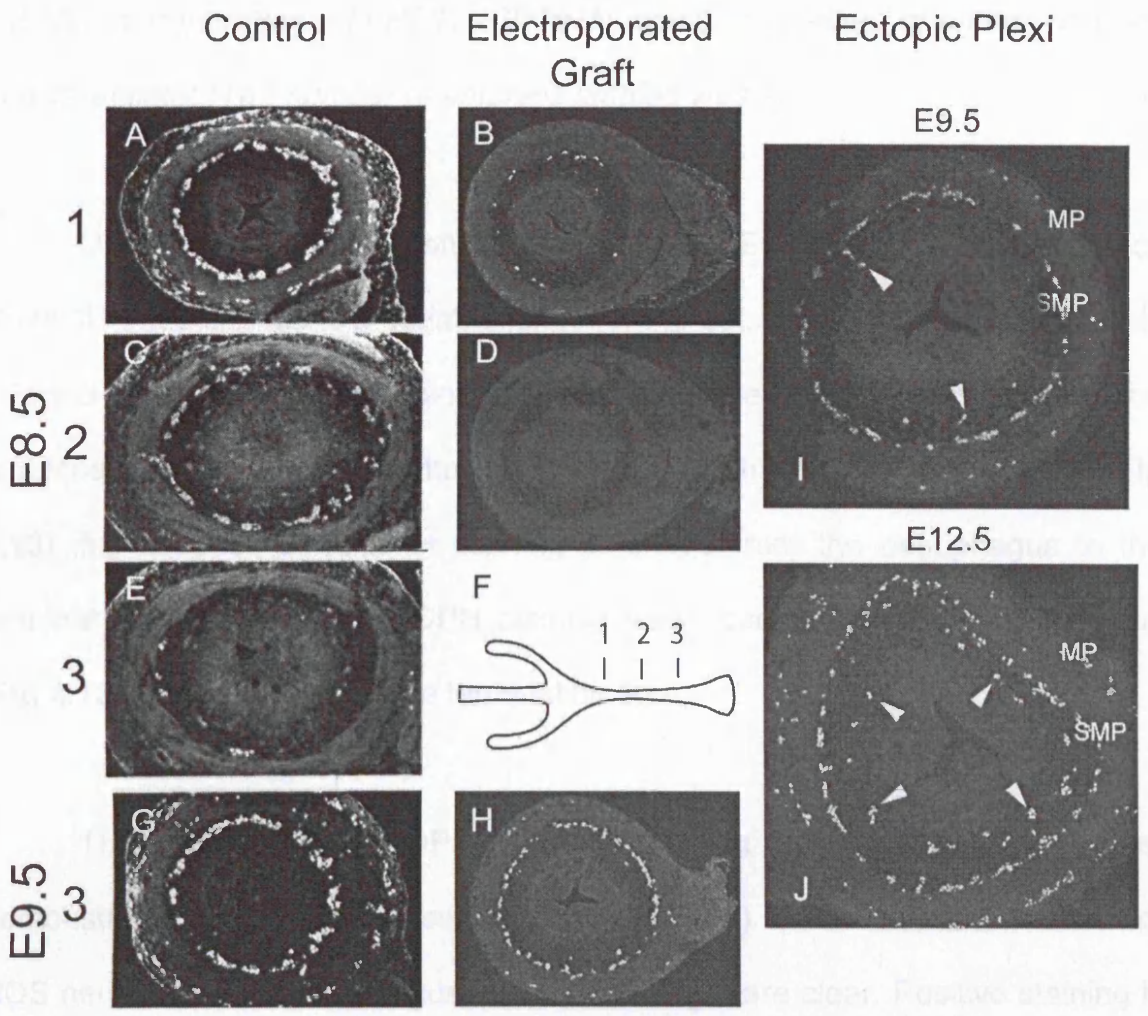

Figure 4.12: Migrational delay of enteric precursors in quail/chick electroporations

(A,C,E) sections of hindgut regions corresponding to those indicated in (F) taken from quail/chick grafts at E8.5. (A) At position 1, QCPN positive cells were present in the submucosal and myenteric plexi. Migration of neural crest cells from the submucosal to myenteric plexus was just beginning at position 2 (C). At the most terminal level QCPN positive cells were present in the submucosal plexus (E). In comparison, tissue from a RET9-ICD707N electroporated graft at position 1 contained only a few cells in the submucosal plexus and none in the myenteric. No QCPN positive cells were found caudal of position 2. At E9.5, QCPN positive cells were present in the terminal hindgut of electroporated embryos (H) and were migrating towards the myenteric plexus. (I,J) show ectopic plexi within electroporated gut arising from centripetal migration from the submucosal plexus.

4.2.10 Electroporation with RET9-ICD707N results in a failure of enteric neurons to differentiate: (The number of embryos studied was 7)

Of the embryos successfully incubated until E14.5, 80% displayed a lack of NADPH staining along a variable length of the gut. The region most commonly affected extended from a point approximately one centimetre caudal to the duodenal junction with the stomach, to the caecum. In the most severe case **(Fig 4.13)** this absence of NADPH staining extended from the oesophagus to the terminal hindgut. Limited NADPH staining was observed in the proventriculus **(Fig 4.13 B)** and one half of the terminal hindgut.

The absence of NADPH positive staining in these guts is further demonstrated using flatmounted sections **(Fig 4.14)** In this instance the lack of NOS neurons in the oesophagus, crop, and midgut are clear. Positive staining is present in the stomach although it appears weaker and reduced. In the terminal hindgut NADPH staining appears comparable to the control.

Occasional isolated populations of NOS neurons could be seen amidst the long stretches of otherwise NADPH staining deficient regions of gut **(Fig 4.15)**. These "islands" ranged in size from single rings of ganglia **(Fig 4.15 E)** to long regions of 20mm which were restricted to one side of the gut **(Fig 4.15 A-D)**. In a number of the embryos recovered, the terminal hindgut contained NOS neurons despite the majority of the mid and hindgut lacking them. The transitional zone between these two regions shows quite an abrupt front **(Fig 4.15 F)**.

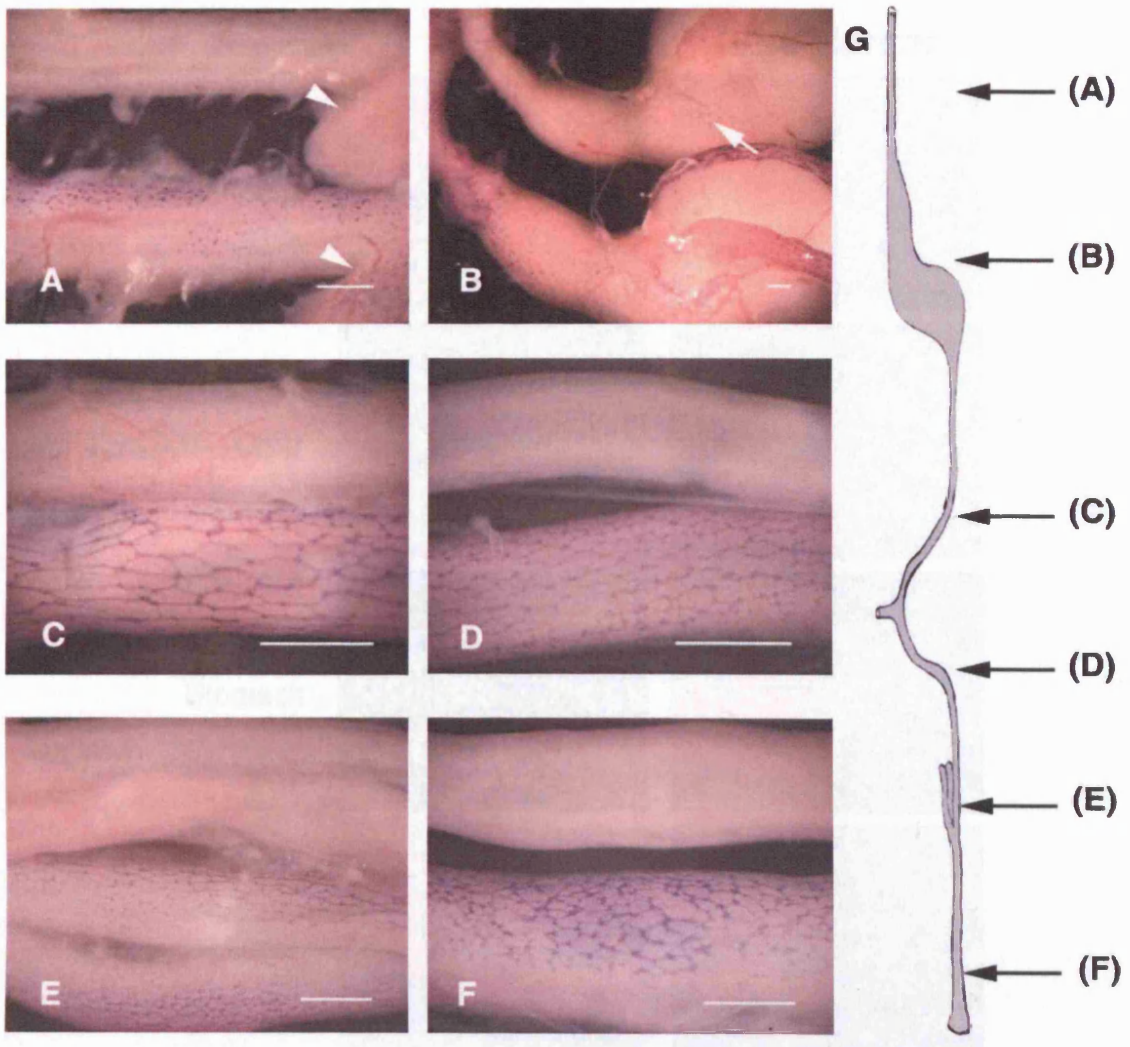

Fig 4.13: Absence of NADPH staining in RET9IC-D707N electroporated embryos:

Panels A-F compare control (bottom tissue) against D707N with severe aganglionosis (top tissue). A-F correspond to regions marked in panel G. A,C-F show normal NOS neuron networks stained by NADPH arranged in a web-like formation. In comparison the D707N tissue in these panels appear pale and devoid of NADPH staining indicating the absence of NOS neurons. B shows normal staining in the stomach of the control and positive staining of NADPH in the stomach and proventriculus. The stomach also appear to be smaller in the D707N embryo.
(Scale bars = 1mm)

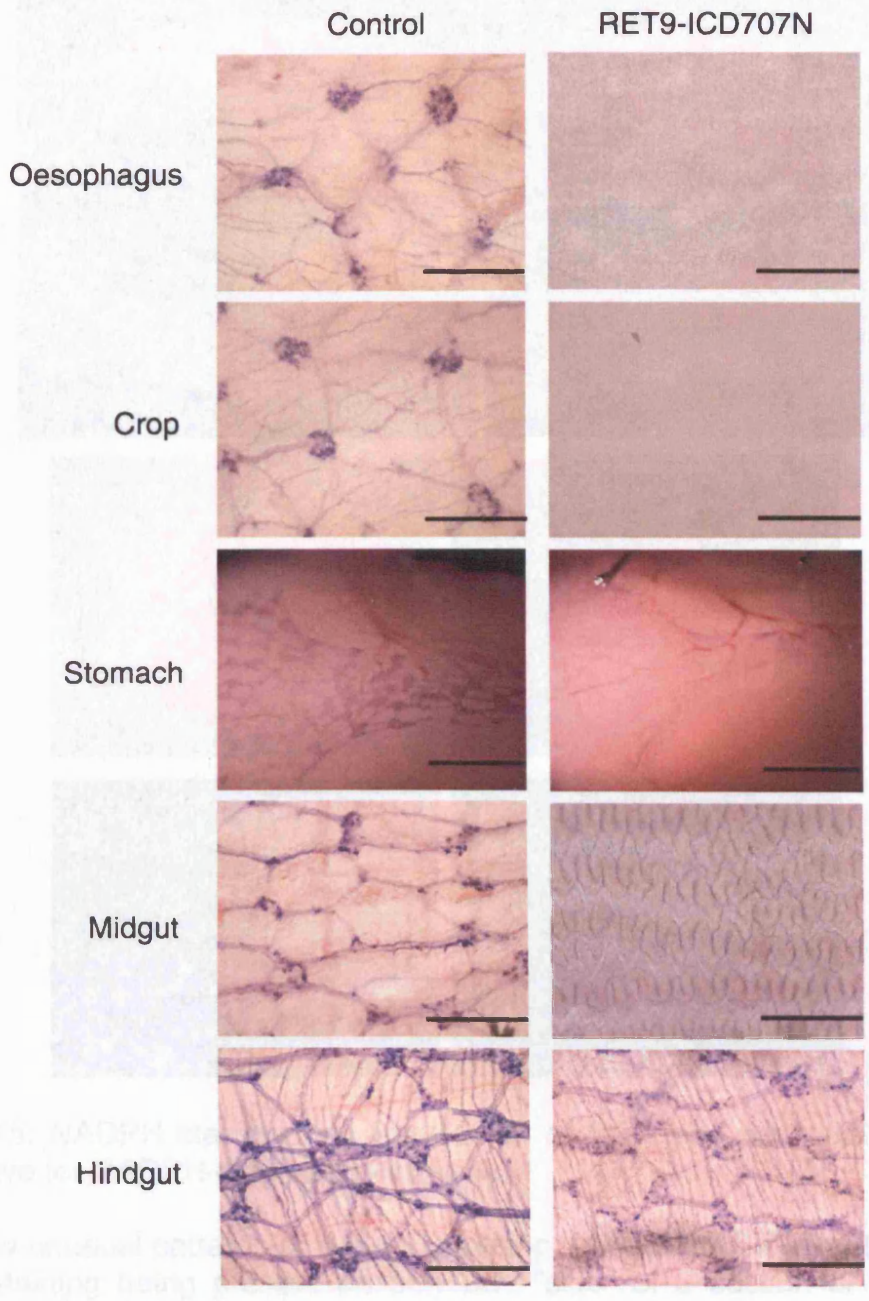

Fig 4.14: Flatmounts of E14.5 RET9-ICD707N electroporated gut compared to controls, staining with NADPH for NOS neurons:

At E14.5 control embryos (Left hand column) display strong positive NADPH staining along the full length of the gut . In comparison, oesophagus, crop and midgut of RET-ICD707N electroporated embryos (right hand column) lack NOS neurons. Whilst positive staining is found in the stomach and hindgut of these RET9-ICD707N embryos, it is weaker and fewer cells are apparent.
Scale Bars: 20μm excluding stomach 1mm

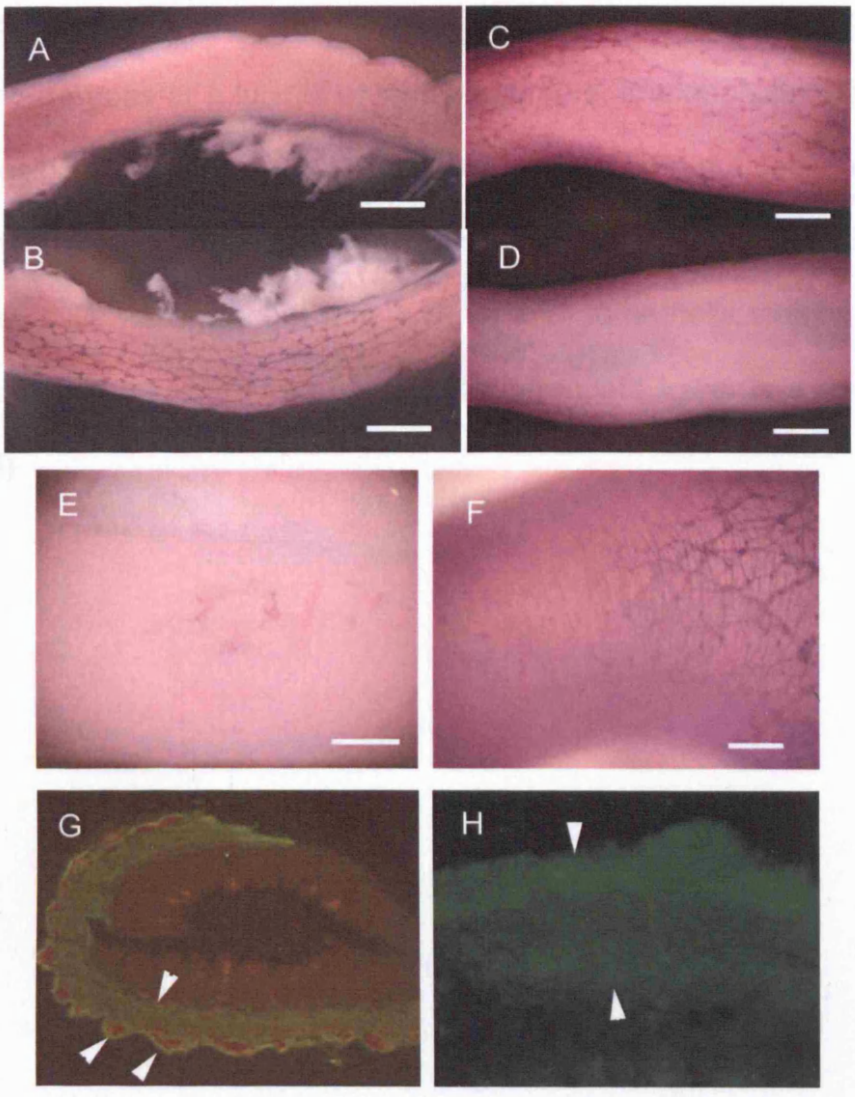

Figure 4.15: NADPH staining and expression of NCC and neuronal markers in gut negative for NADPH-diaphorase staining.

(A-F) show unusual patterns of NADPH staining. (A/B) and (C/D) are examples of NADPH staining being present on only one "side" of a section of midgut and hindgut respectively. (E) illustrates the appearance of an NADPH staining "island" consisting of a single ring of ganglia. (F) the transition zone between NADPH negative gut and NADPH positive terminal hindgut.
(G) immunohistochemical staining for $p75^{NT}R$ (red) and αSMA (green) illustrate that neural crest derived cells were located in the myenteric and submucosal plexi of NADPH negative gut (arrowheads). (H) furthermore these cells were very weakly expressing PGP9.5, a neuronal differentiation marker (arrowheads).
(Scale bars (A-F) = 1mm.)

To investigate whether this lack of NADPH staining indicated a lack of differentiated neurons or a lack of enteric precursors, immunohistochemistry was performed using antibodies against $p75^{NTR}$ and PGP9.5 on gut sections **(Fig 4.15 G,H)**. Such staining revealed that in regions lacking NADPH reactivity neural crest derived cells were present **(Fig 4.15 G)** and some cells stained weakly for PGP9.5 indicating that they had begun to differentiate towards a neuronal fate **(Fig 4.15 H)**.

4.3 Discussion:

In this study the *in vivo* role of RET as a dependence receptor was investigated using electroporation of chick vagal neural crest to introduce constructs designed to perturb this proposed pathway. In order to compare RET expression with the location of apoptotic cells in the early chick embryo *in situ* hybridisation and Tunel staining techniques were employed.

Although the receptor tyrosine kinase RET has a well established role in ENS development as a receptor for the trophic ligand GDNF (Durbec et al. 1996a; Natarajan et al. 2002) there is strong evidence for RET functioning as a dependence receptor *in vitro* (Bordeaux et al. 2000). However, the idea that RET could function as a dependence receptor had not been tested *in vivo* to date. Apoptosis has not been associated with the development of NCC derived enteric precursors, the extensive proliferation required to fully populate the gut from such a small initial migratory pool makes such an association counter-intuitive. Therefore, it was first necessary to confirm the existence of apoptosis within enteric precursor cell populations and to correlate this to the expression of RET in these same populations of cells.

In situ hybridisation using probes for *ret* revealed a strong expression domain in the neural tube between Rhombomere 6 and somite 5. This domain overlaps with the location of vagal neural crest formation. Similar analysis by Robertson et al concurs with this finding. These authors describe expression in

this region extending caudally to somite 7 (Robertson et al. 1995). In addition to this domain, Robertson et al reported expression within the nephritic ducts and at the boundary of Rhombomeres 3 and 4. It is possible that no *ret* expression was observed in the nephritic ducts in this work due to insufficient permeabilisation of the chick embryo which displays a robustness to this procedure.

To complement the *ret in situ* data, Tunel staining was performed to compare *ret* expression with apoptosis in the developing embryo. Here the use of Tunel staining at HH10 revealed apoptotic cells along the neural tube in the region of the forming vagal derived neural crest and at the boundary of Rhombomeres 3 and 4. This correlates with *ret* expression patterns seen here and in previous work (Homma et al. 2000; Schiltz, Benjamin, and Epstein 1999). No apoptotic cells were observed in the region of the nephritic ducts, a region of *ret* expression as described by Homma. This may be due to the presence of RET's receptor GDNF in these structures (Homma et al. 2000). GDNF was not found to be expressed in the neural tube and so it remains a possibility that the apoptosis present in the midline arises as a result of the proposed dependence receptor mechanism.

Tunel positive cells were present in the streams of migrating NCC, as suggested by *sox10* positive *in situ,* around the otic vesicle at E2.5. Sox10 positive NCC were located in the second pharyngeal arch and presumptive foregut regions. *ret* positive neural crest derived cells were present in the first and second pharyngeal arches and the presumptive foregut. GDNF expression was found at the boundaries between the pharyngeal arches and foregut mesoderm

(Homma et al. 2000) correlating nicely with those regions of *ret* expression which did not overlap with Tunel staining.

The patterns of *ret* expression at E3.5 and E4.5 revealed an interesting pattern which may influence the migratory behaviour of ENS precursors. Most clearly shown at E4.5, the expression of *ret* by migrating ENS precursors was restricted to the caudal most cells at the wavefront of colonisation. ENS precursors throughout the oesophagus and stomach were *sox10* positive but lacked *ret* expression. In mice, strong *ret* expression persists within cells behind the migration wavefront (Pachnis, Mankoo, and Costantini 1993). However, only a subset of vagal derived neural crest cells express RET in the first instance in the mouse (Anderson, Stewart, and Young 2005). This suggests a fundamental difference in the regulation of RET expression between the mouse and chick models.

Electroporation is a well-established method for introducing genetic material to the chick at early embryonic stages. Considerable effort was made here to ensure that the physical procedure of electroporation did not affect the development of the neural crest or other tissues. In validation experiments, the GFP reporter expressed strongly within vagal NCC populations and could be detected in tissues six days after electroporation. GFP labelled cells migrated along previously described pathways with no deviation in developmental timing or target location. Later embryos showed no clear difference in ENS formation when assessed with NADPH staining for NOS neurons at E14.5. Thus it can be

concluded that electroporation is an effective and accurate method for introducing DNA into NCC within chick embryos with no undesired side-effects.

The Caspase-9DN construct was used to investigate the effect of reducing cell death in developing neural crest cell populations. At E2.5, NCC were more numerous on the side of embryos electroporated with Caspase-9DN compared with the control side. At E14.5 hyperganglionosis of the oesophagus and crop was observed using NADPH staining compared to PcDNA3 electroporated controls. This confirms the apoptosis observed in the Tunel staining described earlier and implicates capase-9 in the activation of an effector caspase (caspase-3) by an unspecified means.

Caspase-9 was shown to be required for the cleavage of RET *in vitro* (Bordeaux et al. 2000), but these results cannot implicate RET in the apoptosis seen here as caspase-9 is involved downstream of the RET receptor and may interact with other proteins. The restriction of hyperganglionosis arising from Caspase-9DN electroporation to the foregut may be as a result of the plasmid expressing the caspase-9DN construct being diluted out in the rapidly proliferating NCC population. The protocol establishing experiments revealed that GFP expression was only maintained until E8 at the latest and few GFP cells were rarely observed caudal to the stomach. Use of a retroviral capase-9DN vector could result in a hyperganglionosis of the entire ENS.

The unusual morphology of the surface ectoderm and dorsal neural tube suggests a morphological reason for apoptosis occurring at the HH10 stage.

Apoptosis of cells in this region may be required for the separation of the overlying ectoderm from the forming mesenchymal tissue. Removal of the apparatus required for this prevents accurate sculpting of this region and leads to a protruding ridge in the affected area.

Experiments were performed with the RET9IC-wt construct to test the hypothesis that ectopic expression of this intracellular domain would provide sufficient substrate for active caspase-3 to cleave and release the apoptotic fragment as seen *in vitro* (Bordeaux et al. 2000). However, no change in NCC number or in the structure of the ENS was observed.

Endogenous RET levels were not altered in any way during the experiment, nor were the receptor domains blocked. Thus any intrinsic survival signals which NCCs were transducing may have overridden the apoptotic signal from the introduced RET9IC-wt. The only cells that might have been affected in this case would have been non-RET expressing cells in the surrounding tissue, such as the mesenchyme, but no gross change in the survival of these cells was noted. Introduction of small interfering RNAs (siRNAs) to full length RET or GDNF at the same time as RET9IC-wt may circumvent this effect should it be occurring. The siRNA would inhibit translation of the target mRNA and remove the supportive signalling.

Use of such a technique would result in a RET9 deficient phenotype which past experiments using mice have demonstrated to result in an aganglionic phenotype (de Graaff et al. 2001). It may be impossible to restrict RET inhibition

to the timeframe in which it is hypothesised that it plays a part in regulating apoptosis and not functioning in a chemotactic role.

The RET9IC-D707N construct was intended to serve as a control for the RET9IC-wt containing plasmid. However, at E8.5, E9.5 and E14.5 embryos electroporated with RET9IC-D707N displayed a delay in migration and differentiation of vagal derived NCC enteric precursors. Electroporated quail-chick grafts at E8.5 possessed a wavefront of vagal derived enteric precursors several millimetres behind control electroporated grafts. Whilst cells had successfully migrated to the submucosal and myenteric plexi at the most caudal end of the gut by E14.5, NADPH staining revealed that cells had not yet differentiated to a terminal neuronal phenotype.

A possible cause of the delay in migration and subsequently differentiation of these cells could be due to interaction of the endogenous RET with the electroporated RET9IC-D707N. If these receptors were, for example, forming a heterodimer, then the autophosphorylation of RET and subsequent downstream signalling could be adversely affected. Such an interaction should not result in cell death either as the inappropriate binding of the two alleles would alter the conformation of the endogenous RET intracellular domain and mask the caspase-sensitive cleavage sites. The mutation at position 707 is 55 residues upstream of the nearest documented mutation that induces a loss of kinase activity (Manie et al. 2001). To investigate this, co-immunoprecipitation experiments using antibodies to the full length RET extracellular domain and a

tag on RET9IC-D707N would reveal whether ligand-independent binding between the two alleles is occurring.

The apparent ectopic plexus seen in the quail/chick electroporated grafts is difficult to interpret in light of its absence from electroporations of RET9IC-D707N into chicks. It may be that this effect is secondary and results from additional delay in the migration of the neural crest cells in the grafted embryos which leads to a failure of these cells to respond correctly to environmental cues.

Concluding Statement:

The work contained within this thesis addresses two separate issues concerning ENS development. Whilst the immunohistochemical analysis of the formation of a normal functioning ENS in humans stands as a complete work, the investigation into RET's role as a dependence receptor has developed into the beginning of a larger body of work requiring further analysis to fully dissect the potential roles of RET during ENS development.

Characterising spatiotemporal pattern of colonisation and development of the gastrointestinal tract with respect to the ENS, ICCs, and smooth muscle in the human revealed similarities between human patterns and that of mammalian models. Whilst some of the timepoints used in this study overlap with similar works there are significant differences in the findings between the studies. It would be interesting to now go on to use this information to investigate the signals and physical boundaries controlling neural crest colonisation of the gut. Using tissue culture methods to grow lengths of human gut alongside a source of ENS precursors, the precise window for the successful migration and development of NCC into a functioning ENS may be found. It may be possible to use this knowledge to develop cell-based therapies for ENS defects such as Hirschsprung's disease and achalaisa. Knowing which signalling molecules are required to promote sufficient proliferation of introduced ENS precursors to aganglionic gut and their subsequent differentiation would be key to this. Understanding the physical limitations to ENS precursor migration would provide an indication of the best locations / physical spacing to inject such cells.

The second part of this thesis, investigating the role of RET as a dependence receptor in ENS formation, produced some interesting and yet confounding results. Certainly further work is required to address the issues of interaction between endogenous RET and introduced, truncated alleles of RET. The multiple roles of RET in survival, migration, and apoptosis mean that investigating any one function without disrupting the others is very complex. Interactions between RET alleles may adversely affect downstream signalling or autophosphorylation of the protein. Although the role of RET as a dependence receptor gains no direct support from *in vivo* work, the circumstantial evidence is mounting. Apoptosis and RET expression co-inciding at appropriate timepoints and the demonstration that capase-9 dependent apoptosis occurs within early vagal neural crest populations, can only serve to increase support for RET playing a dependence receptor role *in vivo*.

Given sufficient time to continue this investigation, there are a number of key areas one would wish to address; the lack of a phenotype using RET9IC-wt and the delay in migration and differentiation seen with RET9IC-D707N would be ideal starting points. Although the phenotype observed with RET9IC-D707N is very interesting, the more important of these two points to resolve would be the generation of a RET9IC-wt phenotype. To do so electroporation of siRNAs specific to the full length form of RET should be performed in conjunction with electroporation of the RET9IC-wt plasmid. This technique would adversely affect the chemotactic roles of RET later in development compounding possible phenotypes and making analysis of late stages challenging. However, the use of this technique to observe initial changes in neural crest cell number at E2.5 in the

manner used for the Caspase-9DN construct seems valid. Successful electroporation of these constructs could result in increased apoptosis in the forming vagal neural crest. Removal of endogenous RET transduced survival signals would allow the cleavage of the introduced RET allele to induce cell death via release of the pro-apoptotic fragment. This could then be rescued by electroporating Caspase-9DN at the same time point. The use of three modifying constructs and a reporter gene would present a significant technical challenge, especially if each was on a separate construct. The combination of two or more constructs into a single plasmid would probably be necessary to convince critics of the ability to target large numbers of individual cells with all of the required factors.

Approaching the second component of this investigation with the benefit of hindsight, significant changes to the systems employed would be used. The use of late stage embryonic material to investigate ENS phenotypes was unwise lacking sufficient data concerning changes to the initial neural crest cell populations when subjected to electroporation. By employing an *in vivo* approach to the early effects of the various constructs quantitative observations were restricted and the acquisition of data was substantially more difficult than by certain *in vitro* methods. The initial data concerning cell number and behaviour within targeted vagal neural crest cell populations should be done using neural tube cultures allowing time-lapse photography of the behaviour of these cells and easy quantification of cell number and migration ability as determined by speed and distance. Full *in vivo* experimentation should then be persued with sufficient supporting data from these experiments.

The constructs themselves would ideally be redesigned to incorporate an IRES site and associated GFP sequence to guarantee association between GFP expression and the presence of the test construct. In the event that the construct proved too large to read through the IRES site reliably then a tag such as a triple Myc sequence should be attached to the experimental construct to allow identification by antibody staining.

References

Airaksinen MS and Saarma M (2002) The GDNF family: signalling, biological functions and therapeutic value. *Nat.Rev.Neurosci.* 3 (5):383-394.

Albertin G et al (1996) Fine mapping of the human endothelin-converting enzyme gene by fluorescent in situ hybridization and radiation hybrids. *Biochem.Biophys.Res.Commun.* 221 (3):682-687.

Amiel J et al (2001) Large-scale deletions and SMADIP1 truncating mutations in syndromic Hirschsprung disease with involvement of midline structures. *Am.J.Hum.Genet.* 69 (6):1370-1377.

Amiel J et al (2003) Polyalanine expansion and frameshift mutations of the paired-like homeobox gene PHOX2B in congenital central hypoventilation syndrome. *Nat.Genet.* 33 (4):459-461.

Anderson RB, Stewart AL, and Young HM (2005) Phenotypes of neural-crest-derived cells in vagal and sacral pathways. *Cell Tissue Res.*:1-15.

Arinami T et al (1991) Chromosomal assignments of the human endothelin family genes: the endothelin-1 gene (EDN1) to 6p23-p24, the endothelin-2 gene (EDN2) to 1p34, and the endothelin-3 gene (EDN3) to 20q13.2-q13.3. *Am.J.Hum.Genet.* 48 (5):990-996.

Attie T et al (1995) Diversity of RET proto-oncogene mutations in familial and sporadic Hirschsprung disease. *Hum.Mol.Genet.* 4 (8):1381-1386.

Attie-Bitach T et al (1998) Expression of the RET proto-oncogene in human embryos. *Am.J.Med.Genet.* 80 (5):481-486.

Ayme S and Philip N (1995) Possible homozygous Waardenburg syndrome in a fetus with exencephaly. *Am.J.Med.Genet.* 59 (2):263-265.

Badner JA et al (1990) A genetic study of Hirschsprung disease. *Am.J.Hum.Genet.* 46 (3):568-580.

Baetge G, Schneider KA, and Gershon MD (1990) Development and persistence of catecholaminergic neurons in cultured explants of fetal murine vagus nerves and bowel. *Development* 110 (3):689-701.

Ball DW et al (1993) Identification of a human achaete-scute homolog highly expressed in neuroendocrine tumors. *Proc.Natl.Acad.Sci.U.S.A* 90 (12):5648-5652.

Baloh RH et al (2000) The GDNF family ligands and receptors - implications for neural development. *Curr.Opin.Neurobiol.* 10 (1):103-110.

Baloh RH et al (1997) TrnR2, a novel receptor that mediates neurturin and GDNF signaling through Ret. *Neuron* 18 (5):793-802.

Barnett MW et al (2002) Signalling by glial cell line-derived neurotrophic factor (GDNF) requires heparan sulphate glycosaminoglycan. *J.Cell Sci.* 115 (Pt 23):4495-4503.

Baynash AG et al (1994) Interaction of endothelin-3 with endothelin-B receptor is essential for development of epidermal melanocytes and enteric neurons. *Cell* 79 (7):1277-1285.

Benailly HK et al (2003) PMX2B, a new candidate gene for Hirschsprung's disease. *Clin.Genet.* 64 (3):204-209.

Benedeczky I, Fekete E, and Resch B (1993) Ultrastructure of the developing muscle and enteric nervous system in the small intestine of human fetus. *Acta Physiol Hung.* 81 (2):193-206.

Bloch KD et al (1989) cDNA cloning and chromosomal assignment of the gene encoding endothelin 3. *J.Biol.Chem.* 264 (30):18156-18161.

Bondurand N et al (1999) A molecular analysis of the yemenite deaf-blind hypopigmentation syndrome: SOX10 dysfunction causes different neurocristopathies. *Hum.Mol.Genet.* 8 (9):1785-1789.

Bordeaux MC et al (2000) The RET proto-oncogene induces apoptosis: a novel mechanism for Hirschsprung disease. *EMBO J.* 19 (15):4056-4063.

Borrello MG et al (1995) RET activation by germline MEN2A and MEN2B mutations. *Oncogene* 11 (11):2419-2427.

Brandt CT, Tam PK, and Gould SJ (1996) Nitrergic innervation of the human gut during early fetal development. *J.Pediatr.Surg.* 31 (5):661-664.

Bredesen DE, Mehlen P, and Rabizadeh S (2005) Receptors that mediate cellular dependence. *Cell Death.Differ.* 12 (8):1031-1043.

Britsch S et al (2001) The transcription factor Sox10 is a key regulator of peripheral glial development. *Genes Dev.* 15 (1):66-78.

Burns AJ (2005) Migration of neural crest-derived enteric nervous system precursor cells to and within the gastrointestinal tract. *Int.J.Dev.Biol.* 49 (2-3):143-150.

Burns AJ, Champeval D, and Le Douarin NM (2000) Sacral neural crest cells colonise aganglionic hindgut in vivo but fail to compensate for lack of enteric ganglia. *Dev.Biol.* 219 (1):30-43.

Burns AJ, Delalande JM, and Le Douarin NM (2002) In ovo transplantation of enteric nervous system precursors from vagal to sacral neural crest results in extensive hindgut colonisation. *Development* 129 (12):2785-2796.

Burns AJ and Le Douarin NM (1998) The sacral neural crest contributes neurons and glia to the post-umbilical gut: spatiotemporal analysis of the development of the enteric nervous system. *Development* 125 (21):4335-4347.

Burns AJ et al (1997) Interstitial cells of Cajal in the guinea-pig gastrointestinal tract as revealed by c-Kit immunohistochemistry. *Cell Tissue Res.* 290 (1):11-20.

Burns AJ and Le Douarin NM (2001) Enteric nervous system development: analysis of the selective developmental potentialities of vagal and sacral neural crest cells using quail-chick chimeras. *Anat.Rec.* 262 (1):16-28.

Burns AJ, Pasricha PJ, and Young HM (2004) Enteric neural crest-derived cells and neural stem cells: biology and therapeutic potential. *Neurogastroenterol.Motil.* 16 Suppl 1:3-7.

Cacalano G et al (1998) GFRalpha1 is an essential receptor component for GDNF in the developing nervous system and kidney. *Neuron* 21 (1):53-62.

Cacheux V et al (2001) Loss-of-function mutations in SIP1 Smad interacting protein 1 result in a syndromic Hirschsprung disease. *Hum.Mol.Genet.* 10 (14):1503-1510.

Cantrell VA et al (2004) Interactions between Sox10 and EdnrB modulate penetrance and severity of aganglionosis in the Sox10Dom mouse model of Hirschsprung disease. *Hum.Mol.Genet.*

Carrasquillo MM et al (2002) Genome-wide association study and mouse model identify interaction between RET and EDNRB pathways in Hirschsprung disease. *Nat.Genet.* 32 (2):237-244.

Carter CO, Evans K, and Hickman V (1981) Children of those treated surgically for Hirschsprung's disease. *J.Med.Genet.* 18 (2):87-90.

Cecconi F et al (1998) Apaf1 (CED-4 homolog) regulates programmed cell death in mammalian development. *Cell* 94 (6):727-737.

Chalazonitis A et al (2004) Bone morphogenetic protein-2 and -4 limit the number of enteric neurons but promote development of a TrkC-expressing neurotrophin-3-dependent subset. *J.Neurosci.* 24 (17):4266-4282.

Chalazonitis A et al (1998a) Age-dependent differences in the effects of GDNF and NT-3 on the development of neurons and glia from neural crest-derived precursors immunoselected from the fetal rat gut: expression of GFRalpha-1 in vitro and in vivo. *Dev.Biol.* 204 (2):385-406.

Chalazonitis A et al (1998b) Age-dependent differences in the effects of GDNF and NT-3 on the development of neurons and glia from neural crest-derived precursors immunoselected from the fetal rat gut: expression of GFRalpha-1 in vitro and in vivo. *Dev.Biol.* 204 (2):385-406.

Chalazonitis A et al (1994) Neurotrophin-3 induces neural crest-derived cells from fetal rat gut to develop in vitro as neurons or glia. *J.Neurosci.* 14 (11 Pt 1):6571-6584.

Chalazonitis A et al (1998c) Promotion of the development of enteric neurons and glia by neuropoietic cytokines: interactions with neurotrophin-3. *Dev.Biol.* 198 (2):343-365.

Cheung M and Briscoe J (2003) Neural crest development is regulated by the transcription factor Sox9. *Development* 130 (23):5681-5693.

Creedon DJ et al (1997) Neurturin shares receptors and signal transduction pathways with glial cell line-derived neurotrophic factor in sympathetic neurons. *Proc.Natl.Acad.Sci.U.S.A* 94 (13):7018-7023.

Cremazy F et al (1998) Further complexity of the human SOX gene family revealed by the combined use of highly degenerate primers and nested PCR. *FEBS Lett.* 438 (3):311-314.

de Graaff E et al (2001) Differential activities of the RET tyrosine kinase receptor isoforms during mammalian embryogenesis. *Genes Dev.* 15 (18):2433-2444.

Decker RA and Peacock ML (1998) Occurrence of MEN 2a in familial Hirschsprung's disease: a new indication for genetic testing of the RET proto-oncogene. *J.Pediatr.Surg.* 33 (2):207-214.

Decker RA, Peacock ML, and Watson P (1998) Hirschsprung disease in MEN 2A: increased spectrum of RET exon 10 genotypes and strong genotype-phenotype correlation. *Hum.Mol.Genet.* 7 (1):129-134.

Deckwerth TL et al (1996) BAX is required for neuronal death after trophic factor deprivation and during development. *Neuron* 17 (3):401-411.

Delalande, J. M., Cooper, J., and Burns, A. J. Investigation of the signalling mechanisms involved in the development of sacral neural crest-derived enteric nervous system precursors. Neurogastroenterology and Motility 15 (2), 197. 2003.

Denny P et al (1992) A conserved family of genes related to the testis determining gene, SRY. *Nucleic Acids Res.* 20 (11):2887.

Donovan MJ et al (1996) Identification of an essential nonneuronal function of neurotrophin 3 in mammalian cardiac development. *Nat.Genet.* 14 (2):210-213.

Durbec P et al (1996a) GDNF signalling through the Ret receptor tyrosine kinase. *Nature* 381 (6585):789-793.

Durbec PL et al (1996b) Common origin and developmental dependence on c-ret of subsets of enteric and sympathetic neuroblasts. *Development* 122 (1):349-358.

Durick K et al (1995) Tyrosines outside the kinase core and dimerization are required for the mitogenic activity of RET/ptc2. J Biol Chem 270 (42):24642-24645.

Edery P et al (1996) Mutation of the endothelin-3 gene in the Waardenburg-Hirschsprung disease (Shah-Waardenburg syndrome). *Nat.Genet.* 12 (4):442-444.

Ellis HM and Horvitz HR (1986) Genetic control of programmed cell death in the nematode C. elegans. *Cell* 44 (6):817-829.

Ellis L et al (1986) Replacement of insulin receptor tyrosine residues 1162 and 1163 compromises insulin-stimulated kinase activity and uptake of 2-deoxyglucose. *Cell* 45 (5):721-732.

Elshourbagy NA et al (1996) Molecular characterization of a novel human endothelin receptor splice variant. *J.Biol.Chem.* 271 (41):25300-25307.

Encinas M et al (2001) c-Src is required for glial cell line-derived neurotrophic factor (GDNF) family ligand-mediated neuronal survival via a phosphatidylinositol-3 kinase (PI-3K)-dependent pathway. *J.Neurosci.* 21 (5):1464-1472.

Eng C et al (1998) Genomic structure and chromosomal localization of the human GDNFR-alpha gene. *Oncogene* 16 (5):597-601.

Enomoto H et al (1998) GFR alpha1-deficient mice have deficits in the enteric nervous system and kidneys. *Neuron* 21 (2):317-324.

Epstein DJ et al (1993) A mutation within intron 3 of the Pax-3 gene produces aberrantly spliced mRNA transcripts in the splotch (Sp) mouse mutant. *Proc.Natl.Acad.Sci.U.S.A* 90 (2):532-536.

Epstein ML et al (1994) Mapping the origin of the avian enteric nervous system with a retroviral marker. *Dev.Dyn.* 201 (3):236-244.

Ernfors P et al (1994) Lack of neurotrophin-3 leads to deficiencies in the peripheral nervous system and loss of limb proprioceptive afferents. *Cell* 77 (4):503-512.

Esteban I et al (1998) A neuronal subpopulation in the mammalian enteric nervous system expresses TrkA and TrkC neurotrophin receptor-like proteins. *Anat.Rec.* 251 (3):360-370.

Fang DC, Jass JR, and Wang DX (1998) Loss of heterozygosity and loss of expression of the DCC gene in gastric cancer. *J.Clin.Pathol.* 51 (8):593-596.

Fantl WJ, Escobedo JA, and Williams LT (1989) Mutations of the platelet-derived growth factor receptor that cause a loss of ligand-induced conformational change, subtle changes in kinase activity, and impaired ability to stimulate DNA synthesis. *Mol.Cell Biol.* 9 (10):4473-4478.

Fatigati V and Murphy RA (1984) Actin and tropomyosin variants in smooth muscles. Dependence on tissue type. *J.Biol.Chem.* 259 (23):14383-14388.

Faure S et al (2002) Endogenous patterns of BMP signaling during early chick development. *Dev.Biol.* 244 (1):44-65.

Fekete E et al (1996) Sequential pattern of nerve-muscle contacts in the small intestine of developing human fetus. An ultrastructural and immunohistochemical study. *Histol.Histopathol.* 11 (4):845-850.

Fekete E, Resch BA, and Benedeczky I (1995) Histochemical and ultrastructural features of the developing enteric nervous system of the human foetal small intestine. *Histol.Histopathol.* 10 (1):127-134.

Focke PJ et al (2001) Enteric neuroblasts require the phosphatidylinositol 3-kinase pathway for GDNF-stimulated proliferation. *J.Neurobiol.* 47 (4):306-317.

Forcet C et al (2001) The dependence receptor DCC (deleted in colorectal cancer) defines an alternative mechanism for caspase activation. *Proc.Natl.Acad.Sci.U.S.A* 98 (6):3416-3421.

Fu M et al (2003) HOXB5 expression is spatially and temporarily regulated in human embryonic gut during neural crest cell colonization and differentiation of enteric neuroblasts. *Dev.Dyn.* 228 (1):1-10.

Fu M et al (2004) Embryonic development of the ganglion plexuses and the concentric layer structure of human gut: a topographical study. *Anat.Embryol.(Berl)* 208 (1):33-41.

Fukuda T, Kiuchi K, and Takahashi M (2002) Novel mechanism of regulation of Rac activity and lamellipodia formation by RET tyrosine kinase. *J.Biol.Chem.* 277 (21):19114-19121.

Furness JB, Costa M. 1987. *The enteric nervous system.*

Gabella G (2002) Development of visceral smooth muscle. *Results Probl.Cell Differ.* 38:1-37.

Gabella G and Trigg P (1984) Size of neurons and glial cells in the enteric ganglia of mice, guinea-pigs, rabbits and sheep. *J.Neurocytol.* 13 (1):49-71.

Gariepy CE, Cass DT, and Yanagisawa M (1996) Null mutation of endothelin receptor type B gene in spotting lethal rats causes aganglionic megacolon and white coat color. *Proc.Natl.Acad.Sci.U.S.A* 93 (2):867-872.

Garver KL, Law JC, and Garver B (1985) Hirschsprung disease: a genetic study. *Clin.Genet.* 28 (6):503-508.

Gershon MD (1999) The enteric nervous system: a second brain. *Hosp.Pract.(Off Ed)* 34 (7):31-8, 41.

Gershon MD, Chalazonitis A, and Rothman TP (1993) From neural crest to bowel: development of the enteric nervous system. *J.Neurobiol.* 24 (2):199-214.

Goldstein AM et al (2005) BMP signaling is necessary for neural crest cell migration and ganglion formation in the enteric nervous system. *Mech.Dev.*

Gorodinsky A et al (1997) Assignment of the GDNF family receptor alpha-1 (GFRA1) to human chromosome band 10q26 by in situ hybridization. *Cytogenet.Cell Genet.* 78 (3-4):289-290.

Goulding MD et al (1991) Pax-3, a novel murine DNA binding protein expressed during early neurogenesis. *EMBO J.* 10 (5):1135-1147.

Gubbay J et al (1990) A gene mapping to the sex-determining region of the mouse Y chromosome is a member of a novel family of embryonically expressed genes. *Nature* 346 (6281):245-250.

Guillemot F et al (1993) Mammalian achaete-scute homolog 1 is required for the early development of olfactory and autonomic neurons. *Cell* 75 (3):463-476.

Hadano S et al (1999) Genomic organization of the human caspase-9 gene on Chromosome 1p36. 1-p36.3. *Mamm.Genome* 10 (7):757-760.

Hahn M and Bishop J (2001) Expression pattern of Drosophila ret suggests a common ancestral origin between the metamorphosis precursors in insect endoderm and the vertebrate enteric neurons. *Proc.Natl.Acad.Sci.U.S.A* 98 (3):1053-1058.

Hansford JR and Mulligan LM (2000) Multiple endocrine neoplasia type 2 and RET: from neoplasia to neurogenesis. *J.Med.Genet.* 37 (11):817-827.

Hayashi Y et al (2001) Activation of BMK1 via tyrosine 1062 in RET by GDNF and MEN2A mutation. *Biochem.Biophys.Res.Commun.* 281 (3):682-689.

Hearn CJ, Murphy M, and Newgreen D (1998) GDNF and ET-3 differentially modulate the numbers of avian enteric neural crest cells and enteric neurons in vitro. *Dev.Biol.* 197 (1):93-105.

Herbarth B et al (1998) Mutation of the Sry-related Sox10 gene in Dominant megacolon, a mouse model for human Hirschsprung disease. *Proc.Natl.Acad.Sci.U.S.A* 95 (9):5161-5165.

Heuckeroth RO et al (1998) Neurturin and GDNF promote proliferation and survival of enteric neuron and glial progenitors in vitro. *Dev.Biol.* 200 (1):116-129.

Hirst GD and Edwards FR (2004) Role of interstitial cells of Cajal in the control of gastric motility. *J.Pharmacol.Sci.* 96 (1):1-10.

Hofstra RM et al (1996) A homozygous mutation in the endothelin-3 gene associated with a combined Waardenburg type 2 and Hirschsprung phenotype (Shah-Waardenburg syndrome). *Nat.Genet.* 12 (4):445-447.

Hofstra RM et al (1999) A loss-of-function mutation in the endothelin-converting enzyme 1 (ECE-1) associated with Hirschsprung disease, cardiac defects, and autonomic dysfunction. *Am.J.Hum.Genet.* 64 (1):304-308.

Holschneider, A. M. and Puri, P. Hirschsprungs Disease and Allied Disorders. Harwood Academic Publishers Australia . 2000.

Homma S et al (2000) Expression pattern of GDNF, c-ret, and GFRalphas suggests novel roles for GDNF ligands during early organogenesis in the chick embryo. *Dev.Biol.* 217 (1):121-137.

Hosoda K et al (1994) Targeted and natural (piebald-lethal) mutations of endothelin-B receptor gene produce megacolon associated with spotted coat color in mice. *Cell* 79 (7):1267-1276.

Hubbard SR and Till JH (2000) Protein tyrosine kinase structure and function. *Annu.Rev.Biochem.* 69:373-398.

Huizinga JD et al (2001) Development of interstitial cells of Cajal in a full-term infant without an enteric nervous system. *Gastroenterology* 120 (2):561-567.

Huizinga JD et al (1995) W/kit gene required for interstitial cells of Cajal and for intestinal pacemaker activity. *Nature* 373 (6512):347-349.

Hunter T (1998) The role of tyrosine phosphorylation in cell growth and disease. *Harvey Lect.* 94:81-119.

Ibanez CF (1998) Emerging themes in structural biology of neurotrophic factors. *Trends Neurosci.* 21 (10):438-444.

Inoue A et al (1989) The human endothelin family: three structurally and pharmacologically distinct isopeptides predicted by three separate genes. *Proc.Natl.Acad.Sci.U.S.A* 86 (8):2863-2867.

Ishizaka Y et al (1989) Human ret proto-oncogene mapped to chromosome 10q11.2. *Oncogene* 4 (12):1519-1521.

Iwamoto T et al (1993) cDNA cloning of mouse ret proto-oncogene and its sequence similarity to the cadherin superfamily. *Oncogene* 8 (4):1087-1091.

Jhiang SM (2000) The RET proto-oncogene in human cancers. *Oncogene* 19 (49):5590-5597.

Jiang Y, Liu MT, and Gershon MD (2003) Netrins and DCC in the guidance of migrating neural crest-derived cells in the developing bowel and pancreas. *Dev.Biol.* 258 (2):364-384.

Jing S et al (1997) GFRalpha-2 and GFRalpha-3 are two new receptors for ligands of the GDNF family. *J.Biol.Chem.* 272 (52):33111-33117.

Jones KR and Reichardt LF (1990) Molecular cloning of a human gene that is a member of the nerve growth factor family. *Proc.Natl.Acad.Sci.U.S.A* 87 (20):8060-8064.

Kapur RP (1999) Early death of neural crest cells is responsible for total enteric aganglionosis in Sox10(Dom)/Sox10(Dom) mouse embryos. *Pediatr.Dev.Pathol.* 2 (6):559-569.

Kapur RP (2000) Colonization of the murine hindgut by sacral crest-derived neural precursors: experimental support for an evolutionarily conserved model. *Dev.Biol.* 227 (1):146-155.

Kapur RP, Yost C, and Palmiter RD (1992) A transgenic model for studying development of the enteric nervous system in normal and aganglionic mice. *Development* 116 (1):167-175.

Kendall RL et al (1999) Vascular endothelial growth factor receptor KDR tyrosine kinase activity is increased by autophosphorylation of two activation loop tyrosine residues. *J.Biol.Chem.* 274 (10):6453-6460.

Kenny SE et al (1999) Ontogeny of interstitial cells of Cajal in the human intestine. *J.Pediatr.Surg.* 34 (8):1241-1247.

Kim J et al (2003) SOX10 maintains multipotency and inhibits neuronal differentiation of neural crest stem cells. *Neuron* 38 (1):17-31.

Kotzbauer PT et al (1996) Neurturin, a relative of glial-cell-line-derived neurotrophic factor. *Nature* 384 (6608):467-470.

Krygier S and Djakiew D (2001) The neurotrophin receptor p75NTR is a tumor suppressor in human prostate cancer. *Anticancer Res.* 21 (6A):3749-3755.

Kuhlbrodt K et al (1998a) Sox10, a novel transcriptional modulator in glial cells. *J.Neurosci.* 18 (1):237-250.

Kuhlbrodt K et al (1998b) Functional analysis of Sox10 mutations found in human Waardenburg-Hirschsprung patients. *J.Biol.Chem.* 273 (36):23033-23038.

Kuida K et al (1998) Reduced apoptosis and cytochrome c-mediated caspase activation in mice lacking caspase 9. *Cell* 94 (3):325-337.

Kunieda T et al (1996) A mutation in endothelin-B receptor gene causes myenteric aganglionosis and coat color spotting in rats. *DNA Res.* 3 (2):101-105.

Lane PW and Liu HM (1984) Association of megacolon with a new dominant spotting gene (Dom) in the mouse. *J.Hered.* 75 (6):435-439.

Lang D et al (2000b) Pax3 is required for enteric ganglia formation and functions with Sox10 to modulate expression of c-ret. *J.Clin.Invest* 106 (8):963-971.

Lang D et al (2000a) Pax3 is required for enteric ganglia formation and functions with Sox10 to modulate expression of c-ret. *J.Clin.Invest* 106 (8):963-971.

Lang D and Epstein JA (2003) Sox10 and Pax3 physically interact to mediate activation of a conserved c-RET enhancer. *Hum.Mol.Genet.* 12 (8):937-945.

Laudet V, Stehelin D, and Clevers H (1993) Ancestry and diversity of the HMG box superfamily. *Nucleic Acids Res.* 21 (10):2493-2501.

Le Douarin N, Kalcheim C. 1999. *The Neural Crest.*

Le Douarin NM and Teillet MA (1973) The migration of neural crest cells to the wall of the digestive tract in avian embryo. *J.Embryol.Exp.Morphol.* 30 (1):31-48.

Lecoin L, Gabella G, and Le Douarin N (1996) Origin of the c-kit-positive interstitial cells in the avian bowel. *Development* 122 (3):725-733.

Leibl MA et al (1999) Expression of endothelin 3 by mesenchymal cells of embryonic mouse caecum. *Gut* 44 (2):246-252.

Lin LF et al (1993) GDNF: a glial cell line-derived neurotrophic factor for midbrain dopaminergic neurons. *Science* 260 (5111):1130-1132.

Lipson AH and Harvey J (1987) Three-generation transmission of Hirschsprung's disease. *Clin.Genet.* 32 (3):175-178.

Lipson AH, Harvey J, and Oley CA (1990) Three-generation transmission of Hirschsprung's disease. *Clin.Genet.* 37 (3):235.

Liu X et al (1996) Oncogenic RET receptors display different autophosphorylation sites and substrate binding specificities. *J.Biol.Chem.* 271 (10):5309-5312.

Lockshin RA and Zakeri Z (2004) Apoptosis, autophagy, and more. *Int.J.Biochem.Cell Biol.* 36 (12):2405-2419.

Lunam CA and Smith TK (1996) Morphology and projections of neurons in Remak's nerve of the domestic fowl revealed by intracellular injection of biocytin. *Cell Tissue Res.* 284 (2):215-222.

Maisonpierre PC et al (1991) Human and rat brain-derived neurotrophic factor and neurotrophin-3: gene structures, distributions, and chromosomal localizations. *Genomics* 10 (3):558-568.

Maka M, Stolt CC, and Wegner M (2005) Identification of Sox8 as a modifier gene in a mouse model of Hirschsprung disease reveals underlying molecular defect. *Dev.Biol.* 277 (1):155-169.

Malas S, Peters J, and Abbott C (1994) The genes for endothelin 3, vitamin D 24-hydroxylase, and melanocortin 3 receptor map to distal mouse chromosome 2, in the region of conserved synteny with human chromosome 20. *Mamm.Genome* 5 (9):577-579.

Manie S et al (2001) The RET receptor: function in development and dysfunction in congenital malformation. *Trends Genet.* 17 (10):580-589.

Marsden VS et al (2002) Apoptosis initiated by Bcl-2-regulated caspase activation independently of the cytochrome c/Apaf-1/caspase-9 apoptosome. *Nature* 419 (6907):634-637.

Masumoto K et al (2000) The formation of the chick ileal muscle layers as revealed by alpha-smooth muscle actin immunohistochemistry. *Anat.Embryol.(Berl)* 201 (2):121-129.

Matsuoka R et al (1996) Human endothelin converting enzyme gene (ECE1) mapped to chromosomal region 1p36.1. *Cytogenet.Cell Genet.* 72 (4):322-324.

McKeown SJ, Chow CW, and Young HM (2001) Development of the submucous plexus in the large intestine of the mouse. *Cell Tissue Res.* 303 (2):301-305.

McKeown SJ et al (2005) Sox10 overexpression induces neural crest-like cells from all dorsoventral levels of the neural tube but inhibits differentiation. *Dev.Dyn.* 233 (2):430-444.

Mehlen P et al (1998) The DCC gene product induces apoptosis by a mechanism requiring receptor proteolysis. *Nature* 395 (6704):801-804.

Milbrandt J et al (1998) Persephin, a novel neurotrophic factor related to GDNF and neurturin. *Neuron* 20 (2):245-253.

Mohammadi M et al (1996) Identification of six novel autophosphorylation sites on fibroblast growth factor receptor 1 and elucidation of their importance in receptor activation and signal transduction. *Mol.Cell Biol.* 16 (3):977-989.

Moore MW et al (1996) Renal and neuronal abnormalities in mice lacking GDNF. *Nature* 382 (6586):76-79.

Murakami H et al (1999) Rho-dependent and -independent tyrosine phosphorylation of focal adhesion kinase, paxillin and p130Cas mediated by Ret kinase. *Oncogene* 18 (11):1975-1982.

Myers SM et al (1995) Characterization of RET proto-oncogene 3' splicing variants and polyadenylation sites: a novel C-terminus for RET. *Oncogene* 11 (10):2039-2045.

Nagar B et al (1996) Structural basis of calcium-induced E-cadherin rigidification and dimerization. *Nature* 380(6572):360-364.

Nakamuta M et al (1991) Cloning and sequence analysis of a cDNA encoding human non-selective type of endothelin receptor. *Biochem.Biophys.Res.Commun.* 177 (1):34-39.

Natarajan D et al (2002) Requirement of signalling by receptor tyrosine kinase RET for the directed migration of enteric nervous system progenitor cells during mammalian embryogenesis. *Development* 129 (22):5151-5160.

Newman CJ et al (2003) Interstitial cells of Cajal are normally distributed in both ganglionated and aganglionic bowel in Hirschsprung's disease. *Pediatr.Surg.Int.* 19 (9-10):662-668.

Nishijima E et al (1990) Formation and malformation of the enteric nervous system in mice: an organ culture study. *J.Pediatr.Surg.* 25 (6):627-631.

Nozaki C et al (1998) Calcium-dependent Ret activation by GDNF and neurturin. *Oncogene* 16 (3):293-299.

Pachnis V, Mankoo B, and Costantini F (1993) Expression of the c-ret proto-oncogene during mouse embryogenesis. *Development* 119 (4):1005-1017.

Paratcha G et al (2001) Released GFRalpha1 potentiates downstream signaling, neuronal survival, and differentiation via a novel mechanism of recruitment of c-Ret to lipid rafts. *Neuron* 29 (1):171-184.

Paratore C et al (2002) Sox10 haploinsufficiency affects maintenance of progenitor cells in a mouse model of Hirschsprung disease. *Hum.Mol.Genet.* 11 (24):3075-3085.

Paratore C et al (2001) Survival and glial fate acquisition of neural crest cells are regulated by an interplay between the transcription factor Sox10 and extrinsic combinatorial signaling. *Development* 128 (20):3949-3961.

Pasini B et al (1995) The physical map of the human RET proto-oncogene. *Oncogene* 11 (9):1737-1743.

Passarge E (1967) The genetics of Hirschsprung's disease. Evidence for heterogeneous etiology and a study of sixty-three families. *N.Engl.J.Med.* 276 (3):138-143.

Pattyn A et al (1997) Expression and interactions of the two closely related homeobox genes Phox2a and Phox2b during neurogenesis. *Development* 124 (20):4065-4075.

Peters-van der Sanden MJ et al (1993) Ablation of various regions within the avian vagal neural crest has differential effects on ganglion formation in the fore-, mid- and hindgut. *Dev.Dyn.* 196 (3):183-194.

Peterziel H, Unsicker K, and Krieglstein K (2002) TGFbeta induces GDNF responsiveness in neurons by recruitment of GFRalpha1 to the plasma membrane. *J.Cell Biol.* 159 (1):157-167.

Pezeshki G, Franke B, and Engele J (2001) Evidence for a ligand-specific signaling through GFRalpha-1, but not GFRalpha-2, in the absence of Ret. *J.Neurosci.Res.* 66 (3):390-395.

Pichel JG et al (1996) Defects in enteric innervation and kidney development in mice lacking GDNF. *Nature* 382 (6586):73-76.

Pingault V et al (1998) SOX10 mutations in patients with Waardenburg-Hirschsprung disease. *Nat.Genet.* 18 (2):171-173.

Pingault V et al (1997) Human homology and candidate genes for the Dominant megacolon locus, a mouse model of Hirschsprung disease. *Genomics* 39 (1):86-89.

Pomeranz HD and Gershon MD (1990) Colonization of the avian hindgut by cells derived from the sacral neural crest. *Dev.Biol.* 137 (2):378-394.

Pomeranz HD, Rothman TP, and Gershon MD (1991) Colonization of the post-umbilical bowel by cells derived from the sacral neural crest: direct tracing of cell migration using an intercalating probe and a replication-deficient retrovirus. *Development* 111 (3):647-655.

Pong K et al (1998) Inhibition of phosphatidylinositol 3-kinase activity blocks cellular differentiation mediated by glial cell line-derived neurotrophic factor in dopaminergic neurons. *J.Neurochem.* 71 (5):1912-1919.

Popsueva A et al (2003) GDNF promotes tubulogenesis of GFRalpha1-expressing MDCK cells by Src-mediated phosphorylation of Met receptor tyrosine kinase. *J.Cell Biol.* 161 (1):119-129.

Potterf SB et al (2000) Transcription factor hierarchy in Waardenburg syndrome: regulation of MITF expression by SOX10 and PAX3. *Hum.Genet.* 107 (1):1-6.

Puffenberger EG et al (1994) A missense mutation of the endothelin-B receptor gene in multigenic Hirschsprung's disease. *Cell* 79 (7):1257-1266.

Puliti A et al (1997) Assignment of mouse Gfra1, the homologue of a new human HSCR candidate gene, to the telomeric region of mouse chromosome 19. *Cytogenet.Cell Genet.* 78 (3-4):291-294.

Pusch C et al (1998) The SOX10/Sox10 gene from human and mouse: sequence, expression, and transactivation by the encoded HMG domain transcription factor. *Hum.Genet.* 103 (2):115-123.

Raoul C, Henderson CE, and Pettmann B (1999) Programmed cell death of embryonic motoneurons triggered through the Fas death receptor. *J.Cell Biol.* 147 (5):1049-1062.

Reddy T and Kablar B (2004) Evidence for the involvement of neurotrophins in muscle transdifferentiation and acetylcholine receptor transformation in the esophagus of Myf5(-/-):MyoD(-/-) and NT-3(-/-) embryos. *Dev.Dyn.* 231 (4):683-692.

Renault B et al (1995) Localization of the human achaete-scute homolog gene (ASCL1) distal to phenylalanine hydroxylase (PAH) and proximal to tumor rejection antigen (TRA1) on chromosome 12q22-q23. *Genomics* 30 (1):81-83.

Roberts DJ (2000) Molecular mechanisms of development of the gastrointestinal tract. *Dev.Dyn.* 219 (2):109-120.

Robertson K and Mason I (1995) Expression of ret in the chicken embryo suggests roles in regionalisation of the vagal neural tube and somites and in development of multiple neural crest and placodal lineages. *Mech.Dev.* 53 (3):329-344.

Roix JJ et al (2001) Molecular and functional mapping of the piebald deletion complex on mouse chromosome 14. *Genetics* 157 (2):803-815.

Rolle U et al (2002) Altered distribution of interstitial cells of Cajal in Hirschsprung disease. *Arch.Pathol.Lab Med.* 126 (8):928-933.

Rothman TP et al (1996) Increased expression of laminin-1 and collagen (IV) subunits in the aganglionic bowel of ls/ls, but not c-ret -/- mice. *Dev.Biol.* 178 (2):498-513.

Rothman TP, Goldowitz D, and Gershon MD (1993) Inhibition of migration of neural crest-derived cells by the abnormal mesenchyme of the presumptive aganglionic bowel of ls/ls mice: analysis with aggregation and interspecies chimeras. *Dev.Biol.* 159 (2):559-573.

Salomon R et al (1996) Germline mutations of the RET ligand GDNF are not sufficient to cause Hirschsprung disease. *Nat.Genet.* 14 (3):345-347.

Sanchez MP et al (1996) Renal agenesis and the absence of enteric neurons in mice lacking GDNF. *Nature* 382 (6586):70-73.

Sang Q et al (1999) Innervation of the esophagus in mice that lack MASH1. *J.Comp Neurol.* 408 (1):1-10.

Sanicola M et al (1997) Glial cell line-derived neurotrophic factor-dependent RET activation can be mediated by two different cell-surface accessory proteins. *Proc.Natl.Acad.Sci.U.S.A* 94 (12):6238-6243.

Sariola H and Saarma M (2003) Novel functions and signalling pathways for GDNF. *J.Cell Sci.* 116 (Pt 19):3855-3862.

Schepers GE, Teasdale RD, and Koopman P (2002) Twenty pairs of sox: extent, homology, and nomenclature of the mouse and human sox transcription factor gene families. *Dev.Cell* 3 (2):167-170.

Schiltz CA, Benjamin J, and Epstein ML (1999) Expression of the GDNF receptors ret and GFRalpha1 in the developing avian enteric nervous system. *J.Comp Neurol.* 414 (2):193-211.

Schlessinger J and Ullrich A (1992) Growth factor signaling by receptor tyrosine kinases. *Neuron* 9 (3):383-391.

Schmidt M et al (1994) Molecular characterization of human and bovine endothelin converting enzyme (ECE-1). *FEBS Lett.* 356 (2-3):238-243.

Schneider A et al (1999) NF-kappaB is activated and promotes cell death in focal cerebral ischemia. *Nat.Med.* 5 (5):554-559.

Schuchardt A et al (1994) Defects in the kidney and enteric nervous system of mice lacking the tyrosine kinase receptor Ret. *Nature* 367 (6461):380-383.

Sela-Donenfeld D and Kalcheim C (1999) Regulation of the onset of neural crest migration by coordinated activity of BMP4 and Noggin in the dorsal neural tube. *Development* 126 (21):4749-4762.

Sela-Donenfeld D and Kalcheim C (2000) Inhibition of noggin expression in the dorsal neural tube by somitogenesis: a mechanism for coordinating the timing of neural crest emigration. *Development* 127 (22):4845-4854.

Serbedzija GN et al (1991) Vital dye labelling demonstrates a sacral neural crest contribution to the enteric nervous system of chick and mouse embryos. *Development* 111 (4):857-866.

Serbedzija GN and McMahon AP (1997) Analysis of neural crest cell migration in Splotch mice using a neural crest-specific LacZ reporter. *Dev.Biol.* 185 (2):139-147.

Seri M et al (1997) Frequency of RET mutations in long- and short-segment Hirschsprung disease. *Hum.Mutat.* 9 (3):243-249.

Shefelbine SE et al (1998) Mutational analysis of the GDNF/RET-GDNFR alpha signaling complex in a kindred with vesicoureteral reflux. *Hum.Genet.* 102 (4):474-478.

Shepherd IT, Beattie CE, and Raible DW (2001) Functional analysis of zebrafish GDNF. *Dev.Biol.* 231 (2):420-435.

Shepherd IT et al (2004) Roles for GFRalpha1 receptors in zebrafish enteric nervous system development. *Development* 131 (1):241-249.

Shepherd IT and Raper JA (1999) Collapsin-1/semaphorin D is a repellent for chick ganglion of Remak axons. *Dev.Biol.* 212 (1):42-53.

Shimada K et al (1995) Cloning and functional expression of human endothelin-converting enzyme cDNA. *Biochem.Biophys.Res.Commun.* 207 (2):807-812.

Smith DM et al (2000) Roles of BMP signaling and Nkx2.5 in patterning at the chick midgut-foregut boundary. *Development* 127 (17):3671-3681.

Smith TK and Lunam CA (1998) Electrical characteristics and responses to jejunal distension of neurons in Remak's juxta-jejunal ganglia of the domestic fowl. *J.Physiol* 510 (Pt 2):563-575.

Sock E et al (2001) Idiopathic weight reduction in mice deficient in the high-mobility-group transcription factor Sox8. *Mol.Cell Biol.* 21 (20):6951-6959.

Soullier S et al (1999) Diversification pattern of the HMG and SOX family members during evolution. *J.Mol.Evol.* 48 (5):517-527.

Southard-Smith EM, Kos L, and Pavan WJ (1998) Sox10 mutation disrupts neural crest development in Dom Hirschsprung mouse model. *Nat.Genet.* 18 (1):60-64.

Spouge D and Baird PA (1985) Hirschsprung disease in a large birth cohort. *Teratology* 32 (2):171-177.

Stein E et al (1998) Eph receptors discriminate specific ligand oligomers to determine alternative signaling complexes, attachment, and assembly responses. *Genes Dev.* 12 (5):667-678.

Stein J. F (1982) "An introduction to neurophysiology" Blackwell Scientific Publications.

Stennicke HR et al (1999) Caspase-9 can be activated without proteolytic processing. *J.Biol.Chem.* 274 (13):8359-8362.

Sundqvist M and Holmgren S (2004) Neurotrophin receptors and enteric neuronal development during metamorphosis in the amphibian Xenopus laevis. *Cell Tissue Res.* 316 (1):45-54.

Suvanto P et al (1996) Localization of glial cell line-derived neurotrophic factor (GDNF) mRNA in embryonic rat by in situ hybridization. *Eur.J.Neurosci.* 8 (4):816-822.

Tahira T et al (1990) Characterization of ret proto-oncogene mRNAs encoding two isoforms of the protein product in a human neuroblastoma cell line. *Oncogene* 5 (1):97-102.

Takahashi M et al (1993) Characterization of the ret proto-oncogene products expressed in mouse L cells. *Oncogene* 8 (11):2925-2929.

Takahashi M, Ritz J, and Cooper GM (1985) Activation of a novel human transforming gene, ret, by DNA rearrangement. *Cell* 42 (2):581-588.

Takayanagi R et al (1991) Multiple subtypes of endothelin receptors in porcine tissues: characterization by ligand binding, affinity labeling and regional distribution. *Regul.Pept.* 32 (1):23-37.

Tansey MG et al (2000) GFRalpha-mediated localization of RET to lipid rafts is required for effective downstream signaling, differentiation, and neuronal survival. *Neuron* 25 (3):611-623.

Taraviras S et al (1999) Signalling by the RET receptor tyrosine kinase and its role in the development of the mammalian enteric nervous system. *Development* 126 (12):2785-2797.

Tassabehji M et al (1992) Waardenburg's syndrome patients have mutations in the human homologue of the Pax-3 paired box gene. *Nature* 355 (6361):635-636.

Thuneberg L (1982) Interstitial cells of Cajal: intestinal pacemaker cells? *Adv.Anat.Embryol.Cell Biol.* 71:1-130.

Thuneberg L, Rumessen JJ, and Mikkelsen HB (1982) Interstitial cells of Cajal - an intestinal impulse generation and conduction system? *Scand.J.Gastroenterol.Suppl* 71:143-144.

Tomac AC et al (2000) Glial cell line-derived neurotrophic factor receptor alpha1 availability regulates glial cell line-derived neurotrophic factor signaling: evidence from mice carrying one or two mutated alleles. *Neuroscience* 95 (4):1011-1023.

Torihashi S, Horisawa M, and Watanabe Y (1999) c-Kit immunoreactive interstitial cells in the human gastrointestinal tract. *J.Auton.Nerv.Syst.* 75 (1):38-50.

Torihashi S et al (1996) Enteric neurons express Steel factor-lacZ transgene in the murine gastrointestinal tract. *Brain Res.* 738 (2):323-328.

Ullrich A and Schlessinger J (1990) Signal transduction by receptors with tyrosine kinase activity. *Cell* 61 (2):203-212.

Van de Putte T et al (2003) Mice lacking ZFHX1B, the gene that codes for Smad-interacting protein-1, reveal a role for multiple neural crest cell defects in the etiology of Hirschsprung disease-mental retardation syndrome. *Am.J.Hum.Genet.* 72 (2):465-470.

van Weering DH and Bos JL (1998) Signal transduction by the receptor tyrosine kinase Ret. *Recent Results Cancer Res.* 154:271-281.

van Weering DH et al (1998) Expression of the receptor tyrosine kinase Ret on the plasma membrane is dependent on calcium. *J.Biol.Chem.* 273 (20):12077-12081.

Vaos GC (1989) Quantitative assessment of the stage of neuronal maturation in the developing human fetal gut--a new dimension in the pathogenesis of developmental anomalies of the myenteric plexus. *J.Pediatr.Surg.* 24 (9):920-925.

Wakamatsu N et al (2001) Mutations in SIP1, encoding Smad interacting protein-1, cause a form of Hirschsprung disease. *Nat.Genet.* 27 (4):369-370.

Wallace AS and Burns AJ (2003) Spatiotemporal migration of neural crest cells within the human gastrointestinal tract. *Neurogastroenterol.Motil.* (15):201.

Wallace AS and Burns AJ (2005) Development of the enteric nervous system, smooth muscle and interstitial cells of Cajal in the human gastrointestinal tract. Cell Tissue Res. 2005 319 (3):367-82.

Wang ZB, Liu YQ, and Cui YF (2005) Pathways to caspase activation. *Cell Biol.Int.* 29 (7):489-496.

Ward SM et al (1995) Impaired development of interstitial cells and intestinal electrical rhythmicity in steel mutants. *Am.J.Physiol* 269 (6 Pt 1):C1577-C1585.

Ward SM et al (1994) Mutation of the proto-oncogene c-kit blocks development of interstitial cells and electrical rhythmicity in murine intestine. *J.Physiol* 480 (Pt 1):91-97.

Wegner M (1999) From head to toes: the multiple facets of Sox proteins. *Nucleic Acids Res.* 27 (6):1409-1420.

Wester T et al (1999) Interstitial cells of Cajal in the human fetal small bowel as shown by c-kit immunohistochemistry. *Gut* 44 (1):65-71.

Woodward MN et al (2000) Time-dependent effects of endothelin-3 on enteric nervous system development in an organ culture model of Hirschsprung's disease. *J.Pediatr.Surg.* 35 (1):25-29.

Worley DS et al (2000) Developmental regulation of GDNF response and receptor expression in the enteric nervous system. *Development* 127 (20):4383-4393.

Wright EM, Snopek B, and Koopman P (1993) Seven new members of the Sox gene family expressed during mouse development. *Nucleic Acids Res.* 21 (3):744.

Wu JJ et al (1999) Inhibition of in vitro enteric neuronal development by endothelin-3: mediation by endothelin B receptors. *Development* 126 (6):1161-1173.

Wu JJ, Rothman TP, and Gershon MD (2000) Development of the interstitial cell of Cajal: origin, kit dependence and neuronal and nonneuronal sources of kit ligand. *J.Neurosci.Res.* 59 (3):384-401.

Yamada K et al (2001) Nonsense and frameshift mutations in ZFHX1B, encoding Smad-interacting protein 1, cause a complex developmental disorder with a great variety of clinical features. *Am.J.Hum.Genet.* 69 (6):1178-1185.

Yan H et al (2004) Neural cells in the esophagus respond to glial cell line-derived neurotrophic factor and neurturin, and are RET-dependent. *Dev.Biol.* 272 (1):118-133.

Yntema and Hammond (1954) The origin of intrinsic ganglia of trunk viscera from vagal neural crest in the chick embryo. *J.Comp Neurol.* 101 (2):515-541.

Yokoyama M et al (1996) Identification and cloning of neuroblastoma-specific and nerve tissue-specific genes through compiled expression profiles. *DNA Res.* 3 (5):311-320.

Yorimitsu K et al (1995) Cloning and sequencing of a human endothelin converting enzyme in renal adenocarcinoma (ACHN) cells producing endothelin-2. *Biochem.Biophys.Res.Commun.* 208 (2):721-727.

Young HM, Bergner AJ, and Muller T (2003) Acquisition of neuronal and glial markers by neural crest-derived cells in the mouse intestine. *J.Comp Neurol.* 456 (1):1-11.

Young HM et al (1999) Expression of Ret-, p75(NTR)-, Phox2a-, Phox2b-, and tyrosine hydroxylase-immunoreactivity by undifferentiated neural crest-derived cells and different classes of enteric neurons in the embryonic mouse gut. *Dev.Dyn.* 216 (2):137-152.

Young HM et al (1996) Origin of interstitial cells of Cajal in the mouse intestine. *Dev.Biol.* 180 (1):97-107.

Young HM et al (1998) A single rostrocaudal colonization of the rodent intestine by enteric neuron precursors is revealed by the expression of Phox2b, Ret, and p75 and by explants grown under the kidney capsule or in organ culture. *Dev.Biol.* 202 (1):67-84.

Young HM et al (2001) GDNF is a chemoattractant for enteric neural cells. *Dev.Biol.* 229 (2):503-516.

Yuan J et al (1993) The C. elegans cell death gene ced-3 encodes a protein similar to mammalian interleukin-1 beta-converting enzyme. *Cell* 75 (4):641-652.

Zhu L et al (2004) Spatiotemporal regulation of endothelin receptor-B by SOX10 in neural crest-derived enteric neuron precursors. *Nat.Genet.*

Zwijsen A, Verschueren K, and Huylebroeck D (2003) New intracellular components of bone morphogenetic protein/Smad signaling cascades. *FEBS Lett.* 546 (1):133-139.

Appendix: Wallace and Burns (2005)

Cell Tissue Res (2005) 319: 367–382
DOI 10.1007/s00441-004-1023-2

REGULAR ARTICLE

Adam S. Wallace · Alan J. Burns

Development of the enteric nervous system, smooth muscle and interstitial cells of Cajal in the human gastrointestinal tract

Received: 16 July 2004 / Accepted: 19 October 2004 / Published online: 26 January 2005
© Springer-Verlag 2005

WEEK 8